GROWTH DIFFERENTIATION FACTOR 11: GENETIC REGULATION AND IMPLICATIONS FOR HUMAN DISEASE

by

ABIGAIL STARCHER

(Under the Direction of Robert Pazdro)

ABSTRACT

Growth Differentiation Factor 11 (GDF11) serves vital roles in the developing embryo, governing organogenesis and axial patterning, yet surprisingly little is known about its function or genetic regulation in the adult mammal. Over the past several years, some studies have suggested that GDF11 has a rejuvenating effect on the heart by suppressing and even reversing cardiac hypertrophy. However, it is unclear whether those effects are actually due to its homolog, myostatin, which is structurally similar and signals through the same pathways. The work presented in this thesis outlines a translational systems approach to define the genetics of GDF11 better understand its true role in disease pathology. Importantly, the approach has underscored novel genes and pathways that will form the foundation for future GDF11 research.

INDEX WORDS: GDF11, myostatin, rejuvenating, aging, cardiac hypertrophy, asthma, hypothyroidism

# GROWTH DIFFERENTIATION FACTOR 11: GENETIC REGULATION AND IMPLICATIONS FOR HUMAN DISEASE

by

ABIGAIL STARCHER

B.S., The University of Florida, 2019

A Thesis Submitted to the Graduate Faculty of The University of Georgia in Partial Fulfillment of the Requirements for the Degree

MASTER OF SCIENCE

ATHENS, GEORGIA

2021

# GROWTH DIFFERENTIATION FACTOR 11: GENETIC REGULATION AND IMPLICATIONS FOR HUMAN DISEASE

by

ABIGAIL STARCHER

| | |
|---|---|
| Major Professor: | Robert Pazdro |
| Committee: | Arthur Grider |
| | Chad Paton |

Electronic Version Approved:

Ron Walcott
Vice Provost for Graduate Education and Dean of the Graduate School
The University of Georgia
August 2021

# DEDICATION

I would like to dedicate this thesis to my family and friends who have provided invaluable support and encouragement throughout my time at UGA. To my parents, Doug and Linda, who empowered me to pursue my passions and cheered me on along the way; to my sisters, Allison, Amanda, and Amelia, who were always only a call away and provided needed laughs and perspective; and to my fiancé, Josh, who challenged me to be courageous and continually put forth my best effort, thank you. Most of all this investigation of GDF11 is dedicated to the One who designed it all in His infinite wisdom and beautiful creativity. It is because of God science will be an endless playground of exploration, and I am thankful for the privilege to enjoy it.

ACKNOWLEDGEMENTS

Completing this degree would not have been possible without the incredible people at UGA. I am thankful to Gabie Daniel, Emily Crowell, and Kali Haney for the weekend adventures and daily laughs, to my fellow interns for their friendship and consolidation, to Dr. Grossman for supporting us as aspiring dietitians and answering endless questions, to Rebecca Gould and my wonderful labmates, Jessica Strosahl, Olivia Delgado, and Steven Craig, for their constant willingness to help, to Dr. Ye for his guidance and training, to Drs. Cotwright, Laing, and Grider for teaching with excellence, and to Dr. Pazdro for pushing me to always do my best.

TABLE OF CONTENTS

Page

LIST OF TABLES

Page

LIST OF FIGURES

Page

# CHAPTER 1

# INTRODUCTION

## Purpose of the Study

Growth Differentiation Factor (GDF11) has been implicated as a protective factor against multiple chronic and degenerative conditions. Yet to this point, mouse and human studies have been plagued by limitations that prevented a full understanding of GDF11 and its impact on disease. The work presented in this thesis seeks to use an innovative systems genetics approach, leveraging the relative advantages of mouse and human studies, to define the genetic factors that control GDF11 levels in the adult and how those factors impact chronic disease risk. It has been prepared in manuscript format with with all chapters after the second either submitted for review or to be submitted. Chapter two serves as the literature review of GDF11. Chapter three contains the initial *in vivo* study conducted using a cohort of Diversity Outbred (DO) mice to examine the relationship between cardiac structure and function and circulating GDF11 levels. Precise genetic mapping also identified a putative genetic regulator which was further explored *in silico* in chapter three. Subsequent bioinformatic analysis of GDF11 in chapter four provided evidence of GDF11 as an intermediate genetic regulator of hypothyroidism and respiratory ailments such as asthma. Chapter six summarizes the conclusions of the combined body of research presented in this thesis. The appendix provides direction for mechanistic validation of results outlined in chapter three.

CHAPTER 2

LITERATURE REVIEW

## I. Introduction

Heart disease continues to be the leading cause of death for both men and women in the United States and around the world, disproportionately affecting older people. To address this public health crisis, especially in an increasingly aging population, it is essential to develop a better understanding of the mechanisms that drive the onset of heart disease in its various forms. In 2013, a seminal parabiosis study demonstrated that the abnormal thickening of ventricle walls, known as cardiac hypertrophy, in aged mice can be reversed by exposure to young blood, a change credited to the circulating protein Growth Differentiation Factor 11. Interestingly, intraperitoneal injections of the protein administered to aged mice had similar rejuvenating effects in the heart. Naturally, those findings earned a significant amount of attention and excitement, yet in the subsequent years, some research studies have shown that the opposite relationship exists between GDF11 and cardiac hypertrophy or no relationship at all. To help address these controversies, we posited that systems genetics would be a powerful tool to resolve the relationship between GDF11 and cardiac hypertrophy. We used a translational approach that paired an innovative mouse model of human genetics, the Diversity Outbred population, and powerful human databases to elicit genetic regulators of GDF11 and explore its connection to human disease.

## II. Heart Failure and Cardiac Hypertrophy: an Overview

The Aging Heart

*Heart Failure Statistics:* In 2019, heart failure claimed the lives of nearly 9 million people worldwide, representing 16% of total deaths [1]. In the United States alone, an estimated 6.2 million adults over the age of 20 had heart failure between 2013 and 2016 according to National Health and Examination Survey (NHANES) data [2]. It was estimated that in 2012 the total direct and indirect costs of the disease to the nation was $30.7 billion dollars [3, 4], and that by 2030 it will be a staggering $69.8 billion, the equivalent of $244 for every US adult [4]. Heart failure, like many other degenerative diseases, disproportionately afflicts older people: 80% of those diagnosed with heart disease are 65 years or older with incidence and prevalence increasing with age [5]. In fact, acute heart failure is the number one reason for hospitalization of people in that age group [5]. Furthermore, many chronic diseases, such as coronary artery disease, hypertension, genetic cardiomyopathies, and HIV, contribute to the development of heart failure [6].

*Cardiac Hypertrophy as a Key Contributor to Heart Failure:* Heart failure is a complex disease that exists in different forms and is often preceded by various conditions and environmental and genetic factors [7]. A primary driving condition of heart failure is cardiac hypertrophy, or the enlargement of the heart as a result of increased workload that often leads to impaired circulation of blood throughout the body due to reduced ventricle filling ejection of blood or reduced ventricular filling [6-8]. Initially, cardiomyocyte and/or cardiac tissue hypertrophy is an adaptive response necessary to keep up with increased demand, but if the stress is sustained over a prolonged period of time, the

changes often eventually become maladaptive [8]. Such cardiac changes can be induced by various pathologies (often age-related), intrinsic aging of the heart, or intense exercise.

*Determinants of Pathological Cardiac Hypertrophy*: Pathological cardiac hypertrophy is largely caused by sarcomeric gene mutations, responsible for 40-60% of cases [9], yet can also induced by chronic disease or intrinsic aging of the heart [10]. In the former case, many disease states such as hypertension, remodeling following a myocardial infarction, and valvular abnormalities contribute to either pressure- or volume-based stress increases and result in forced cardiac adaptation [11, 12]. In the older population, pathological cardiac hypertrophy is often secondary to the development of other cardiovascular diseases (CVDs) and comorbidities that increase in prevalence with age [13, 14]. It is characterized by increased LV thickness and a functional decline in the heart's contractility and filling capabilities, in part due to excessive fibrosis that stiffens the cardiac muscle [15].

Another contributor to cardiac hypertrophy is the intrinsic aging of the heart that occurs outside of CVDs and other pathological factors. The natural aging of the heart muscle involves structural and functional changes, including LV hypertrophy, that render the heart more susceptible to stress and poor cardiovascular outcomes [10]. The Framingham Heart Study and the Baltimore Longitudinal Study on Aging demonstrated that LV hypertrophy and a decline in diastolic function increases prevalence with aging in healthy individuals without cardiovascular disease (CVD) [16, 17]. Such non-pathologically-induced age-related cardiac hypertrophy has also been noted in rodents and flies [10].

The progression of chronic disease-induced pathological and age-related hypertrophy share many similarities on a mechanistic level [10]. For example, as the heart hypertrophies, there is increased cardiomyocyte death, by necrosis, autophagy, and apoptosis, which contributes to impaired contractility of the muscle and induces maladaptive ventricular remodeling [10, 18]. Another mechanism involved in pathological cardiac hypertrophy is interstitial fibrosis accumulation during extracellular matrix (ECM) remodeling, which increases cardiac stiffness and reduces the heart's impairing the ventricle's filling and contracting capacity [19-21]. Furthermore, this fibroblast over-production of collagen, seen particularly in chronic pathological overload such as a myocardial infarction, disrupts myocardial excitation-contraction coupling [19, 20, 22]. Excitation-contraction coupling is typically modulated by $Ca^{2+}$ molecules, however in a hypertrophic heart, this signaling is impaired by reduced uptake of $Ca^{2+}$ into the sarcoplasmic reticulum [23-25]. Additionally, cardiac hypertrophy increases the tissue's oxygen demand, while simultaneously decreasing perfusion pressure, the gradient that drives left ventricular (LV) coronary perfusion, making it more difficult to supply adequate oxygen to the heart muscle [10, 26]. Finally, while cardiac hypertrophy does stimulate some upregulation of mitochondrial biogenesis, proliferation can rarely match the increasing energy demands, resulting in an energy deficiency [27, 28].

*Physiological Determinants of Adaptive Cardiac Hypertrophy:* While cardiac hypertrophy is common in the elderly due to age-related causative hemodynamic stressors and intrinsic aging of the heart muscle [17], it is not exclusive to the aging process and is not always pathological: increased cardiac demand can also result from excessive aerobic exercise, as noted above, informally referred to as an "athletic heart"

[29, 30]. Exercise-induced and pathological cardiac hypertrophy both result in LV enlargement [11]. However, a key distinction is that mild to moderate hypertrophy induced by aerobic exercise often proves to be a beneficial adaptation that results in enhanced cardiac performance by increasing stroke volume, oxygen consumption with improved relaxation, and contractility [29-31]. An exercise-induced increase in the hemodynamic load causes cardiomyocytes to synthesize new contractile proteins and assemble new sarcomeres, thus expanding the cardiac cells homogenously [12, 32]. The expansion can result in an increased LV chamber, seen in endurance training, or increased heart wall thickness, as for strength training [12].

The molecular differences that determine the maladaptive or beneficial outcomes between pathologically-induced and exercise-induced hypertrophy include protein kinase C, gp130 and G-protein signaling, calcineurin regulation, mitogen-activated protein kinase (MAPK) pathways and more, yet are beyond the central theme of this review [33]. Importantly, cardiac hypertrophy is not always maladaptive (i.e. exercise-induced), and not all cardiac hypertrophy stems from chronic disease (i.e. natural cardiac aging).

*Concentric Versus Eccentric*: All forms of cardiac hypertrophy can be described as concentric or eccentric hypertrophy, or a combination of the two, as determined by the etiology as well as the specific morphological manifestation [12]. Concentric cardiac hypertrophy is characterized by increased wall thickness due to the increasing short-axis diameter of myocytes, and is often a result of pressure overload [34, 35]. Concentric hypertrophy is commonly induced by chronic hypertension, congenital heart disease, or intense strength training [12, 36]. On the other hand, eccentric cardiac hypertrophy is the result of chronic volume overload, as in the case of endurance training, which

characteristically results in myocyte lengthening, producing dilated LV and thinner LV walls [34, 37]. Both forms of hypertrophy result in an increase in LV mass as detected by echocardiography [34]. These hypertrophic alterations can contribute to heart failure, which is associated with higher mortality rates and increased risk of cardiovascular events [38, 39].

## III. Cardiac Hypertrophy and GDF11: Implications in Heart Disease

GDF11 as the "Fountain of Youth"

*Cardiac Hypertrophy Reversal*: Growth Differentiation Factor 11 (GDF11), also known as Bone Morphogenetic Protein 11 (BMP11), is a circulating protein belonging to the transforming growth factor beta (TGF-β) superfamily [40]. It was first implicated as a rejuvenating factor in 2013 when Loffredo et al. demonstrated GDF11's anti-aging effects on cardiac muscle [41]. The team used heterochronic parabiosis to elicit the biological mechanisms underlying cardiac hypertrophy in aging. This technique involved surgically linking the circulatory systems of pairs of living mice of the same gender for four weeks (first females, then males to evaluate sex effect). The test pairs were comprised of one old (23 months) C57B1/6 and one

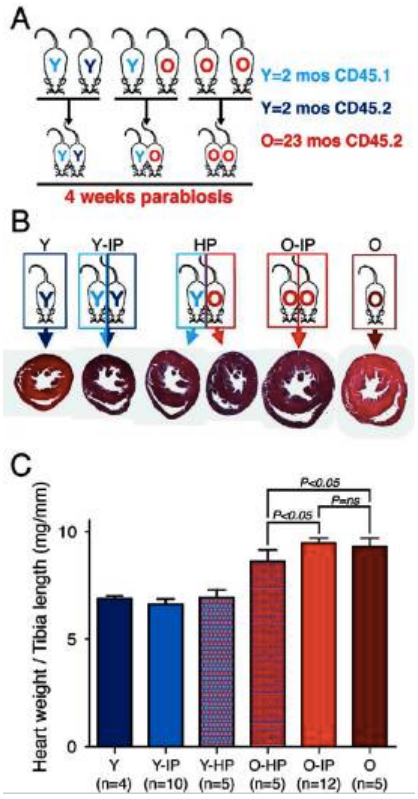


**FIGURE 2.1 - Parabiosis Results.** From Loffredo, et al. 2013. [71]

young (2 months) C57BL/6 mouse forming heterochronic parabiotic (HP) pairs and were compared against isochronic parabiotic (IP) pairs of young-to-young and old-to-old (Figure 2.1). Thus, maintaining the IP pairs allowed for the observed changes to be more specifically related to a blood borne factor as opposed to hemodynamic, behavioral, or surgical effects.

After four weeks, the hearts of the old mice in the HP pairs showed significantly decreased heart size as measured by heart weight to tibial length ratio (HW/TL) and a blinded comparison of short-axis histological sections taken from midventricle [41]. The team used HW/TL because it corrects for body frame variations [42] and has been previously used for older mice [43, 44]. Hypertrophic reversal had important implications on the cellular level as well: aging hearts showed significantly reduced cardiomyocyte cross-sectional area when compared to aging hearts of the IP pairs. Furthermore, Loffredo et al. noted molecular remodeling. The cardiac markers atrial natriuretic peptide (ANP) and brain natriuretic peptide (BNP), which typically increase with cardiac hypertrophy were markedly reduced in the old mice of the HP pairs.

The team used a similar study design to evaluate the effects of blood pressure changes during the intervention, and found it was highly unlikely for hemodynamic effects to be a significant contributing factor to the observed results [41]. Likewise, no significant changes were noted in the young or old IP pairs, further suggesting the effects were due to a rejuvenating factor within the blood. Loffredo et al. performed comprehensive serum and plasma screens to determine the causal blood-borne factor. GDF11 was identified by a broad scale proteomics analysis, an aptamer-based technology, to be the age-reversing agent. Furthermore, the team noted GDF11 is widely

expressed throughout the body, and its expression in the spleens of old mice was reduced compared to that in young mice [45]. Follow-up tests were performed using recombinant GDF11 (rGDF11) both *in vitro* and *in vivo* (0.1 mg/kg), reversing hypertrophy in both instances to the same extent as in the parabiosis portion of the study. In conclusion, Loffredo and colleagues proposed GDF11 is a potent age-regulated blood-borne factor that reverses the effects of age-related cardiac hypertrophy.

*Rejuvenating Effects on Skeletal Muscle*, *Vasculature and Neurogenesis*: One year later in 2014, the same research team from Harvard University garnered further evidence in support of GDF11 acting as a rejuvenating factor in the skeletal muscle, and vasculature and neurogenesis in the brain, enhancing the excitement surrounding the protein [46, 47]. After administering intraperitoneal injections of recombinant GDF11 (rGDF11, 0.1 mg/kg) into aged mice, they found an increased satellite cell frequency and an increase in the percent of satellite cells with intact DNA [46]. No change in satellite cell profile was noted in the young population. Additionally, they injured the tibialis anterior muscle following prior 7 day rGDF11 treatment in aged mice and found a strong rejuvenating effect on the activity of the satellite cells, restoring it to a youthful caliber. Next, they interrogated rGDF11's effect on physical functional and saw an overall improved grip strength and exercise endurance in the treated aged mice.

Other negative and potentially debilitating effects of aging include decline of cognitive function and neurogenesis [48]. The Harvard research team applied a similar approach as the original study- using HP and IP pairs, this time for five weeks, to examine the rejuvenating effects of young blood on these systems [47]. Rejuvenating factors in young blood induced vascular remodeling, which resulted in increased

neurogenesis and improved vascular discrimination in aged mice. Furthermore, GDF11 in isolation as provided *in vivo* as rGDF11 treatments (0.1 mg/kg mouse body weight), enhanced neurogenesis and benefit cerebral vasculature in aging mice, though not to the same extent as the parabiosis old HP mice. Finally, rGDF11 treatments *in vitro* (40 ng/ml) confirmed its direct and beneficial effect on capillary endothelial cells via the p-SMAD pathway.

Summary of Early Rejuvenating GDF11 Literature

Evidence thus far supports GDF11 as a potent anti-aging circulatory protein. In three different studies, rGDF11 injections in aged mice showed reversal of age-related cardiac hypertrophy, skeletal muscle enhancement, and vasculature and neurogenesis improvement, respectively [41, 46, 47]. All three studies primarily used C57Bl/6 ($CD45.1^{-}CD45.2^{+}$) or young B6.SJL ($CD45.1^{+}CD45.2^{-}$) mice from the Jackson Laboratory (JAX) or the Institute on Aging (NIA), which are inbred strains and, thus, approximately 99% homozygous at all genetic loci. Additionally, the above groundbreaking experiments quantified GDF11 levels in the mice- whether to detect directionality in age or confirm the effectiveness of rGDF11 injections- by using a proteomic aptamer-based quantification method [41, 46]. Loffredo and his team used SomaLogic Inc.'s (Boulder, CO) proteomics discovery platform, SOMAscan™, and SOMAmers (Slow Off-rate Modified Aptamers) to bind to the target protein, GDF11, in the plasma [41]. Sinha et al. also quantified GDF11 from the plasma [46] using an enzyme-linked immunosorbent assay (ELISA) kit (specifically TGF-β1 Immunoassay Quantikine® ELISA Catalog # MB100B and Myostatin Immunoassay Quantikine® ELISA Catalog) followed by Western blotting for their quantification method. It is

unclear what quantification method the vascular and neurogenic study used from the publication, however since it was conducted by roughly the same team, it is likely that they used the same method as one of the above [47].

## IV. Recent Controversy

GDF11: Protective, Harmful, or Irrelevant?

After these studies, however, the story of the "miraculous" anti-aging protein became more doubtful as subsequent publications offered conflicting results [40]. The directionality throughout aging was called into question and is still largely debated, so too is GDF11's effect on age-related cardiac hypertrophy. rGDF11 has been explored as a treatment and prevention for cardiac incidents and as a predictor of mammalian lifespan, but also with uncertain results. There were a variety of publications on GDF11's effect on different organ systems and diseases, but for the purpose of this review, the studies analyzed will be those with relevance to GDF11's role in cardiac muscle and heart disease, specifically.

GDF11's Directionality Throughout the Lifespan

*Antibody Quantification*: Loffredo concluded that rGDF11 has a rejuvenating effect in part because GDF11 naturally declines with age [41], however, Egerman et al. challenged this conclusion by demonstrating that GDF11 and myostatin (Mstn), a closely-related protein also within the TGF-β superfamily, instead *increase* with age [49]. His team developed an immunoassay to detect and quantify the GDF11 in both human and rat sera, stating the prior reagents used were not specific enough to distinguish and

accurately quantify the proteins. In fact, they tested the SOMAmer technology and antibody used in the Loffredo and Sinha studies and found that they did cross-react with Mstn [49]. Smith et al. later corroborated these results, adding that the anti-GDF11 antibody used by Loffredo and Sinha could not detect non-reduced forms of GDF11 or Mstn [50]. Western blot analysis revealed the combination of Mstn and GDF11 also increased in mouse sera [50]. The following year in 2016, Chen and colleagues complimented Egerman's study by following the same ELISA protocol to quantify serum GDF11 levels in a population of 169 healthy postmenopausal women aged 47-78 randomly selected from Changsha, China [51]. They also found an increase in GDF11 concentrations with age in this human population. Zhang et al. also used ELISA kits to measure serum GDF11 levels in humans and mice, both with osteoporosis [52]. GDF11 concentrations were markedly reduced in old human and mice participants compared to young humans and mice, respectively. However, it is unclear whether the scientists measured plasma or serum levels due to their interchangeable use of the words throughout the report. Additionally, GDF11 mRNA levels in the bone marrow of old mice were significantly less than that of young mice. In 2018, Liu et al. turned their attention to the potential effects of GDF11 as a therapeutic agent in the liver while also assessing the age-related directionality of GDF11 [53]. Specifically, the team investigated GDF11 in the context of hepatocellular injury and liver regeneration after an induced liver ischemia reperfusion injury (IRI) in both young and old mice. They used immunoblotting techniques to show that serum GDF11 increases with age as well as after IRI. Additionally, hepatic GDF11 protein expression levels increases with age.

Conversely, in 2016, Ahn and colleagues used a similar ELISA based kit (MyBioSource, San Diego, CA) to quantify GDF11 levels in the serum of 69 small breed dogs aged 7 and 17 years old [54]. They reported no significant association between age and circulating serum GDF11 levels. Similarly, in 2017, Yang et al. used an ELISA kit to evaluate GDF11 levels in the plasma of 51 healthy Chinese subjects and 41 elderly Chinese patients with varying degrees of age-related cognitive decline [55]. Unlike the aforementioned study [54], Yang et al. analyzed GDF11 levels in the plasma as opposed to serum [55]. They also reported no concentration directionality associated with age in a healthy Chinese population, which reflects the results of a larger study conducted on Chinese adults with metabolic syndrome (N = 381) that quantified serum GDF11 by ELISA [56]. However, a notable limitation of both studies are that the study subjects were all male subjects [55, 56]. Additionally, Kalampouka et al. used an ELISA kit from R&D (Minneapolis, MN) to measure plasma GDF11 concentrations in 12 healthy male adults (6 young, 6 old), and found no significant change with age [57]. However, the small sample size was a limiting factor.

A couple studies among the controversy did support the initial age-related decline reported by Loffredo et al. [41]. Tian et al. analyzed the effects of not only aging, but also diabetes mellitus (DM), and antiplatelet drugs on GDF11 concentration and found that GDF11 declines with age [58]. They measured GDF11 in the plasma of adult humans with an ELISA kit from Ray Biotech (Peachtree Corners, GA). Likewise, Añón-Hidalgo et al. examined the effects of age and type 2 DM, as well as obesity on circulating GDF11 levels and documented an age-related decline [59]. They also used an ELISA kit,

however unlike Tian et al., the Añón-Hidalgo team's kit was from BlueGene Biotech (Shanghai, China) and was used to measure serum levels.

*Combined GDF11/8 Quantification*: Egerman et al. had reported an increase in GDF11 and Mstn levels throughout aging based on two distinct Western analysis bands, one at ≈12.5 kDa and the other at ≈25 kDa [49]. The ≈25 kDa chain showed a sharp increase with age and was declared to be GDF11. Much of the original members of Loffredo's research team [41] under the leadership of Poggioli, challenged Egerman's conclusions stating the ≈25 kDa band thought to be GDF11 was instead immunoglobulin (IgG) light chain [60]. This hypothesis was initially formed on the basis that IgG light chain has the molecular weight of ≈25 kDa and increases with age in C57BL/6 mice [61]. They garnered evidence for their claim by demonstrating a great abundance of the ≈25 kDa protein in the serum and a failure of the band to migrate at ≈12.5 kDA under reducing conditions as GDF11 should. They used liquid chromatography-mass spectrometry/mass spectrometry (LC-MS/MS) to confirm that IgG light chain was the protein responsible for the ≈25 kDa band. Additionally, they performed the same Western quantitative analysis on sera from recombinase activating gene 1 (*Rag1*) knockout mice, which are unable to produce immunoglobulin. As they expected, the ≈25 kDa band was absent. Using the same anti-GDF11 antibody as Egerman, Poggioli and his team quantified circulating combined serum GDF11/8 levels by Western Blot in mice, rats, horses, and sheep at various ages. They found the band corresponding to the reduced GDF11/8 monomer to significantly decrease with age. Furthermore, the *Gdf11* gene expression declined in various mouse tissues, but not in skeletal muscle. Finally, Walker

et al. from Poggioli's research team noted Egerman's immunoassay rat and human sample sizes were not large enough to yield results with sufficient statistical power [62].

Shortly after Egerman's publication was released in 2015, Oxford Journals released a study by Olson and his team entitled "Association of growth differentiation factor 11/8, putative anti-ageing factor, with cardiovascular outcomes and overall mortality in humans: analysis of the Heart and Soul and HUNT3 cohorts" [63]. As the name aptly implies, the research team analyzed associations between cardiovascular measures/outcomes, such as LV hypertrophy, and the combination of GDF11 and Mstn in human plasma. While measuring the proteins in combination reflected the strategy demonstrated in Poggioli's study, Olson et al. quantified the protein levels by using using the aptamer-based proteomic platform, SOMAscan™ like the Loffredo and Sinha research groups [41, 46]. Higher combination GDF11/8 levels were found to belong to younger participants [63]. The contributing proportions of each protein were not elicited, so the results neither add nor to subtract from prior arguments.

Rodgers and Eldridge published a critique of ELISA kits, reporting high cross-reactivity among the homologous proteins [64]. Instead they determined circulating Mstn levels decrease with age and, using *Mstn* knockout mice, GDF11 was detected in such comparatively low concentrations, it was deemed physiologically irrelevant. However, LC-MS/MS quantification methods in subsequent studies detected substantially higher concentrations than immunoassay results indicate as detailed below [65] and reflect that the potency of a hormone may not be accurately reflected by its circulating concentration, anyway.

*Mass Spectrometry Technique*: Due to the dense controversy surrounding antibody detection methods, Schafer et al. leveraged an immunoplexed LC-MS/MS quantification method to more reliably distinguish between the two proteins in the plasma of healthy men and women 20 to over 80 years of age [66]. Furthermore, they applied the technique to draw associations between clinical phenotypes and circulating levels, which will be discussed in a later section. The detection method involved immunoaffinity purification using antibodies prior to LC-MS/MS. Schafer and colleagues reported GDF11 did not change with age. Mstn decreased in men, but no significant change as a factor of aging was noted in women. This reported behavior of Mstn could provide an explanation as to why Olson et al. found both proteins to decline when measured together: it may not be that GDF11 is declining, but only that Mstn in males is declining enough to show significance [63]. For all its merits, the study offered its limitations such as being unable to distinguish between latent and mature GDF11 and Mstn as bound versus unbound GDF11 and Mstn.

In 2019, Semba et al. overcame the above limitations by use of a similar quantification method with unique advantages. They utilized antibody-free immunoaffinity-selected reaction monitoring (SRM) in combination with LC-MS/MS to examine the relationship of GDF11, Mstn, and their inhibitors, with age and skeletal muscle strength in healthy adult humans [67]. They distinctly quantified six inhibiting proteins including Mstn and GDF11 prodomains. Inhibitors bind to and alter the biological performance of Mstn and GDF11, and could prevent epitopes, recognized by antibodies, from binding, leading to an underestimation of circulating protein levels.

Thus, using anti-body free detection method such as LC-MS/MS allowed the team to include the inhibited Mstn and GDF11 in the analysis.

Semba et al. quantified plasma protein levels in 160 healthy American adults, 80 men and 80 women, ages 22-93 years old [67]. The Mstn mature protein and GDF11 mature protein were not significantly correlated with age, although GDF11 did increase with age insignificantly, and the GDF11 prodomain showed a positive correlation with age ($p = 0.001$). As they expected, they detected higher plasma protein levels than those reported with immunoassays and immunoaffinity-SRM assays due to the inhibitors' effect. Such results add evidence to the conclusion that slight to no GDF11 and GDF8 associations with age exist in adult humans [66]. Additionally, they suggest the concentrations of GDF8 and GDF11 antagonists, which did show significant changes with age, could have greatly influenced prior anti-body based detection methods.

Camparini and his team built upon the present technique by developing a parallel reaction monitoring (PRM) LC-MS/MS assay with immune precipitation (IP) to detect and distinguish between Mstn and GDF11 using stable isotope-labeled (SIL) peptides in C57Bl/6 mice [68]. Their highly specific and novel quantification method was not to debunk a prior LC-MS/MS study's findings, but rather to add to the growing body of evidence of non-antibody-based techniques. Analysis of six young female mice and six old female mice revealed serum levels of both GDF11 and Mstn decline with age. The study supported Loffredo's original conclusion of age-related decline [41] but did so with innovative methods that could reliably distinguish between the two proteins. However, the small sample size must be noted as a limitation of the study.

*Gene Expression:* In the 2015 study conducted by Egerman et al., RNA-seq on skeletal muscle from rats at various ages was performed in addition to sera immunobody methods [49]. Interestingly, GDF11 expression dramatically increased with age, while Mstn expression decreased with age, as confirmed by qPCR. Poggioli et al. also examined GDF11 expression as an additional feature of their study, quantifying it in the spleen, kidney and quadriceps muscles in young (2 months) and old (24 months) mice [60]. Spleens and kidneys of old mice showed significant reduction in gene expression, whereas there was no difference in skeletal muscle gene expression between young and old mice.

GDF11 expression was again measured in 2016, when Du and his team set out to determine GDF11's association with not only age but also myocardial regeneration after ischemia reperfusion injury [69]. GDF11 mRNA in the myocardium of 3-month-old mice was compared to that of 21-month-old mice by RT-PCR analysis. They concluded GDF11 expression decreases with age as well as after myocardial injury.

Factors Contributing to Controversy

*Controversy Largely Due to Structural Similarity of Myostatin*: Many factors contribute to the pervasive controversy throughout the GDF11 literature, but perhaps the most confusion is caused by GDF11's similarity to Mstn [40]. Mstn, also known as GDF8, is a closely related protein within the TGF-β superfamily and also a circulating blood-borne factor [62, 70]. The two proteins are highly homogenous: they share roughly 90% of their amino acid sequence in their mature domains, differing by only 11 residues [40, 71-73]. Additionally GDF11 and GDF8 bind the same receptors (ACVR1B/ALK4, ACVR1A/ALK5 and ACVR1C/ALK7) [46, 74, 75], though GDF11 does so with a

stronger affinity [72], and both can activate the Smad 2/3 intracellular pathway [76-81]. Follistatin acts as an inhibitor to many members of the TGF-β family, including both GDF11 and Mstn [82], but the mature forms of both proteins are also inhibited by the more selective GASP1 and GASP2 proteins [83, 84]. Similar to other TGF-β superfamily members, GDF11 and Mstn are both synthesized as precursor proteins and must be proteolytically processed to form active carboxy-terminal dimers [76, 84]. Suh and Lee analyzed the evolutionarily constrained regions (ECRs) of both proteins via the webtool Aminode [85] and determined the mature domains of each were, unsurprisingly, highly conserved among vertebrate species [84]. However, only the pro-domain of GDF11 showed high sequence conservation highlighting the functional significance of this region. This finding is particularly interesting since the pro-domains of GDF8 and GDF11 share only 45% amino acid sequence identity, which suggest the variation in this region contributes to differing functions of each protein [84].

The literature has shown that despite their close relation, GDF11 and Mstn play distinct and often dissimilar roles in the body [84]. GDF11 is widely expressed and its roles in development and in homeostasis are varied [70, 86, 87]. Sinha et al. proposed findings supporting its regenerative effect on muscle including improved exercise endurance *in vivo*. Additionally, they demonstrated *in vitro*, rGDF11 can increase aged satellite cell proliferation and differentiation, while recombinant Mstn had no effect [46]. Mstn is primarily expressed in skeletal muscle and acts as a potent muscle growth suppressor [70, 76]. Additionally, the genetic deletion of *Mstn* causes hypertrophy in skeletal muscle [88-90], whereas the deletion of *Gdf11* leads to abnormal organ development and skeletal patterning [91]. Teasing apart their respective endogenous

effects by embryonic deletion is complicated by the fact that *Gdf11*-null mice, but not *Mstn*-null, show perinatal lethality [91]. GDF11's broad, though uncertain, roles in the heart also set it apart from Mstn and will be discussed presently.

*Insufficient Specificity of Quantification Methods:* Various techniques and anti-body based kits have been used to quantify GDF11 and Mstn (whether together or separately) in humans, rats, mice, and dogs [64] (Table 2.1). The initial anti-body based methods proved to be insufficiently specific to distinguish between the two homologs [92], and since Mstn is found in nearly 500 fold the concentration of GDF11, combined measures tell us little about the age-dependent nature of GDF11 alone [64].

*Variables Among Models Used:* Beyond the quantification method used, the experimental models may further complicate the pool of evidence. Participants of various health statuses provided unique information but did not contribute to a non-diseased baseline measurement of GDF11 concentrations [62]. Likewise, gender of study subject seemed to impact results and the literature on each male, female, and combined contributes to mixed results [68]. Other considerations in regard to factors contributing to the age-dependent controversy include the dose and quality of rGDF11 administered [14], statistical power (i.e. sample size), and genetic influence [55]. Zhou et al. in 2016, demonstrated 74.52% of the variation seen in circulating levels of GDF11 in different strains of mice was due to genetic background or strain used [93].

*Blood Component Discrepancy:* Furthermore, there may be distinctions between GDF11 levels within different blood components (i.e. plasma versus serum) [55]. Bueno et al. quantified GDF11 levels in each the serum, plasma, and platelet lysate from 23 adult volunteers [94]. They concluded GDF11 concentrations in the serum were higher

than in the plasma, and an age-related increase was seen in the serum only with no age-association to plasma GDF11 levels. Platelet GDF11 is over 10 times more concentrated than in serum or plasma indicating that GDF11 is perhaps stored in platelets [94]. The higher level in serum could be attributed to GDF11 being released from platelets similarly to how it has been described for other platelet-contained factors [95]. The excitement surrounding the study however is tempered with a small sample size and use of an ELISA kit for quantification, which has been noted to cross-react with Mstn [92].

**TABLE 2.1 - Directionality of GDF11 Levels with Age.** Adapted from Egerman, M.A. & Glass, D.J. [92]. Species is denoted by M for mouse, H for human, R for rat, Ho for horse, or D for dog. The method used to quantify GDF11 in each study is named in short in the far right column.

| GDF11 Level with Age | Study | Date | Blood Component | Species | Quantifying Method |
|---|---|---|---|---|---|
| Decreases | Loffredo et al. [41] | 2013 | Plasma | M | SOMAmer; Immunoblotting |
| | Zhang et al. [52] | 2015 | Serum | M, H | ELISA |
| | Du et al. [69] | 2016 | Gene Expression | M | |
| | Tian et al. [58] | 2018 | Plasma | H | ELISA |
| | Añón-Hidalgo et al. [59] | 2019 | Serum | H | ELISA |
| | Camparini et al. [68] | 2020 | Serum | M | PRM LC-MS/MS with IP |
| GDF11/GDF8 Decreases | Olson et al. [63] | 2015 | Plasma | H | SOMAmer |
| | Poggioli et al. [60] | 2016 | Serum | M, R, Ho, S | ELISA |
| | Bueno et al. [94] | 2016 | Serum/Plasma | H | ELISA |
| Increase | Chen et al. [51] | 2016 | Serum | H | ELISA (In-House) |
| | Egerman et al. [49] | 2015 | Serum | M, R, H | ELISA (In-House) |
| | Liu et al. [53] | 2018 | Serum | M | Immunoblotting |

| | | | | | |
|---|---|---|---|---|---|
| No Change | Schafer et al. [66] | 2016 | Serum | H | Immunoplexed LC-MS/MS |
| | Ahn et al. [54] | 2016 | Serum | D | ELISA |
| | Yang et al. [55] | 2017 | Plasma | H | ELISA |
| | Kalampouka et al. [57] | 2018 | Plasma | H | ELISA |
| | Semba et al. [67] | 2018 | Plasma | H | SRM assay LC-MS/MS |
| | Xu et al. [56] | 2020 | Serum | H | ELISA |

GDF11 and Cardiac Hypertrophy

*GDF11 Reverses Age-Related Cardiac Hypertrophy*: As outlined above, Loffredo et al. began the discussion of GDF11 as an age-reversing agent particularly in the context of age-related cardiac hypertrophy in 2013 [41]. Aged partners of the heterochronic (O-HP) pairs demonstrated notably smaller hearts than their old IP counterparts as measured histologically by left ventricular wall thickness after 4 weeks. HW/TL was also significantly lower in O-HP mice than the control, as was cardiomyocyte size. The experiment was run on both sexes individually with the same results. Next, the Loffredo team tested GDF11's anti-hypertrophic effects *in vitro* by treating neonatal cardiomyocytes with three different concentrations of rGDF11 or Mstn for 24 hours. Interestingly, cells treated by GDF11 exhibited activation of TGF-β as evidenced by increased pSMAD2 and pSMAD3 as well as suppression of Forkhead transcription factor phosphorylation leading the authors to conclude GDF11 has a direct rejuvenating effect at the cell level. Cells simultaneously treated with Mstn also stimulated TGF- β signaling pathways, however it did not lead to a dose-dependent inhibition of phenylephrine-mediated hypertrophy in the cardiomyocytes.The results thus far were sufficient to prompt a third randomized and blinded trial, this time examining the effects of rGDF11

(0.1 mg/Kg) *in vivo* [41]. They determined GDF11 levels at this dose remained elevated in the plasma for 24 hours following injection. rGDF11 treatments were administered daily for 30 days to old (23-month-old) C57Bl/6 female mice. As mentioned above, HW/TL ratio and cardiomyocyte size were significantly reduced compared to the saline-injected control group. They did not report changes in body weight.

In 2016, the same research group under the direction of Poggioli followed up their initial study by demonstrating the antihypertrophic effects of rGDF11 in both young (2 months) and old (22 months) mice in a dose-dependent manner [60]. The prior study administered 0.1 mg/kg for 28 days, whereas Poggioli et al. reported significant decreases in cardiomyocyte cross-sectional area and HW/TL at 0.5 and 1.0 mg/kg per day of rGDF11 for 9 days. Interestingly, they reported body weight reduction for both age groups, though only significant in older mice. Furthermore, a single dose of rGDF11 *in vivo* (1 mg/kg) activated SMAD2 and SMAD3 signaling in the myocardium one hour following injection. In 2018, Duran et al. complimented these findings with their own investigation of GDF11's effects on neonatal rat cardiomyocytes [96]. GDF11 induced $Ca^{2+}$ increases in the cells and increased the phosphorylation levels as well as the luciferase activity of Smad2/3 in a dose-dependent manner. Furthermore, pre-treatment of GDF11 blunted the hypertrophic response of the cells when exposed to two different hypertrophy-inducing stimulants. Duran and colleagues concluded that GDF11 utilizes $Ca^{2+}$ signaling and utilizes the Smad2/3 pathway to prevent cardiomyocyte hypertrophy *in vitro*.

Also in 2018, Zhang et al. investigated the effects of GDF11 on Angiotensin II (ANG II)-induced cardiac hypertrophy in mice tissue and in cardiomyocytes in culture

[97]. They also examined differences in expression markers for volume overload such as BNP, ANP, and beta-MHC, similarly to Loffredo et al. [41]. Favorable *in vivo* and *in vitro* results led the authors to declare GDF11 attenuates ANG II-induced cardiac hypertrophy and expression of overload markers by downregulating C-C motif chemokine 11 (CCL11) [97].

*GDF11 Improves CVD and Cardiac Injury Outcomes:* Various studies also evaluated GDF11's protective effect against specific cardiovascular diseases and injuries, such as ischemic cardiac injury, myocardial infarction (MI), and ischemic reperfusion injury (IRI). Ischemic cardiac injury is the cardiomyocyte cell death and consequent tissue damage caused by partial or complete blockage of the heart's arteries, as in the case of a heart attack or MI [98]. MI can result from constriction of the blood vessel from plaque buildup or a blood clot and may be life-threatening. Ischemic cardiac injury is the primary contributor to heart failure [69]. IRI is the cell dysfunction and death following the restoration of blood flow to the tissue after an MI event [99]. The magnitude of the IRI is typically reflective of the duration and extent of the ischemia [100].

Du et al. examined the association of endogenous GDF11 expression levels of mice with MI and IRI as well as the impact of exogenous GDF11 following such events [69]. Myocardial GDF11 mRNA levels were measured prior to cardiovascular injury and compared against expression following injury. They found that just three days following IRI, GDF11 expression levels significantly increase in both young and old mice [69]. However, the mice in the MI group demonstrated an age-dependent GDF11 expression response following injury. Endogenously expressed GDF11 mRNA increased in the injury border zone of young mice, yet decreased in the same region of old mice seven

days after the injury, leading the team to suggest GDF11 may play a role in ischemic remodeling. Such findings mirrored those of a similar study by Hudobenko et al. in which GDF11 levels significantly declined following an ischemic stroke in aged mice [101]. Next, Du et al. analyzed the effects of exogenous GDF11 administration on the heart particularly following MI. Instead of intraperitoneal injections of rGDF11 like prior studies [41, 60], Du et al. employed targeted yet non-invasive tissue-specific GDF11 gene delivery to the heart [69]. Ultrasound-targeted microbubble destruction (UTMD)-mediated GDF11 plasmid delivery resulted in improved cardiac function, increased angiogenesis, and decreased infarct size in old mice following ischemia reperfusion injury [69]. Du et al. declared GDF11 useful in treatment following myocardial injury.

In 2019, Su et al. reported preventative benefits of exogenous GDF11 delivered prior to acute IRI [102]. The team injected 24 Sprague-Dawley rats with rGDF11 prior to inducing IRI. GDF11-treated rats showed reduced arrhythmia severity and were more successful in attenuating MI. GDF11 also decreased oxidative damage, generally increased cardiac function, and protected the heart from severe reperfusion damage following IRI.

The cardioprotective effects of GDF11 were supported by Olson et al. in their analysis of the Heart and Soul and HUNT3 participants [63]. In this human study, combined GDF11/8 levels were measured using SOMAmer technology and were found to be associated with lower risk of cardiovascular events and death. Specifically, LV hypertrophy was less common in the participants of the highest quartile of GDF11/8 compared to those in the lowest quartile. Additionally, highest quartile participants had lower risk of hospitalization due to heart failure, stroke, and MI after multivariant

adjustment. However, the lack of differentiation between the two proteins made it impossible to imply which protein was responsible for the cardiovascular traits. Additionally, GDF11 and GDF8 could have a synergistic or antagonistic effect on one another with one protein's function outperforming the other.

*GDF11 Does Not Rescue Age-Related Cardiac Hypertrophy:* Mounting literature simultaneously emerged debunking the rejuvenating claims of GDF11. Smith et al. replicated the rGDF11 administration portion of Loffredo's ground-breaking study [41] and were able to achieve elevated levels of rGDF11 in the blood, however the effects reported were nearly the exact opposite [50]. After 28 days of treatment, Smith found no significant differences in heart weight nor body weight. Cardiac structure (including cardiomyocyte cross-sectional area, internal ventricle dimension, and septal wall thickness) and function (i.e. ejection fraction) were not significantly different between the treated mice and control. *In vitro*, GDF11 actually had a hypertrophic effect on neonatal rat ventricular myocytes.

Although Loffredo and Smith's conclusions could not be more opposite, their reported HW/TL measures were very similar [103]. Smith reinterpreted Loffredo's data to find that his mice dropped significant overall body mass, thus HW/TL ratios gave the appearance of only the heart reducing size [41]. In a healthy aging population, heart weight naturally increases with body weight, thus Smith and colleagues concluded HW/TL is incapable of distinguishing between pathological hypertrophy and physiological growth in adult animals, as tibia length does not continue growing [50]. So, what Loffredo was likely reporting was the normal heart mass increase seen with whole-

body growth in aging as opposed to disproportionate pathological cardiac hypertrophy induced by chronic hypertension, MI, genetic defects, or other health impairments [104].

In support of Smith's conclusion, in 2018 Jin et al. also found that gene delivery of GDF11 reduced heart size in mice, but not when normalized to similarly reduced body weight [105]. Harper et al. suggests more indicative measures of pathological cardiac hypertrophy include increased HW/BW, decreased cardiomyocyte number attributable to cell death, increased cardiomyocyte size, and increased fibrosis [104, 106, 107]. Rodgers and Eldridge proposed that GDF11 and Mstn should share similar actions due to ligand homology and mutual affinities for ActRIIB receptors [64]. This rationale is counter to the rejuvenating and anti-hypertrophic reports recently circulated regarding GDF11's role in the adult heart.

*GDF11 Does Not Improve CVD and Cardiac Injury Outcomes:* In 2016, Schafer et al. conducted a similar experiment to Olson and colleagues, comparing GDF11 and Mstn levels to cardiovascular disease and outcomes in a human population [63, 66]. However, unlike Olson, Schafer and team used a highly specific LC-MS/MS assay to distinguish between GDF11 and Mstn, and evaluate effects on health outcomes accordingly. In their study sample of 41 women and 55 men aged 65-94, plasma GDF11 levels were not correlated with hypertension or hyperlipidemia prevalence. Additionally, GDF11 was positively associated with a diabetes diagnosis and previous cardiac conditions, particularly with previous coronary artery bypass, as well as high risk categorization before surgery. No differences in aortic stenosis severity or related cardiac dysfunction (measured by aortic valve velocity, valve area and index, LV mass, mean gradient, and ejection fraction) were related to GDF11 levels. Mstn was also not

correlated with hypertension or hyperlipidemia prevalence, nor did significant associations arise with comorbid conditions.

Ahn et al. used an ELISA kit to examine serum GDF11 levels from dogs at different stages of chronic mitral valve insufficiency (CMVI), which is characterized by myxomatous mitral valvular degeneration and subsequent regurgitation, and is the most common cardiac disease in dogs [54]. They hypothesized circulating GDF11 levels may be lower in subjects with advanced CMVI-related heart failure, further contributing to disease progression, based off past reports [41]. However, Ahn et al. reported no associations of GDF11 with echocardiographic variables of heart function or the severity of CMVI-associated heart failure, and thus determined GDF11 would not make an adequate biomarker or therapeutic agent [54].

Beyond passive associations between GDF11 and cardiovascular disease measures, Zhang et al. in 2019 examined the effects of GDF11 as a direct treatment following isoproterenol (ISO)-induced heart failure in rats [108]. Although plasma GDF11 levels were unchanged, both GDF11 mRNA expression and GDF11 protein significantly increased in heart tissue following ISO-induced injury *in vivo*. Next, to examine the potential role of a local GDF11 increase, rGDF11 or endogenous GDF11 knockdown effects were observed in ISO-treated H9C2 cells in culture. Interestingly, rGDF11 treatment resulted in decreased cell proliferation, increased reactive oxygen species levels, and worsening cellular apoptosis, while GDF11 knockdown cells showed the opposite. Thus, the authors concluded GDF11 worsened ISO-induced heart failure. Similarly, in 2018, Xiufeng et al. observed that genetic deletion of GDF11 in rat endothelial cells attenuated right ventricular hypertrophy of the heart [109] and

Akhmedov et al. reported GDF11 injections increased sensitivity of the heart to myocardial infarction in mice [110].

*GDF11 Contributes to Bodily Wasting and Frailty:* A strong predictor in humans of poor-postoperative outcomes is frailty [66], often defined using Cardiovascular Health Study (CHS) criteria: unintentional weight loss, reduced endurance, grip strength, gait speed, and physical activity [111]. In addition to associations with adverse health outcomes, diabetes, and higher prevalence of CVD, Schafer et al. noted individuals with higher GDF11 levels were more likely to be frail according to the CHS criteria [66].

Although Harper et al. reported GDF11 treatment reduces pressure overload-induced pathological cardiac hypertrophy and associated fibrosis, they also noted high doses caused severe cachexia and wasting in mice [112]. The highest dose tested (0.5 mg/kg) resulted in dramatic weight loss, lethargy, and even death. Thus, GDF11 used as a therapeutic agent may have devastating effects if the dose is not precise to age and body mass.

Similarly, other *in vivo* studies examining the effects of GDF11 administration in mice reported induced wasting as well as cardiac and skeletal muscle dysfunction [113-115]. In 2017, Zimmers et al. evaluated the effects of exogenous GDF11 on various muscle types in 10-week old mice [113]. They found whole body wasting and skeletal muscle loss, similar to what might be expected following treatment with Mstn. While they did note decreased LV muscle wall thickness and decreased cardiomyocyte cross-sectional area after only 14 days of injection in the heart, they also reported declined cardiac function in the treated mice suggesting a cachexic effect of GDF11 rather than therapeutic.

Likewise, Roh et al. analyzed FSTL3 levels in a human cohort and reported a positive association with age, frailty, and heart failure, suggesting the ActRII pathway activation is a risk factor for impaired cardiac function [116]. Circulating levels of FSTL3 can be used as an indicator of systemic Activin Type II (ActRII) receptor signaling activity, which is a net readout of Mstn, GDF11, and ActivinA stimulation [116]. The team also noted that mice with increased FSTL3 expression demonstrated decreased cardiac function and when signaling activity was blocked by an antibody, cardiac function restoration was observed.

**TABLE 2.2 - Impact of GDF11 on Cardiac Hypertrophy, CVD, and Frailty.** Species is denoted by M for mouse, H for human, R for rat, or D for dog. *Study measured and drew associations with combined GDF11/Mstn levels, so results are not GDF11-specific.

| GDF11 Effect | Study | Date | Model Used | Study Type | Aged Model |
|---|---|---|---|---|---|
| Protected Against/Reversed Cardiac Hypertrophy | Loffredo et al. [41] | 2013 | M | In Vivo/In Vitro | Yes |
| | Poggioli et al. [60] | 2016 | M | In Vivo | Yes |
| | Duran et al. [96] | 2018 | R | In Vitro | No |
| | Zhang et al. [97] | 2018 | M | In Vivo/In Vitro | No |
| Protective/Restorative Effect on CVDs | Olson et al.* [63] | 2015 | H | In Vivo | Yes |
| | Du et al. [69] | 2017 | M | In Vivo | Yes |
| | Su et al. [102] | 2019 | R | In Vivo | No |
| | Hudobenko et al. [101] | 2020 | M | In Vivo | Yes |
| Did Not Reverse/Prevent Cardiac Hypertrophy | Smith et al. [50] | 2015 | M; R | In Vivo/In Vitro | Yes |
| | Jin et al. [117] | 2018 | M | In Vivo | No |

| | | | | | |
|---|---|---|---|---|---|
| Did Not Protect/Treat CVDs | Schafer et al. [66] | 2016 | H | In Vivo | Yes |
| | Ahn et al. [54] | 2016 | D | In Vivo | No |
| | Yu et al. [109] | 2018 | R | In Vivo | No |
| | Akhmedov et al. [110] | 2018 | M | In Vivo | No |
| | Zhang et al. [108] | 2019 | R; H | In Vivo/In Vitro | No |
| Induced Bodily Wasting/Frailty | Schafer et al. [66] | 2016 | H | In Vivo | Yes |
| | Zimmers et al. [113] | 2017 | M | In Vivo | No |
| | Hammers et al. [114] | 2017 | M | In Vivo | No |
| | Harper et al. [112] | 2018 | M | In Vivo | No |
| | Roh et al. [116] | 2019 | H | In Vivo | Yes |

*Pressure Overload-Induced Cardiac Hypertrophy and GDF11:* In the initial study in 2013 by Loffredo et al., the team contrasted the dramatic effects GDF11 had on age-related pathological hypertrophy with hypertrophy induced by transverse aortic constriction (TAC) [41]. Half of the mice received 30 days of rGDF11 treatment (N = 10), while the other half received sham injections (N = 9). Echocardiography was performed 15 days prior to sacrifice, morphometry of the hearts was measured by HW/TL ratio, and cardiomyocyte cross sectional area and percent fibrosis were quantified. There was no significant difference between the two groups, suggesting GDF11's restorative effect is specific to natural age-related hypertrophy, and not in induced pressure-overload hypertrophied heart.

The apparent inconsistency in GDF11's function can be explained in part by the molecular differences between the type of stressor inducing cardiac hypertrophy. Loffredo's results perhaps highlight the differences between age-related hypertrophy and other forms of pathological hypertrophy, which have been noted elsewhere [118]. TAC-, which is used to model pressure-overload, ANG II-, phenylephrine- and testosterone-induced cardiac hypertrophy do not encompass all aspects of the neurological and biochemical cardiac changes involved in aging [10, 16]. Thus results from such studies cannot be used to negate or support GDF11's role in age-related cardiac hypertrophy, specifically.

Harper et al. conducted a dose-specific investigation of rGDF11 on TAC-induced cardiac hypertrophy in mice, similarly to Loffredo et al. [41] and thus comparable [112]. Only at a dose ten fold that of Loffredo's did Harper and team note a significant reduction in pathological hypertrophy. At this dose, systolic function measured by echocardiography improved and dysfunctional ventricular remodeling, particularly ventricular dilation, was reduced. rGDF11 also reduced TAC-induced interstitial cardiac fibrosis. Larger size reduction effects were seen at the highest dose tested (5.0 mg/Kg), however they were accompanied by severe wasting and lethargy.

*Factors Contributing to Controversy:* As seen in Tables 2.1 and 2.2, the GDF11 literature is sparse and inconsistent. Many potential factors contribute to the variable reported effects of GDF11 in cardiac-aging and heart disease. First, a major hurdle in many of the studies was reliably distinguishing between homologous GDF11 and Mstn, as reviewed in the prior section. In many cases this inability could have lead to incorrect measures of exogenous GDF11 used as a therapeutic or inaccurate associations of

endogenous GDF11 with measures of heart disease. Second, results of studies examining the effects of exogenous GDF11 have not been fully reproducible even when using similar dose administrations partly due to the different sources and qualities of rGDF11 [84]. For example, Poggioli et al. pointed out the existence of batch-to-batch concentration variations of rGDF11, which manufacturers confirmed [60]. Third, environmental and genetic influences remain unaddressed. Variation in the C57Bl/6 mice colonies and substrains could impact responses to rGDF11 [103]. Although C57Bl/6 mice are inbred, genetic drift can occur in all mice strains, altering genes [119]. Thus, the use of substrains can impair study replication. Food source, as well as caging and housing environments likely varied among labs and could also impact results.

*GDF11 versus Mstn:* Currently, controversy remains as to whether GDF11 and Mstn's similar roles reflect their mature structural homology, or if the amino acid differences in their prodomains results in the proteins functioning in opposite manners [84]. Some point to their distinct developmental roles as supporting evidence for their sustained divergent roles in adulthood [104]. In the context of skeletal muscle, exogenous Mstn and, at high doses, GDF11 (Table 2.2) appear to induce whole-body wasting [120]. The involvement of Mstn in the mature cardiac muscle is nearly equally as ambiguous as GDF11's [84], further complicating the comparison between the two proteins.

## V. The Discovery, Function, and Regulation of GDF11

GDF11: History and Reported Functions in Development and Beyond

*Discovery and Involvement in Embryonic Development:* In 1999, McPherron et al. used the closely related Myostatin gene (*MSTN*), which they had discovered two years

prior [121], as a probe to be the first to clone both human and mouse GDF11 [91]. Nakashima and colleagues discovered GDF11 expression in the murine embryo by use of RNA template from rat incisor pulps [122]. They found it was expressed as early as 8.5 days after conception with the highest expression levels found in the tail buds. Since then, GDF11 has been determined to serve vital developmental roles in the embryo, particularly in regulating anterior-posterior patterning of the axial skeleton [91], inducing mesoderm and neural tissue [123, 124], regulation of neurogenesis [125], governing pancreatic islet progenitor cell number and maturation [126, 127], and in liver development [128]. In the developing chick, Gamer et al. demonstrated GDF11 serves as a negative regulator of myogenesis and chondrogenesis [129].

*Implications as a Cancer Therapeutic:* Farooq and his team determined that histone deacetylases (HDACs) must inhibit GDF11, an inhibitor of cell proliferation, in order for normal hepatic development to occur in zebrafish [128]. Likewise, Zhang et al. examined the HDAC-GDF11 axis and showed specific classes of HDACs can activate GDF11 to reverse abnormal cell growth, a valuable revelation for the field of oncology research [130]. Subsequent investigations of GDF11's role as a cancer suppressor ensued but with mixed results: some found beneficial protective effects against liver [131] and breast [132] cancer, while others reported deleterious effects in colorectal [133] and oral [134] cancer. GDF11's conflicting relationship with cancer development could be attributed to a number of variables including tissue type, grade of differentiation, and stage and aggressiveness of the cancer [40].

*Roles of GDF11 in the Adult Largely Unknown:* GDF11, also known as Bone Morphogenetic Protein 11 (BMP11), belongs to the transforming growth factor beta

(TGF-β) superfamily [40]. Proteins in this family play important and often overlapping roles in the development of various tissues, particularly in bone and cartilage [135], and in several human pathologies such as cancer, and autoimmune, cardiovascular, and fibrotic diseases [136]. However, GDF11 specifically has few conclusive roles in the adult mammal [127]. Among its suggested associations are its interference with inflammation in part by blocking the TNF-α and subsequently NF-κB and JNK signaling pathways [137-139], its involvement in the homeostasis of bone regulation [92], its actions in metabolism regulation [40], and its effects on the developed heart and skeletal muscle, which have been discussed at length (see sections II and III).

Regulation of GDF11 in Levels in Circulation

*Heritability and Genetic Construct:* Prior calculations conducted by our lab reported high heritability of GDF11 (0.75), however the estimate was likely inflated due to the use of an ELISA kit that failed to distinguish between GDF11 and Mst [93]. Heritability estimates in our present study report modest heritability for GDF11 levels (0.23) and a moderate heritability for Mstn levels (0.57)[1].

The protein-coding *GDF11* gene is highly conserved across vertebrate species [140] and encodes the preproprotein ligand [73, 84, 141]. In the human genome, *GDF11* is located on Chromosome 12 on the forward strand and has two splice variants, 174 orthologs, and 31 paralogs [142]. In mice, the *Gdf11* gene is located on the reverse strand of Chromosome 10 and has one splice variant, 174 orthologs, and 32 paralogs [142].

[1] Starcher AE, Peissig K, Stanton JB, Churchill GA, Cai D, Maxwell JT, Grider A, Love K, Chen S, Coleman A, Strauss E, Pazdro R. A systems approach using Diversity Outbred mice distinguishes the cardiovascular effects and genetics of circulating GDF11 from those of its homolog, myostatin. Submitted to *G3*, June 7, 2021.

Human and mouse GDF11 proteins share 99.5% amino acid sequence identity [123]. The GDF11 protein in mice is processed, transported, and stored similarly to human GDF11.

*Expression, Transcription and Processing:* In humans, GDF11 is widely expressed in all major organs and tissues including the spleen, endometrium, and heart [143, 144]. The spleen and heart express similar levels of GDF11 mRNA; most of GDF11 expression in the spleen is produced in the lymphocytes and macrophages, while fibroblasts are responsible for the majority of expression in the myocardium [127]. The highest expression is in the hippocampal region of the brain and the lowest is in the liver [127]. Recently, Bueno et al. showed high GDF11 expression in platelets [94]. Murine *Gdf11* is likewise expressed in many organs and tissues including the pancreas, kidney, intestine, nervous system, and skeletal muscle [45, 70, 123, 145].

Transcription of *Gdf11* can be inhibited by HDACs, as demonstrated by Farooq et al. mentioned previously [128]. Alternatively, the promoter region can be activated by treatment of the antibiotic trichostatin A (TSA), which blocks HDACs [130]. Following mRNA translation, the GDF11 peptide is cleaved by pro-protein convertase subtilisin/kexin type 5 (PCSK5), forming its non-covalent latent complex that contains an N-terminal inhibitory pro-domain as well as two disulfide-linked carboxyl-terminal active domain, and is released into circulation [146, 147]. Often times the latent complex will be sequestered to the extracellular matrix in proximity to their target cells [148, 149].

*Extracellular Regulation:* The activity state of GDF11 and Mstn in circulation determines their relative bioavailability, and, consequently, projected impact [103]. Mature GDF11 and Mstn, like many members of the TGF- β family, can be inhibited extracellularly by a variety of circulating proteins including follistatin [49, 150],

follistatin-related protein 3 (FSTL3) [151-153], WFIKKN1 [83], WFIKKN2 [83], GDF-associated serum protein-1 (GASP-1) and GASP-2 [62, 87, 150, 154], and the respective prodomains of Mstn [49, 121, 155, 156] and GDF11 [157]. The latent GDF11 and Mstn complexes are cleaved by members of BMP1/Tolloid family of metalloproteinases [86] to release the prodomain and yield the disulfide-linked homodimer active form [73, 84]. Active GDF11 is transported and stored in endosomes, lysosomes, peroxisomes, and lipid droplets, however more information is needed to understand when storage takes place, for how long, and how GDF11 is released [86].

GDF11 Cellular Signaling

*Canonical Signaling:* Like most members of the TGF-β family, GDF11-mediated signaling is Smad-dependent as well as Smad-independent [40, 158, 159] (Figure 2.2). Ligands of the TGF-β family classically bind to serine/threonine kinase receptors, activating intracellular cytoplasmic molecules belonging to the Smad family, known as receptor-Smads (R-Smad) and include Smad2/3 and Smad1/5/8 [86]. R-Smads recruit common Smads (co-Smad, Smad4) which then translocate and accumulate in the nucleus [86]. The complex then regulates expression of its target genes [136, 160, 161]. Smad2/3 is well documented, while only two studies have demonstrated GDF11 activating Smad1/5/8 [86, 162, 163].

*Non-Canonical Signaling:* Alternatively, Smad-independent signaling may also be employed resulting in the activation of MAP kinases (p38, ERK, JNK), small GTP-binding proteins, and phosphatidylinositol-3-kinase/AKT to modulate the downstream cellular response [160, 164-166]. The primary non-canonical pathway GDF11 signals through is likely MAPK; through this pathway, GDF11 can activate AKT, JNK and p38

routes [40, 158, 159] or inhibit activation of JNK or NF-κB, as demonstrated by Su et al. in their investigation of GDF11's effects on IR [102].

*GDF11's Regulatory Roles:* There is little conclusive evidence determining GDF11's regulatory effect on its target genes. Since GDF11 and Mstn signal through identical pathways, resolving the dispute surrounding their distinct roles in the heart may require tissue-specific expression studies to elicit local differences [104]. While GDF11 and Mstn are circulating factors, they appear to also serve as a paracrine signals, modulating function in target cells [127]. The two proteins' primary mode of action (systemic hormones versus local autocrine/paracrine signals) remains uncertain [62].

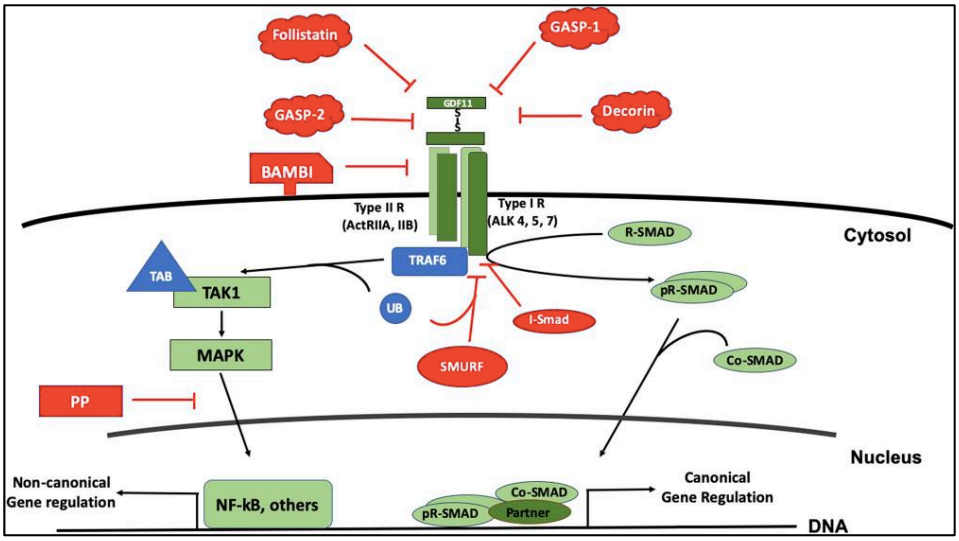


**FIGURE 2.2 - GDF11 Cellular Signaling**. Image from Simoni-Nieves, et al. 2019 [40].

## VI. Conclusion

Current Gaps in the GDF11 Literature

*Reliable Protein Quantification:* Until the present study, no baseline measurement of endogenous GDF11 and Mstn in the serum of a genetically diverse, statistically powerful adult population existed. Using LC-MS/MS quantification method, we reliably

distinguished between the two homologous proteins to compare heart associations side-by-side. Correlative data on various cardiac measures with circulating GDF11 levels provide fundamental insight into the function of this protein in the mature heart without assuming or inducing pathological hypertrophy. Such data is important to set the foundation for future age-related GDF11 studies.

*Genetically Diverse Model:* C57BL/6 (B6) mice are the most commonly used mouse strain in biomedical research due to their predictability and genetic stability as well as their physically activity and frequency of breeding [167]. They also develop an age-related cardiac phenotype that resembles humans [41]. While minimizing genetic variables has its benefits, including study reproducibility, it also has significant drawbacks, such as representing very little of the genetic diversity of the human population, thus reducing the ability to extrapolate results or reflect a wide array of phenotypes caused by genetic heterozygosity [168]. Using a genetically diverse model is vital for high-resolution mapping to elicit genetic regulators of GDF11, which are currently unknown. Thus, we employed the Diversity Outbred (DO; Jackson Laboratory, Bar Harbor, ME) mouse model which is a heterogeneous stock developed by careful randomized outcross breeding of 160 Collaborative Cross (CC) inbred strains and maintained by continued random breeding [169-171] (Figure 2.3). The result is the most genetically diverse mouse resource available, providing a more accurate model of the human population [171]. While inbred models lack natural variation and have blind spots in complex traits, the heterogeneity of the DO displays a wide range of phenotypes and allows for precise genetic mapping [168, 169, 172]. The natural genetic buffering also sustains a robust and well-bred colony [169].

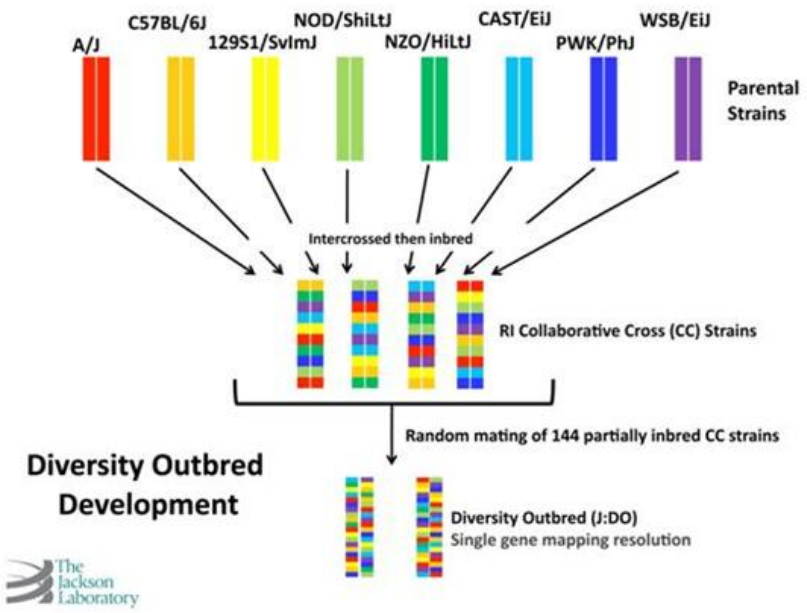


**FIGURE 2.3 - The Diversity Outbred Mouse Model Development.** Image from Lambert, R. 2012 [173]. Eight founder strains are mated to produce the Collaborative Cross (CC) strains, which are randomly mated to develop the Diversity Outbred model.

*GDF11 and Variants as Predictors of Human Heart Disease:* Currently, GDF11's impact on heart failure and, specifically, cardiac hypertrophy remains unresolved. Our present work utilizes various bioinformatic platforms to examine genetic associations of common and rare variants of GDF11 with cardiovascular disease in the human population. Our *in silico* approach analyzes data from thousands of human studies generating highly powered results and eliciting novel connections between our genes of interest and complex human diseases.

Final Summary

GDF11 is a circulatory protein expressed in various tissues throughout the body that activates Smad and non-Smad pathways to regulate gene expression in its target nuclear genes. In recent years, it has been reported to reverse age-related cardiac hypertrophy as well as rejuvenation in the brain, vasculature, and skeletal muscle.

However, GDF11's rejuvenating ability as well as its directionality in age has since been debated. Many factors contribute to the controversy surrounding its effects including its structural similarity to Mstn, a related protein also belonging to the TGF-β superfamily. Further research is needed to elicit genetic regulators of GDF11 as well as establish its role in cardiac hypertrophy as a contributor to heart failure and as an intermediate of other human diseases.

# CHAPTER 3

# A SYSTEMS APPROACH USING DIVERSITY OUTBRED MICE DISTINGUISHES THE CARDIOVASCULAR EFFECTS AND GENETICS OF CIRCULATING GDF11 FROM THOSE OF ITS HOMOLOG, MYOSTATIN[2]

[2] Starcher AE, Peissig K, Stanton JB, Churchill GA, Cai D, Maxwell JT, Grider A, Love K, Chen S, Coleman A, Strauss E, Pazdro R. A systems approach using Diversity Outbred mice distinguishes the cardiovascular effects and genetics of circulating GDF11 from those of its homolog, myostatin. Submitted to *G3*, June 7, 2021.

**Abstract**

Growth differentiation factor 11 (GDF11) is a member of the TGF-β protein family that has been implicated in the development of cardiac hypertrophy. While some studies have suggested that systemic GDF11 protects against cardiomyocyte enlargement and left ventricular wall thickening, there remains uncertainty about the true impact of GDF11 and whether its purported effects are actually attributable to its homolog myostatin. The present study was conducted to resolve the statistical and genetic relationships among GDF11, myostatin, and cardiac hypertrophy in a mouse model of human genetics, the Diversity Outbred (DO) stock. In the DO population, serum GDF11 concentrations positively correlated with cardiomyocyte cross sectional area, while circulating myostatin levels were negatively correlated with body weight, heart weight, and left ventricular wall thickness and mass. Genetic analyses revealed that serum GDF11 concentrations are modestly heritable (0.23) and identified a suggestive peak on murine chromosome 3 in close proximity to the gene *Hey1*, a transcriptional repressor. Bioinformatic analyses located putative binding sites for the Hey1 protein upstream of the *Gdf11* gene in the mouse and human genomes. In contrast, serum myostatin concentrations were more heritable (0.57) than GDF11 concentrations, and mapping identified a significant locus near the gene *FoxO1*, which has binding motifs within the promoter regions of human and mouse myostatin genes. Together, these findings more precisely define the independent cardiovascular effects of GDF11 and myostatin, as well as their distinct regulatory pathways. Hey1 is a compelling candidate for the regulation of GDF11 and will be further evaluated in future studies.

## Introduction

The heart adapts to excessive loading stresses by eccentric or concentric hypertrophy. Eccentric cardiac hypertrophy, a typical response to excessive ventricular preload, is characterized by dilatation of the affected ventricular chamber [12], whereas concentric cardiac hypertrophy, a typical response to excessive ventricular afterload, is associated with increases in cardiomyocyte size and left ventricular wall thickness – features that, while initially adaptive, may ultimately contribute to the development of heart failure [174]. Heart failure is a major public health problem that currently affects 6.5 million Americans [3], roughly 3 million of whom will die within the next five years from related complications [175]. The cumulative prevalence of cardiac hypertrophy and heart failure is projected to increase dramatically in the coming decades, driven by a rapid population increase in those aged 65 and over, the group most profoundly affected by these conditions [176].

In recent years, evidence has shown that age-related cardiac hypertrophy is governed, at least in part, by systemic factors. Using heterochronic parabiosis, Loffredo and colleagues demonstrated that blood from young mice reverses signs of cardiac hypertrophy in aged animals [41], an effect seemingly mediated by the circulating protein growth differentiation factor 11 (GDF11), a member of the transforming growth factor β (TGF-β) superfamily [41, 60]. Circulating GDF11 levels were found to decrease during aging, and restoring GDF11 in aged mice improved histopathological indicators of cardiac hypertrophy, recapitulating the effect of young blood [41]. However, the findings of subsequent studies have called into question the true impact of GDF11 on cardiac

hypertrophy [49, 50, 64, 66, 177], introducing the possibility that GDF11 has a pro-hypertrophic effect, or even no effect at all. Discrepant findings may be attributed in part to methodological limitations of many studies, with the most notable being the use of antibody-based methods that are fundamentally unable to distinguish between GDF11 and its homolog, myostatin [49, 60]. Both proteins belong to the activin/myostatin subclass of the TGF-β superfamily, and these factors share 90% sequence identity within their signaling domains [62, 115]. Their disulfide-linked dimer ligands bind the same ActRIIA, ActRIIB, ALK4, and ALK5 receptors, and induce phosphorylation of SMAD2/3 transcription factors [115]. Though myostatin has an established, anti-hypertrophic effect on muscle [178-181], including a direct regulatory effect on cardiomyocytes [182-185], it still remains unclear whether GDF11 has the same, or distinct, effects on cardiac hypertrophy [50, 115].

The present study was conducted to precisely resolve the relationships among GDF11, myostatin, and cardiac hypertrophy, while simultaneously comparing their genetic architectures to uncover any mechanisms that link them. Circulating GDF11 and myostatin levels were quantified via mass spectrometry to distinguish between these factors in the Diversity Outbred (DO) stock, a translationally relevant model of human genetic diversity, vastly expanding upon previous results gathered using inbred mice. Overall, we discovered unique relationships among GDF11, myostatin, and indicators of cardiac hypertrophy, as well as distinct loci and candidate genes behind each phenotype, and our results point to molecular pathways that will be interrogated in future studies of GDF11 and the heart.

**Materials and Methods**

Animals: Diversity Outbred mice (N=225) were purchased from The Jackson Laboratory (J:DO, JAX stock #009376) [169], and arrived at the University of Georgia at about 5 weeks of age. All animals were housed under conventional conditions in the animal care facilities and received humane care in compliance with the Principles of Laboratory Animal Care formulated by the National Society for Medical Research and the Guide for the Care and Use of Laboratory Animals. The cohort contained an approximately equal number of males and females. Mice were maintained on a 12-hour light-dark cycle and were given *ad libitum* access to water and standard chow (LabDiet, St. Louis, MO, product 5053). Data from eight mice that died or were euthanized before the end of the study due to injuries sustained in fights or other health issues were not included in final histological analyses.

Blood Sampling and Protein Quantification: Blood was collected from the submandibular vein, according to protocols approved by the University of Georgia Animal Care and Use Committee. Serum was isolated and sent to the Brigham Research Assay Core at Brigham and Women's Hospital where GDF11 and myostatin levels were quantified by LC-MS/MS. Briefly, the serum was denatured, reduced, alkylated, and subjected to pH-based fractionation via cation ion exchange SPE, then the elution fraction was digested with trypsin. The concentrated peptide mixture was eluted by liquid chromatography followed by mass spectrometric analysis. Unique proteotypic peptides from GDF11 and

myostatin as well as heavy-labeled unique peptides were used for quantification. Batch effects for GDF11 and myostatin were corrected using the ComBat algorithm.

Echocardiography: Transthoracic chocardiography was performed on DO mice at 16 weeks of age using a VisualSonics Vevo 1100 Imaging System (Toronto, Canada) with a 30-MHz probe. Mice were anesthetized with inhaled 1-2% isoflurane in oxygen and placed in a supine position on a heating platform. M-mode recordings of the left ventricle were obtained from a short-axis view at the level of the mitral valve chordal attachments to the papillary muscles. From these images, measurements from the average of 3-5 consecutive beats were used to calculate the following parameters: interventricular septal thickness at end-diastole and end-systole (IVSd and IVSs, respectively), left ventricular internal diameter at end-diastole and end-systole (LVIDd and LVIDs, respectively) and left ventricular posterior wall thickness at end-diastole and end-systole (LVPWd and LVPWs, respectively). Ejection fraction, fractional shortening, left ventricular mass, and LV volume at end-diastole and end-systole (LVVd and LVVs, respectively) were calculated from these measurements. This procedure was approved by the Institutional Animal Care and Use Committee of the University of Georgia.

Histopathology: At 5-6 months of age, mice were euthanized, and hearts were isolated and fixed in neutral-buffered 10% formalin for 24 hours at room temperature and then paraffin embedded using routine methods. Tissue was serially sectioned and stained using hematoxylin & eosin (for routine histopathologic analysis), Gordon and Sweet's reticulin stain (for determination of cardiomyocyte cross sectional area), and Masson's trichrome

stain (for determination of percent fibrosis). Left ventricular wall thickness, cardiomyocyte cross sectional area, and percent fibrosis were measured using FIJI software (ImageJ).

Genetic Analyses: Tail tips were collected and sent to NEOGEN Genomics (Lincoln, NE) for DNA isolation and genotyping via the Giga Mouse Universal Genotyping Array (GigaMuga) [186], on the Illumina Infinium platform. Genotypes and phenotypic data were imported into the R/qtl2 software for genetic mapping [187]. Genotype probabilities were calculated based on the single nucleotide polymorphism (SNP) genotypes using a hidden Markov Model [188]. Mapping analysis was performed to determine associations between genotype and phenotypes and accounted for kinship using the "leave one chromosome out" (LOCO) method [189]. Statistical significance thresholds were established through permutation tests [190]. For significant quantitative trait locus (QTL) peaks positions, Bayesian credible intervals were calculated to identify the QTL interval. Genes with expression QTL within those intervals were then identified. Genetic mapping results are reported at a genome-wide adjusted family-wise error rate of 0.05, separately for each trait in the mapping analysis. The genome-wide adjustment is a stringent correct for testing multiple markers in the genetic mapping analysis. We did not apply a correction for mapping multiple traits. We mapped a total of 15 traits, but not all traits are independent, as some represent different normalizations of the same underlying data, e.g., heart weight to body weight ratio and heart weight with regression adjustment for body weight.

Bioinformatics was used to illuminate likely binding sites for Hey1 and FoxO1 upstream of their putative target genes. Coordinates of the transcription factors were determined in both the human (hg38) and mouse genome (mm10) through the Integrative Genomics Viewer software (version 2.8.2) [191]. Most likely binding sites were determined by proximity to the promoter region of the gene of interest, determined by Ensembl [192], and by acetylation activity seen through the UCSC Genome Browser (http://genome.ucsc.edu/) using the Human Assembly Dec. 2013 (GRCh38/hg38) and Mouse Assembly Dec. 2011 (GRCm38/mm10) versions for the human and mouse genomes, respectively.

Statistical Analyses: Mass spectrometry data were batch corrected with the Combat algorithm [193] prior to analysis. Pearson correlation coefficient was performed on all anthropometric, histological, echocardiogram, and serum data (after normalizing transformations and batch corrections). Correlations were reported as significant at a p-value of less than 0.05. In Tables 3.1 and 3.2, we report p-values for the evaluation of 48 and 66 correlation statistics, respectively. The tests are not independent because we report results from separate tests for mice of each sex alongside the pooled test results. For simplicity, we report raw p-values without multiple testing adjustments. However, as all test results are presented, it is straightforward to evaluate significance in light of the numbers of test performed.

Data Availability: The DO population is available through The Jackson Laboratory (Bar Harbor, ME; https://www.jax.org/strain/009376). The Reagent Table can be found in the

Supplemental Information on FigShare[3], as can the raw, uncorrected phenotypic data (Table S1), and the GeneSeek data containing the genotypes from each mouse (File S1) as well as the genotype probabilities (File S2) and the script used (File S3). The phenotype QTL viewers are available at https://churchilllab.jax.org/qtlviewer/pazdrodoheart. Marker information containing the genetic map (cM) and physical map (Mbp) for the GigaMUGA, the eight founder strain genotypes, and the GigaMUGA founder genetic maps (cM) and physical maps (Mbp) for each chromosome (File S4) as well as the genetic mapping reports (File S5) can also be found on FigShare.

**Results and Discussion**

In a genetically and phenotypically diverse population of DO mice (N=217; Figure 3.1), we discovered a significant positive correlation between serum GDF11 levels and cardiomyocyte cross sectional area ($r = 0.14$, $p = 0.046$; Table 3.1). When grouped by sex, no significant correlations were found in males, but in females, a negative relationship between GDF11 and postmortem heart wall thickness ($r = -0.20$, $p = 0.036$) emerged. In the 64 DO mice (34 males; 30 females) randomly selected to undergo echocardiography, no significant correlations between GDF11 and measures of heart size or function were noted (Table 3.2).

In contrast to GDF11, transformed myostatin levels were negatively correlated with several measures of cardiac hypertrophy, including heart weight (natural log transformed;

[3] Figshare link will be provided by *G3* editorial staff and made publicly available.

r = -0.29, p < 0.001), heart weight standardized to tibial length (natural log transformed; r = -0.29, p < 0.001), and left ventricular heart wall thickness (r = -0.18, p = 0.008; Table 3.1). We found that myostatin levels tended to be higher in females (t(215) = 3.72, p < 0.001), and similarly, heart wall thickness tended to be lower in females (t(217) = -8.65, p < 0.001; Table 3.1). Additionally, we found a negative correlation between myostatin and total body weight (natural log transformed; r = -0.34, p <0.001), a trend that aligns with past evidence that myostatin negatively regulates body mass [183, 194-196]. When separated by sex, males showed a negative correlation between myostatin and total body weight (r = -0.21, p = 0.033), and percent fibrotic area (r = -0.20, p = 0.040). Females showed a negative relationship between myostatin and total body weight (natural log transformed; p = -0.30, p = 0.001), heart weight (natural log transformed; r = -0.21, p = 0.024), and the ratio of heart weight to tibia length (natural log transformed; r = -0.22, p = 0.019; Table 3.1). In the DO subset that underwent echocardiography, a significant negative correlation emerged between untransformed myostatin levels and left ventricular mass (LVM; r = -0.34, p = 0.006). When separated by sex, the only significant correlation appeared in males: a negative correlation between serum myostatin and LVM (r = -0.38, p = 0.029; Table 3.2). Although these data align with the findings of previous studies establishing the anti-hypertrophic effects of myostatin [178, 197], other rodent studies have reported no effect of myostatin on adult and aged heart mass [198], suggesting that the role of myostatin in the heart is complex and may be context-dependent.

These findings provide novel insight into the distinct relationships between GDF11,

myostatin, and the heart, and most surprisingly do not support a broadly anti-hypertrophic effect for GDF11. That said, it is essential to put these data into proper context. First, the present study assessed DO mice as adult animals aged 5-6 months. As such, the data highlight the fundamental relationships between circulating factors and the heart at a single time point (i.e., adulthood) and may serve as the foundation for future aging studies. Second, LC-MS/MS was used to quantify serum GDF11 and myostatin levels. This technique is highly specific and more sensitive for distinguishing between GDF11 and myostatin than antibody-based methods [67, 68], yet it provides only one aspect of a more complex system. For example, these proteins may circulate freely in the active form or may be bound to inhibitor proteins, such as GASP-1 and GASP-2 [87], which render them inactive. The methods used in the present study measure total circulating concentrations of these proteins, but cannot distinguish between their active and inactive forms. It is possible that the free form of GDF11 has a unique, and stronger, relationship with the heart. All of these limitations should be addressed with more comprehensive future studies.

An additional focus of the present study involved genetic analyses. We calculated heritabilities for serum GDF11 and myostatin concentrations, which revealed a modest heritability for GDF11 levels (0.23) and a moderate heritability for myostatin levels (0.57). The GDF11 heritability estimation is lower than the estimate (0.75) previously reported by our group, which could be explained in part by the fact that the prior study used an ELISA test that likely failed to fully discriminate between GDF11 and myostatin, resulting in a higher heritability estimate reflecting that of myostatin [93].

High-precision gene mapping was then performed using R/qtl2 software [187], and no significant peaks were found for phenotypes related to heart size or histology in normal adulthood. In contrast, mapping serum GDF11 levels revealed a suggestive peak ($p < 0.1$) on murine chromosome 3 within the Bayesian credible interval 3.039589 – 9.983782 Mbp (Figure 3.2A-B). The peak was located in close proximity to the protein-coding gene *Hes Related Family BHLH Transcription Factor with YRPW Motif 1* (*Hey1*; Figure 3.2C-D*)*, a member of the hairy and enhancer of split-related (HESR) family of basic helix-loop-helix (bHLH) transcriptional repressors [199]. Proteins in the HESR family repress target genes via epigenetic modification, mediated by Hdac recruitment and resulting in histone deacetylation [199]. These proteins have been previously linked to cardiovascular development [199-202], with high expression of Hey bHLH transcription factors, such as Hey1 and Hey2, in atrial and ventricular cardiomyocytes as well as in the endocardium [199]. Hey1 in particular promotes heart development by participating in an important signaling cascade for the differentiation of non-chamber atrioventricular canal and inner curvature regions of the heart [201, 203], and regulates expression of other transcription factors involved in cardiac development *in vitro* [199]. In the adult mouse, members of the Hey family have shown an antihypertrophic effect on the heart [204].

*In silico* analyses were used to test whether Hey1 has binding sites proximal to the *Gdf11* gene. Hey1 preferentially binds to the canonical E box sequence 5'-CACGTG-3' in both the murine and human genomes [200, 205, 206]; several Hey1 binding motifs were observed upstream of *Gdf11/GDF11* in both species [191]. The binding motif on mouse

chromosome 10 nearest to *Gdf11* is located at Chr10:128,898,596-128,898,601, only 1,100 base pairs away from the flanking promoter region and 5,196 base pairs from the gene itself (Figure 3.4A). In the human genome, the nearest Hey1 binding site to the *GDF11* gene lies on human chromosome 12 (Chr12:55,729,183-55,729,189), located 13,933 base pairs upstream from the *GDF11* gene and 12,613 base pairs from the flanking promoter region (Figure 3.4A). Further analysis (human genome hg38 assembly) revealed that this particular Hey1 binding sequence lies within highly active histone H3 lysine 27 acetylation (H3K27Ac) and trimethylation of histone H3 lysine 4 (H3K4Me3) regions, which are epigenetic marks strongly correlated with active transcription [207, 208]. It should be noted that this Hey1 binding site may regulate a neighboring gene, such as CD63 (Chr12:55,725,323-55,729,707). Though the binding sites for Hey1 were located outside of the *Gdf11/GDF11* promoter regions in both humans and mice, their proximities to the gene, as well as the acetylation surrounding the motifs – particularly in human DNA – suggest that Hey1 is a plausible candidate gene in the regulation of GDF11 via transcriptional control. We posit that the Hey1 binding site is still located within the upstream regulatory region, especially for mouse *Gdf11*, and that Hey1 inhibits co-activators from binding to enhancers in the distal regulatory regions to modulate *Gdf11* transcription. This model of transcriptional regulation will be tested in future molecular studies.

In parallel, we conducted genetic mapping of serum myostatin levels and discovered a significant locus ($p < 0.05$) on murine chromosome 3 within the Bayesian credible interval of 52.26269 – 52.71985 Mbp (Figure 3.3A-B). The peak is located in close

proximity to protein-coding gene *Forkhead Box O1* (*FoxO1*; Figure 3.3C-D). FoxO1, along with several other Forkhead proteins, plays an essential role in cardiac development [209, 210] and appears to be equally vital in maintaining the function of the adult heart [209, 211]. Multiple studies have shown that FoxO1 increases myostatin expression in myotubes [178, 212-214], though one study of trout myotubes found no effect of FoxO1 on myostatin expression [215]. We identified the FoxO1 binding sequence 5'-TTGTTT-3' sites on murine chromosome 1 [191, 216]; the most likely site fell within the myostatin (*Mstn)* gene itself and within the flanking promoter region (Figure 3.4B). This particular location (Chr1:53,062,323-53,062,328) showed moderate acetylation activity when examined using the UCSC Genome Browser (mm10 assembly), increasing the likelihood that it serves as a site for FoxO1 binding [207, 208]. In the human genome, we searched chromosome 2 near the *MSTN* gene for same motif, TTGTTT, since the Forkhead protein is highly conserved across species [214], and found that it also fell within the gene's promoter region [207] (Figure 3.4B). These findings support a role for FoxO1 in the regulation of myostatin expression and suggest that genetic variants in or near the FoxO1 gene govern circulating myostatin levels.

In summary, the findings of the present study underscore a relatively weak, inconsistent relationship between total serum GDF11 levels and cardiac hypertrophy in a genetically-diverse population of adult mice and support a stronger, consistent anti-hypertrophic role for its homolog, myostatin. To our knowledge, this study is the first to identify a candidate genetic regulator of serum GDF11 concentrations in adults. That gene, Hey1, is a transcriptional repressor with putative binding sites located in close proximity to the

*Gdf11/GDF11* gene in the mouse and human genomes. Hey1 is part of the Notch pathway [217], a signaling cascade that mediates the proliferation and differentiation of cardiomyocytes as well as remodeling the developed heart under stress [217, 218]. These results form the necessary foundation for future studies, which will further interrogate Hey1 as a regulator of GDF11 and cardiovascular disease, and lead to a better understanding of the cardiovascular impact of GDF11 in older adults.

**Tables and Captions**[4]

**TABLE 3.1 - Relationships Among Serum GDF11 and Myostatin Concentrations and Indicators of Cardiac Hypertrophy in DO Mice.** In DO mice, serum GDF11 and ln(myostatin) levels were quantified by LC-MS/MS and body weight and indicators of cardiac hypertrophy were measured. Statistical parametric correlations between serum GDF11 and myostatin concentrations and other variables were determined via Pearson correlation coefficient, and p-values less than 0.05 were deemed to be statistically significant.

| Phenotype | GDF11 r, p-value | | | ln(Myostatin) r, p-value | | |
|---|---|---|---|---|---|---|
| | Overall[a] | M[b] | F[c] | Overall[a] | M[b] | F[c] |
| ln(Body Weight) | -0.016, 0.81 | -0.18, 0.069 | -0.048, 0.62 | **-0.34, < 0.001*** | **-0.21, 0.033*** | **-0.30, 0.001*** |
| ln(Heart Weight) | 0.042, 0.54 | 0.011, 0.91 | -0.11, 0.26 | **-0.29, < 0.001*** | -0.14, 0.15 | **-0.21, 0.024*** |
| Tibia Length | -0.075, 0.28 | 0.042, 0.67 | -0.15, 0.13 | -0.046, 0.50 | -0.10, 0.29 | 0.015, 0.88 |
| ln(Heart Weight/Body Weight) | 0.075, 0.27 | 0.19, 0.053 | -0.047, 0.62 | 0.007, 0.91 | 0.052, 0.60 | 0.10, 0.30 |
| ln(Heart Weight/Tibia Length) | 0.065, 0.35 | 0.003, 0.98 | -0.052, 0.59 | **-0.29, < 0.001*** | -0.13, 0.20 | **-0.22, 0.019*** |
| Wall Thickness | 0.005, 0.94 | 0.078, 0.43 | **-0.20, 0.036*** | **-0.18, 0.008*** | -0.034, 0.73 | -0.094, 0.33 |
| Cardiomyocyte Cross Sectional Area | **0.14, 0.046*** | 0.053, 0.59 | 0.12, 0.20 | -0.11, 0.10 | -0.005, 0.96 | 0.076, 0.43 |

[4] Tables have been sized down from original size to fit formatting requirements.

| | | | | | | |
|---|---|---|---|---|---|---|
| Percent Fibrosis | 0.015, 0.82 | -0.012, 0.90 | 0.054, 0.58 | -0.12, 0.070 | **-0.20, 0.040*** | -0.035, 0.71 |

[a]N = 217
[b]N = 106
[c]N = 111
*Indicates statistical significance

**TABLE 3.2 - Relationships Among Serum GDF11 and Myostatin Concentrations and Indicators of Heart Function in DO Mice.** A total of 64 mice (34 males; 30 females) were randomly selected for echocardiography at approximately 16 weeks of age. Non-normally distributed data were adjusted by a natural log transformation and statistical correlations between serum GDF11 and myostatin concentrations and measures of heart function were determined via Pearson correlation coefficient. A p-value less than 0.05 was considered statistically significant. Myostatin levels were normally distributed in this subset and were therefore not transformed.

| **Phenotype** | **GDF11 r, p-value** | | | **Myostatin r, p-value** | | |
|---|---|---|---|---|---|---|
| | **Overall[a]** | **M[b]** | **F[c]** | **Overall[a]** | **M[b]** | **F[c]** |
| ln(IVSs) | -0.23, 0.23 | -0.020, 0.91 | -0.23, 0.23 | -0.18, 0.17 | -0.23, 0.19 | -0.046, 0.81 |
| IVSd | -0.27, 0.15 | 0.11, 0.56 | -0.27, 0.15 | -0.13, 0.33 | -0.30, 0.086 | 0.030, 0.88 |
| LVIDs | 0.046, 0.81 | -0.093, 0.61 | 0.046, 0.81 | -0.21, 0.10 | 0.004, 0.98 | -0.33, 0.071 |
| LVIDd | 0.081, 0.67 | -0.067, 0.71 | 0.081, 0.67 | -0.23, 0.067 | -0.003, 0.99 | -0.31, 0.098 |
| ln(LVPWs) | 0.025, 0.90 | -0.003, 0.99 | 0.025, 0.90 | -0.085, 0.51 | -0.14, 0.46 | 0.11, 0.57 |
| ln(LVPWd) | -0.12, 0.53 | 0.052, 0.77 | -0.12, 0.53 | -0.091, 0.48 | -0.26, 0.14 | 0.17, 0.38 |
| Ejection Fraction | -0.004, 0.98 | 0.070, 0.70 | -0.004, 0.98 | 0.12, 0.35 | -0.021, 0.91 | 0.28, 0.14 |
| Fractional Shortening | -0.007, 0.97 | 0.050, 0.78 | -0.007, 0.97 | 0.11, 0.40 | -0.029, 0.87 | 0.28, 0.14 |
| LV Mass | -0.15, 0.42 | 0.033, 0.86 | -0.15, 0.42 | **-0.34, 0.006*** | **-0.38, 0.029*** | -0.14, 0.46 |
| ln(LVVs) | 0.064, 0.74 | -0.026, 0.88 | 0.064, 0.74 | -0.18, 0.16 | 0.036, 0.84 | -0.35, 0.061 |
| LVVd | 0.062, 0.75 | -0.11, 0.55 | 0.062, 0.75 | -0.24, 0.058 | -0.030, 0.87 | -0.31, 0.10 |

[a]N = 64
[b]N = 34
[c]N = 30
*Indicates statistical significance

*Note*. IVSs, interventricular septum thickness at end-systole; IVSd, interventricular septum thickness at end-diastole; LVIDs, left ventricular internal dimension at end-

systole; LVIDd left ventricular internal dimension at end-diastole; LVPWs, left ventricular posterior wall thickness at end-systole; LVPWd, left ventricular posterior wall thickness at end-diastole; LV Mass, left ventricular mass; LVVs, Left ventricular volume at end-systole; LVVd, left ventricular volume at end-diastole.

## Figures and Captions[5]

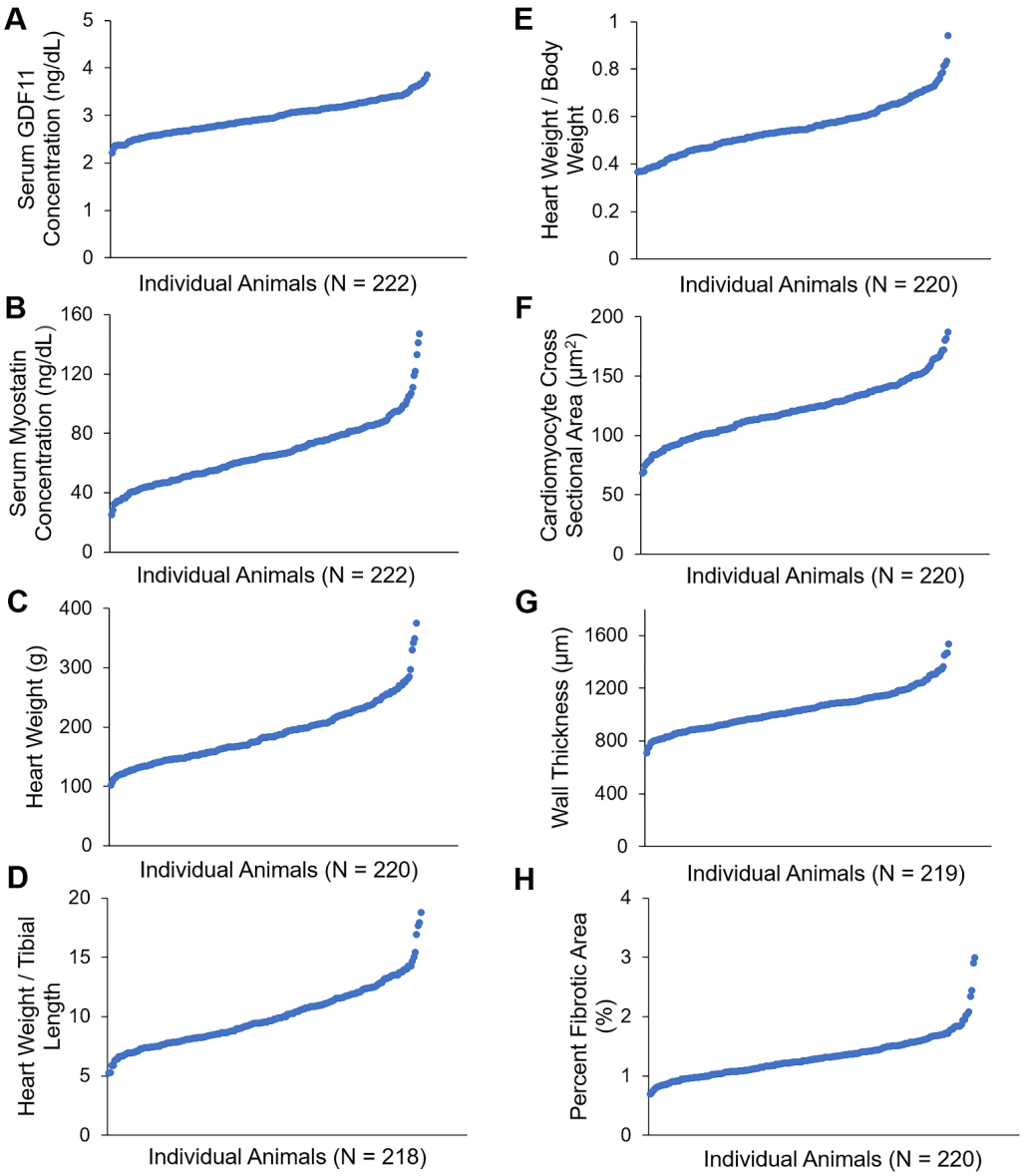


**FIGURE 3.1 - Phenotypic Distribution Across Adult DO Population.** The plotted distribution of uncorrected serum GDF11 (A; ng/dL) and Myostatin (B; ng/dL) levels have confidence intervals of (CI: 2.92, 3.01) and (CI: 63.2, 69.0), respectively. The distributions of heart weight (C; g; (CI: 181, 194)), heart weight to tibial length (D; (CI: 9.64, 10.3)), heart weight to body weight (E; (CI: 0.538, 0.566)), cardiomyocyte cross sectional area (F; µm$^2$; (CI: 118, 124), left ventricular wall thickness (G; µm (CI: 1018,

[5] Figures have been sized down from original size to fit formatting requirements.

1059)), and percent fibrotic area (H; (CI: 1.27, 1.36)) are displayed in the scatter plots above.

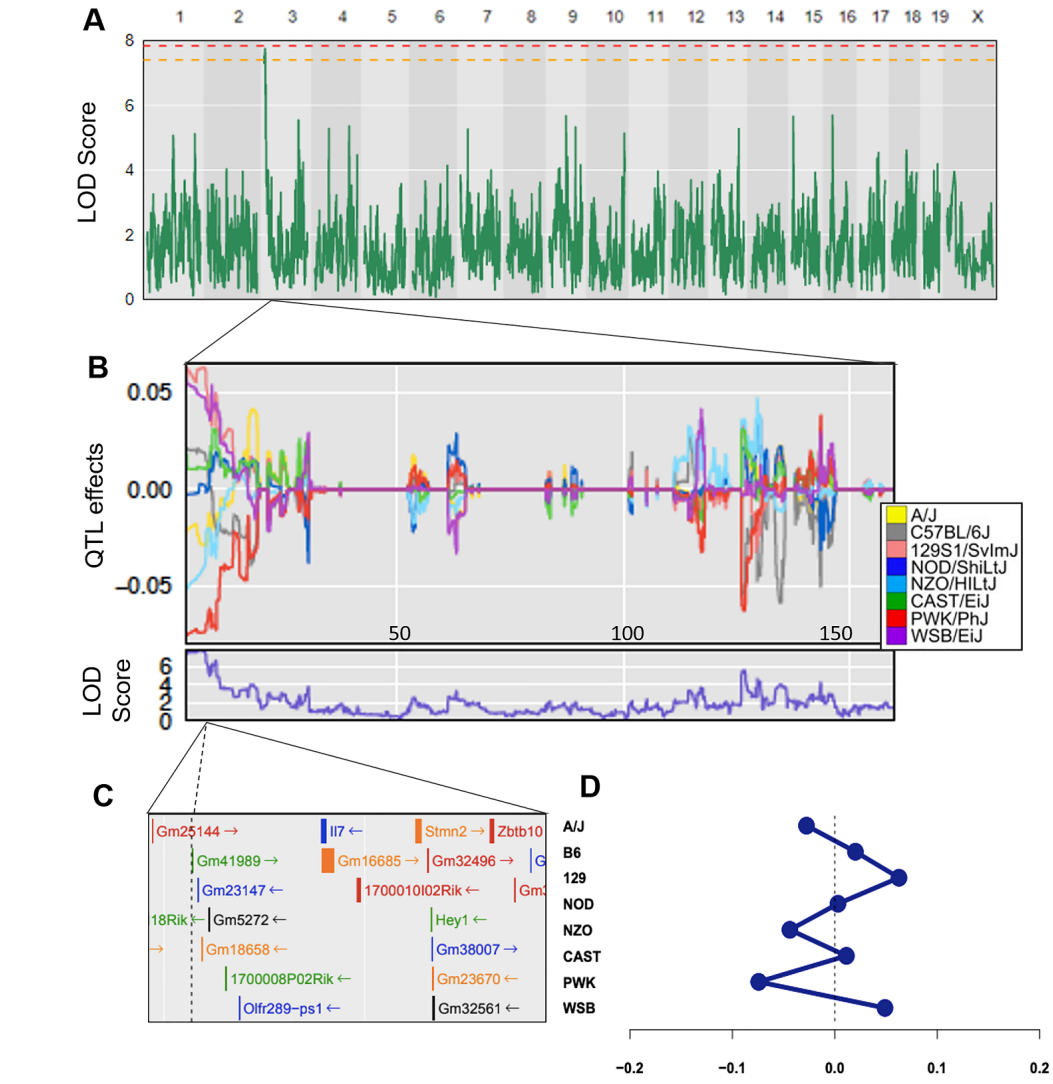


**FIGURE 3.2 - Quantitative Trait Locus (QTL) Mapping of Serum GDF11, Adjusted for Sex, Batch, and Kinship.** Horizontal lines represent permutation testing significant threshold (orange line at *p*-value = 0.1, red line at *p*-value = 0.05). (A) The QTL model for GDF11 revealed a suggestive peak ($p < 0.1$) at Bayesian credible interval 3.039589 – 9.983782 Mbp, with (B and D) additive allele effects from the contributing mouse strains. (C) Genes located near the causative SNP include *Hey1*.

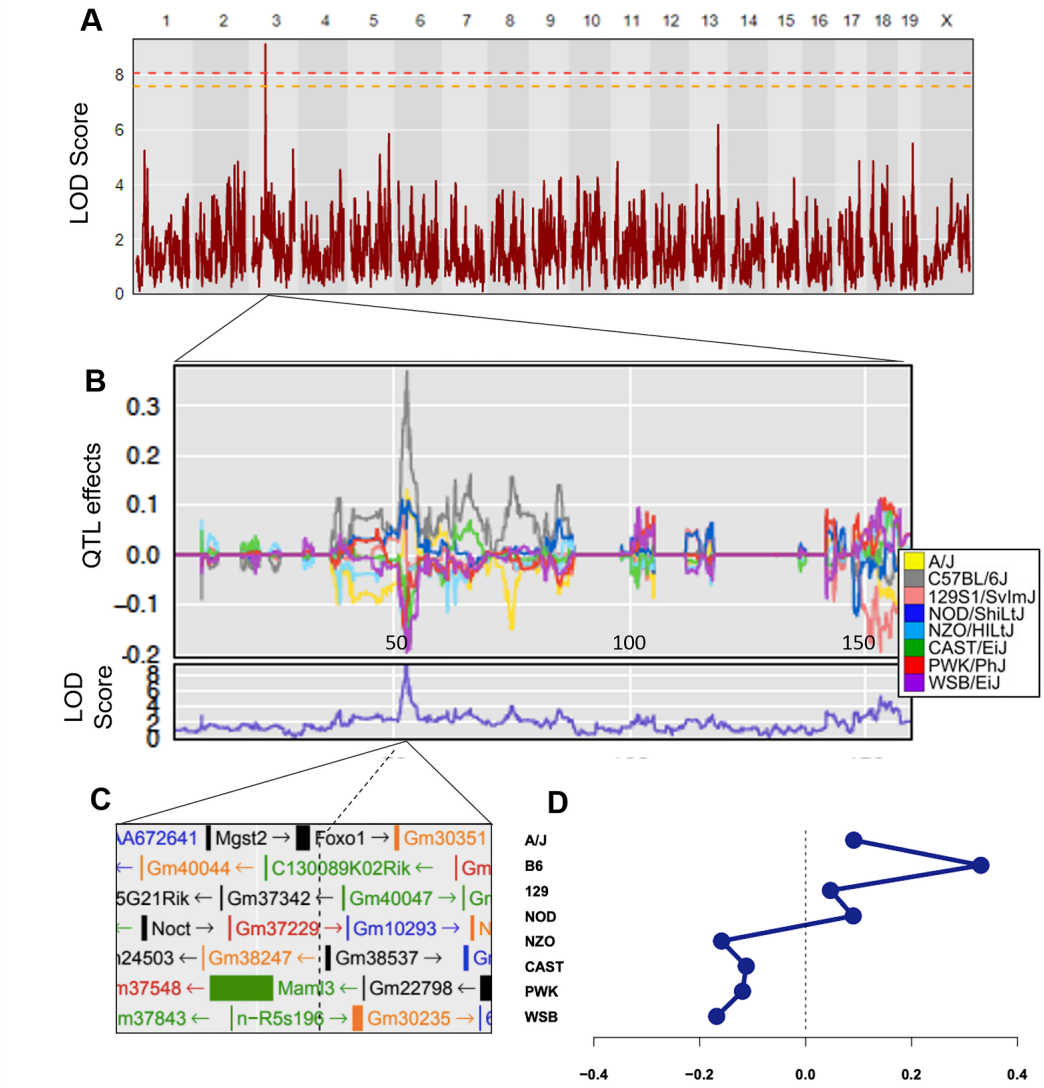


**FIGURE 3.3 - Quantitative Trait Locus (QTL) Mapping of Serum Myostatin, Adjusted for Sex, Batch, and Kinship.** Horizontal lines represent permutation testing significant threshold (orange line at *p*-value = 0.1, red line at *p*-value = 0.05). (A) The QTL model for myostatin revealed a significant peak ($p < 0.05$) at the Bayesian credible interval of 52.26269 – 52.71985 Mbp, with (B and D) additive allele effects from DO parent strains plotted. (C) Genes located near the associated SNP include *FoxO1*.

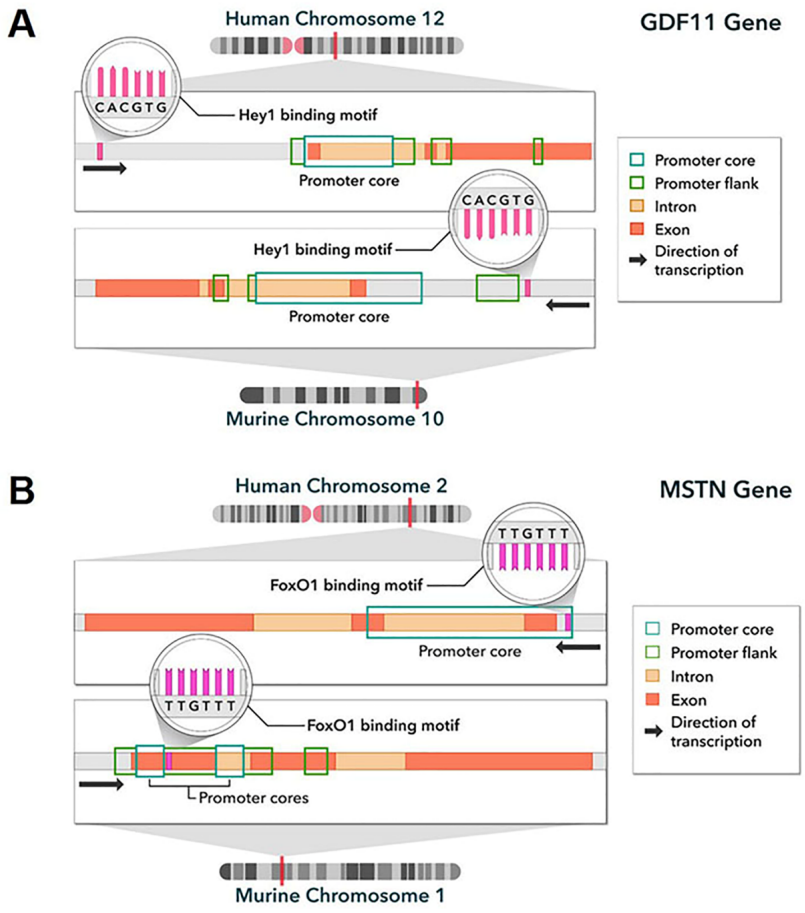


**FIGURE 3.4 - A Model for Transcriptional Regulation of the GDF11 and Myostatin (MSTN) Genes.** (A) Bioinformatics revealed several Hey1 binding sequences (5'-CACGTG-3') upstream of the *Gdf11/GDF11* gene in both humans and mice; the most likely site per species was selected and shown in proximity to the promoter region. (B) Binding sequences of the transcription factor FoxO1 were determined upstream of *Mstn/MSTN* gene in the human and mouse genomes. The most likely binding motif lies within the promoter regions in both species.

**Acknowledgements, Contributions, and Disclosures**

Acknowledgments: The authors wish to thank Ming Shen, Duy Pham, Rebecca Gould, Steven Craig, Isabella Coletta, Andrew Winsauer, Abigayle Simon, Aida Rassam, and Michael Francis for their help with the analyses. The authors also wish to thank Steven Whitford and the staff at the Brigham and Women's Assay Core at Brigham and Women's Hospital (Boston, MA) for conducting serum analyses of GDF11 and myostatin, and Ali Ennis for creating the artwork in this manuscript.

Authors' Contributions: A.E.S. managed project, conducted bioinformatics analyses, and wrote manuscript; K.P. managed mouse colony, phenotypic analyses, and contributed to manuscript; J.B.S. directed histopathology and contributed to study design and manuscript preparation; G.A.C. directed genetic mapping and contributed to study design and manuscript preparation; D.C. and J.T.M managed echocardiography analyses and contributed to the manuscript; A.G. contributed to bioinformatics analyses and manuscript preparation; K.L. directed statistical analyses and contributed to the manuscript; S.Y.C. planned and directed echocardiography and contributed to manuscript; A.E.C. contributed to study design, analyses, and manuscript preparation; E.S. contributed to histopathology and manuscript preparation; R.P. managed project design and implementation, analyses, and manuscript preparation.

Funding: This study was funded by the National Institutes of Health (grant numbers R56 AG053309, R01 GM121551).

Conflicts of Interest/Competing Interests: The authors have no competing interests to disclose.

# CHAPTER 4

# HEY-GDF11 AXIS AS A GENETIC MODULATOR OF CARDIOVASCULAR CONDITIONS[6]

[6] Starcher A, Ye K, Pazdro R. HEY-GDF11 axis as a genetic modulator of cardiovascular conditions. To be submitted to *Gene*.

**Abstract**

Growth Differentiation Factor 11 (GDF11) is a circulating protein that has been suggested to play a role in heart disease, though the effects and extent of that role remain uncertain. Furthermore, little is known about the genetic regulation of GDF11 dictating its expression throughout the body. In our former study, precise genotype mapping of serum GDF11 levels in 217 Diversity Outbred mice produced a suggestive ($p < 0.1$) QTL on chromosome 3 near the the protein-coding gene *Hes Related Family BHLH Transcription Factor with YRPW Motif 1* (*Hey1*). In the present study, we identified associations between variants of GDF11 and cardiovascular disease-related phenotypes as well as variants of the HEY family and similar phenotypes using a layered phenome- and transcriptome-wide exploratory approach. We found our genes of interest demonstrated significant associations with many heart-related disease states and diagnoses including hypertension, endocarditis, and heart failure. Interestingly, GDF11 variants and tissue-specific expression was most often positively associated with several cardiovascular conditions. Overlapping and most often inverse associations among such phenotypes and GDF11 and members of the HEY genes, respectively, support further research into the proposed HEY-GDF11 axis.

## Introduction[7]

Growth Differentiation Factor 11 (GDF11), a member of the transforming growth factor β (TGF-β) superfamily, was first proposed as a blood-borne rejuvenating agent when in

[7] Adapted from Starcher AE, Peissig K, Stanton JB, Churchill GA, Cai D, Maxwell JT, Grider A, Love K, Chen S, Coleman A, Strauss E, Pazdro R. A systems approach using Diversity Outbred mice distinguishes the cardiovascular effects and genetics of circulating GDF11 from those of its homolog, myostatin. Submitted to *G3*, June 7, 2021.

2013, Loffredo and colleagues used heterochronic parabiosis to demonstrate that blood from young mice reverses signs of cardiac hypertrophy in aged animals [41]. Injecting old mice with recombinant GDF11 (rGDF11) produced similar age-reversing effects in the heart [41, 60]. However, the findings of subsequent studies produced conflicting results, calling into question the true impact of GDF11 on cardiac hypertrophy, if any [49, 50, 64, 66, 177]. Likewise, some studies using rGDF11 as protection against or treatment for forms of heart disease and cardiovascular injury yielded beneficial results [69, 101, 102], while others demonstrated no effect [54, 66, 108].

In our previous study, we used a genetically diverse mouse model known as the Diversity Outbred (DO) stock from the Jackson Laboratory (Bar Harbor, ME) to elicit putative genetic regulators of GDF11 and explore associations between circulating serum GDF11 levels and various measures of cardiac function and structure[8]. QTL mapping of serum GDF11 levels revealed a suggestive peak ($p < 0.1$) on murine chromosome 3 within the Bayesian credible (BC) interval 3.039589 – 9.983782 Mbp (Figure 4.1). The peak was located in close proximity to the protein-coding gene *Hes Related Family BHLH Transcription Factor with YRPW Motif 1* (*Hey1)*, a member of the hairy and enhancer of split-related (HESR) family of basic helix-loop-helix (bHLH) transcriptional repressors [199]. Proteins in the HESR family repress target genes via epigenetic modification, mediated by Hdac recruitment and resulting in histone deacetylation [199]. These proteins have been previously linked to cardiovascular development [199-201, 203], with

[8] Starcher AE, Peissig K, Stanton JB, Churchill GA, Cai D, Maxwell JT, Grider A, Love K, Chen S, Coleman A, Strauss E, Pazdro R. A systems approach using Diversity Outbred mice distinguishes the cardiovascular effects and genetics of circulating GDF11 from those of its homolog, myostatin. Submitted to *G3*, June 7, 2021.

high expression of Hey bHLH transcription factors, such as Hey1 and Hey2, in atrial and ventricular cardiomyocytes as well as in the endocardium [199]. Hey1 in particular promotes heart development by participating in an important signaling cascade involved in differentiation [201, 202], and regulates expression of other transcription factors involved in cardiac development *in vitro* [199], thus making it a likely candidate for regulating GDF11. Additionally, in the adult mouse, members of the Hey family have shown an antihypertrophic effect on the heart [204], though their role in the mature heart is poorly understood.

Subsequent *in silico* analyses illuminated putative Hey protein binding motifs (5'-CACGTG-3') upstream of both the murine and human *GDF11* genes. HEY1, HEY2, and HEYL preferentially bind to the same class B E-box sequence (5'-CACGTG-3') and share various overlapping roles in the heart, particularly in modulating cardiac organogenesis [202, 219]. The suggested binding sites in relation to GDF11 have yet to be validated by our lab or any other. Presently, we utilized a layered bioinformatics approach to examine the genetic architecture of heart disease in its many forms as it relates to GDF11, HEY1/2/L, and their genetic variants.

Genome-wide association studies (GWAS) scan the entire genome of the given model to identify genetic variants associated with the phenotype of interest [220]. They are highly powered and offer valuable genetic insights, such as the ability to identify novel genes and pathways connected with common, complex diseases [221]. More recent systematic accumulation and cataloguing of GWAS into databases makes the plethora of

information from individual studies readily accessible [222]. Yet for all its contributions in linking phenotypes to contributing gene variants, GWAS often fail to identify many clinically significant associations and biologically important variants [221, 223]. They also lack the ability to characterize functional single nucleotide polymorphisms (SNPs) within intergenic regions. Furthermore, the stringent significance cutoff of $p < 5.0e\text{-}8$ due to multiple testing can make reaching significance a challenge [221]. A complimentary approach is to reverse the exploration, using genes or variants to identify phenotypes, through phenome-wide association studies (PheWAS). PheWAS are a powerful and unbiased method used to connect disease-associated genetic variants with many phenotypes, while also possessing the ability to identify pleiotropy (i.e., a single locus affecting multiple distinct phenotypes) [220, 224, 225]. Thus, PheWAS allow for illumination of intermediate traits or modulators in a disease pathway that may otherwise go undetected by GWAS [221].

An additional layer of analysis integrates genomic, transcriptomic, and other functional, regulatory information in the form of transcriptome-wide association studies (TWAS) [226]. TWAS leverage GWAS summary-level data to identify the association between gene expression and a complex phenotype [227]. Specifically, TWAS utilize expression quantitative trait loci (eQTL) in relevant tissues to highlight functionally relevant loci in a disease or trait of interest [228]. They allow for highly powered and more easily interpretable identification of trait-associated SNPs by aggregating the effects of several regulatory variants into one testing unit [228, 229]. Furthermore, TWAS provide the

unique advantage of identifying causal mediators of a disease and thus giving insight into the disease biology [230].

The present study extracts and analyzes data from multiple bioinformatic databases in a multi-layered approach to systematically evaluate associations between human GDF11 and HEY1/2/L variants and cardiovascular-related phenotypes. We aim to explore the mechanistic links between GDF11 and heart conditions, HEY1/2/L and heart conditions, as well as any implications of regulation between GDF11 and the HEY genes. First, we leveraged results from over 5,100 GWAS performed on participants of the UK Biobank study to conduct a PheWAS for variants predictive of forms of cardiovascular disease. Next, we evaluated significant *cis*-genetic correlations between heart diseases/contributing conditions and tissue-specific expression of our genes of interest in over 100,000 expression models. For comparison, we took a similar approach using an additional TWAS portal that synthesizes 8.87 million variants from GWAS on thousands of traits with expression data from 49 tissues into a gene-based platform of over 22,500 genes [226, 231]. Our findings supported the relevance of GDF11 and HEY genes in the pathological biology of endocarditis, heart failure, hypertension, and other forms of heart disease. Furthermore, HEY1 and HEY2 expression had converse implications in cardiovascular conditions compared to GDF11 expression, supporting the need for futures studies to validate the HEY-GDF11 axis.

**Methods**

Ethics statement: UK Biobank is a globally accessible, large-scale biomedical database containing genetic and disease information from over 500,000 European individuals [232]. Participants ranged from 40 to 69 years of age between the years 2006 and 2010. The North West Multi-Centre Research Ethics Committee (11/NW/ 0382) approved the UK Biobank project. Informed consent was obtained from each participant prior to collection of biological and anthropometric measurements, lifestyle indicators, blood and urine biomarkers, and information from their medical records [232].

The Genotype-Tissue Expression (GTEx) project collected 15,201 RNA-sequencing samples from 49 tissues of 838 postmortem donors. The organ procurement organizations that collected the biospecimens, Biospecimen Source Sites (BSS) chose to either submit a GTEx research protocol and undergo IRB review or, per the consultation of their Office of Research Subject Protection, forwent further review on account of deceased donors not constituting as human subjects [233, 234]. However, due to the large amount of sequencing data that is made publicly available, GTEx required explicit next-of-kin or otherwise legally authorized representative authorization for study participation [233]. Specific training regulating how BSS obtained consent can be found at http://gtextraining.org/. Only de-identified data according to HIPPAA policy is distributed to GTEx project collaborators (http://www.hhs.gov/ocr/privacy/hipaa/administrative/privacyrule/index.html).

Phenome-wide association study for variants related to cardiovascular conditions: To extract relevant heart-related phenome-wide associations, we utilized the Oxford Brain Imaging Genetics (BIG) Server (version 2.0), an integrative platform of over 5,100 GWAS. Oxford BIG sourced GWAS results from Brain Imaging Derived Phenotypes (n = 3,144 studies) measured on a selection of UK Biobank study participants (n = 9,707) [232, 235], additional UK Biobank GWAS results from the Neale Lab (http://www.nealelab.is/uk-biobank/), amyotrophic lateral sclerosis GWAS [236], Alzheimer's disease GWAS [237], ADHD GWAS from the EAGLE consortium (https://tweelingenregister.vu.nl/eagle-gwa-meta-analyses-summary-results), Magnetic NMR GWAS [238], and BMI, waist circumference and waist/hip ratio from the GIANT consortium data files (http://portals.broadinstitute.org/collaboration/giant/index.php/GIANT_consortium_data_files). Association analysis was performed using BGENIE [239]. We used the significance threshold $p < 5.0e\text{-}8$, commonly used in GWAS [240], when analyzing associations among the heart-related phenotypes and our genes interest.

Transcriptome-wide association study on expression related to cardiovascular conditions: Transcriptome-wide analyses were performed through TWAS Hub (twas-hub.org) and PhenomeXcan [226, 227]. The TWAS Hub synthesizes GWAS and functional data for hundreds of traits and over 100,000 expression models [227]. Summary association statistics came from 30 large-scale (n = 20,000 subjects) GWAS studies, and SNPs with minor allele frequencies of less than 1% were removed [230]. RNA sequencing data originated from CommonMind Consortium (brain, n =613) [241], GTEx (41 tissues)

[242], and the Metabolic Syndrome in Men study (adipose, n = 563) [243, 244], and expression microarray data from the Young Finns Study (blood, n = 1,264) [245, 246], and the Netherlands Twins Registry (n = 1,247) [230, 247]. Associations were considered significant if they reached the tissue-specific threshold determined by Bonferroni correction at an α of 0.05 for each model, as a conservative measure.

PhenomeXcan includes transcriptome-wide gene expression results from 49 tissues using the latest GTEx (v8) data [248] that were then refined by a locus regional colocalization probability (locus RCP), which was used to define putative causal gene contributors (locus RCP > 0.1) [226]. In our analyses, we considered p-values of < 0.01 to be significant and set the record limit to 650 to include all significant associations for GDF11, HEY1, HEY2, and HEYL.

Resources

Oxford Brain Imaging Genetics (BIG) Server (version 2.0): http://big.stats.ox.ac.uk/

TWAS Hub: http://twas-hub.org/

PhenomeXcan: http://apps.hakyimlab.org/phenomexcan/

GeneATLAS: http://geneatlas.roslin.ed.ac.uk/

**Results**

Variants of GDF11 are associated with cardiovascular conditions

We began by analyzing gene-to-phenotype results extracted from thousands of GWAS using data from over 40,000 UK Biobank participants. Of the 86 significant ($p$ < 5.0e-8)

disease phenotypes associated with GDF11 gene variants, five were primary underlying causes of death related to cardiovascular conditions (Table 4.1). Specifically, we observed the GDF11 locus is significantly positively associated with aortic valve disorder ($p$ = 7.6e-18), cardiomegaly ($p$ = 1.0e-9), acute and subacute infective endocarditis ($p$ = 2.2e-14), hypertensive heart disease without congestive heart failure ($p$ = 1.2e-13), heart failure ($p$ = 1.8e-9), and cardiomyopathy ($p$ = 3.4e-9). The effect sizes of the associations were positive and strongest in aortic valve disorder (0.11), indicating a potential detrimental effect of GDF11 in various types of heart disease (Figure 4.1).

Variants of HEY1, HEY2, and HEYL are associated with cardiovascular conditions

While HEY genes are primarily implicated in fetal development of the heart [201, 249], a total of 28 significantly associated cardiovascular-related disease phenotypes suggest they also play an important role in adult heart health. Furthermore, many significant associations between cardiovascular-relevant phenotypes and the HEY genes overlapped, adding evidence to their reported functional redundancy [250, 251]. Specifically, variants of all three genes demonstrated significant associations with endocarditis, unspecified heart failure, and congestive heart failure (Tables 4.2-4.4) and all effect sizes were positive (Figure 4.1).

Of the 107 phenotypes significantly related to the HEY1 locus, 9 were primary underlying causes of death related and one was a non-cancer illness code related to cardiovascular disease (Table 4.2). Among the nine were two forms of endocarditis: acute and subacute infective endocarditis ($p$ = 1.4e-19) and endocarditis of an unspecified valve

($p$ = 1.9e-16). Another two were related to cardiomyopathy: ischaemic cardiomyopathy ($p$ = 6.6e-11) and cardiomyopathy ($p$ = 2.2e-8). Three were forms of heart failure: congestive heart failure ($p$ = 5.3e-16), heart failure ($p$ = 6.0e-15), and hypertensive heart disease with congestive heart failure ($p$ = 3.7e-15). Finally, aortic valve disorder ($p$ = 2.4e-19), cardiomegaly ($p$ = 5.4e-13), and the self-reported non-cancer illness of pericarditis ($p$ = 1.6e-8) were also significantly associated with HEY1 variants.

Variants of HEY2 were significantly associated with 9 heart-related phenotypes, out of the 144 significant associations (Table 4.3). Similarly to HEY1, ICD codes of associations can be grouped according to ailment. Two significant codes were related to endocarditis: acute and subacute infective endocarditis ($p$ = 4.8e-9) and endocarditis of an unspecified valve ($p$ = 2.3e-14). Another two were related to hypertension: hypertensive renal disease ($p$ = 1.0e-8) and hypertensive heart disease without congestive heart failure ($p$ = 2.9e-8). The last coupled associations were cardiomyopathy ($p$ = 4.5e-10) and ischaemic cardiomyopathy ($p$ = 2.40e-10). The latter of the two has the greatest effect size (0.094) for phenome-wide associations with HEY2. Lastly, aortic valve disorder ($p$ = 6.5e-15), heart failure ($p$ = 5.8e-11), and congestive heart failure ($p$ = 1.6e-9) were also associated with HEY2 variants.

Finally, the HEYL locus significantly correlated with 127 phenotypes, 9 of which had implications in heart health (Table 4.4). The following 7 associated phenotypes were primary underlying cases of death: heart failure ($p$ = 7.7e-13), acute and subacute infective endocarditis ($p$ = 9.1e-13), aortic valve stenosis ($p$ = 1.9e-11), ruptured thoracic

aortic aneurysm ($p$ = 7.8e-11), congestive heart failure ($p$ = 7.3e-10), atrial fibrillation and flutter ($p$ = 5.4e-9), and endocarditis of an unspecified valve ($p$ = 2.9e-8). Self-reported pericarditis was observed as a significant non-cancer illness code ($p$ = 6.9e-10) and antihypertensive treatment was associated ($p$ = 7.5e-9). The most significantly associated phenotype was the primary underlying cause of death other specified respiratory disorders ($p$ = 3.1e-44).

Tissue-specific expression of GDF11 is associated with measures of heart health

TWAS provides unique advantages over single eQTL analyses and GWAS in part by capturing the full *cis*-SNP signal [227]. For example in GDF11, we see that for the model listed, the best multivariate predictive model (elastic net with cross-validation $p$ = 3.8e-4, in this case) outperforms the two eQTLs listed ($p$ = 0.75 and $p$ = -0.005). We analyzed the imputed 196 GWAS results from the model non-sun-exposed suprapubic skin from GTEx in the TWAS Hub to determine tissue-specific expression associations with disease. GDF11 expression in this tissue was significantly associated with cardiovascular disease ($p$ = 3.8e-6), high blood pressure ($p$ = 3.0e-5), hypertension ($p$ = 3.0e-5), and vascular/heart problems diagnosed by a doctor ($p$ = 2.0e-5). Interestingly, the former three associations are positive, suggesting GDF11 expression may be upregulated in the pathogenesis of these disease states as a result and/or precursor of the conditions (Figure 4.2). Even after the conservative Bonferroni correction at an α of 0.05 was applied, all listed phenotypes remained significant ($p$ < 2.6e-4).

Furthermore, we analyzed transcriptome-wide expression associations from 49 tissue models in parallel and observed supporting results at a p-value threshold of 0.01 and record limit of 650 (Table 4.1). GDF11 expression in atrial appendage tissue of the heart returned associations with hypertensive heart and/or renal disease ($p = 0.0021$) and hypertensive renal disease ($p = 0.0060$), similar to the results above. Additionally, the diagnosis acute and subacute endocarditis, was significantly associated with GDF11 expression in cell cultured fibroblasts ($p = 0.0038$), mammary breast tissue ($p = 0.0093$), brain/cervical spinal cord C-1 ($p = 0.0093$), and tibial nerve ($p = 0.0093$). Endocarditis was linked to GDF11 expression in cell cultured fibroblasts ($p = 0.0068$). Five different tissues demonstrated significant associations between the expression of GDF11 and the diagnoses of subsequent myocardial infarction: thyroid ($p = 0.0076$), brain/cervical spinal cord C-1 ($p = 0.0096$), tibial nerve ($p = 0.0096$), mammary breast tissue ($p = 0.0096$), and cell cultured fibroblasts ($p = 0.0096$). Finally, expression in four tissues (thyroid, mammary breast tissue, brain/cervical spinal cord C-1, tibial nerve) significantly correlated with heart disease in siblings ($p = 0.0033$, 0.0089, 0.0089, 0.0089, respectively). Again, the tissue-specific expression of GDF11 is positively associated with the cardiovascular-related disease phenotypes (Figure 4.2).

Tissue-specific expression of HEY1/2/L are associated with measures of heart health

In contrast to the TWAS results of GDF11, tissue-specific expression of HEY1 and HEY2 demonstrated sparse, yet significant and mostly negative cardiovascular-related associations (Figure 4.2). HEYL tissue-specific expression did not return any significant heart-related associations (Table 4.4).

In over 100,000 expression models, HEY1 expression was negatively associated with heart disease as an illness of the father ($p = 0.0019$) in the pre-frontal cortex, and high blood pressure as a condition of the father ($p = 0.0042$) in the hypothalamus, though neither reached the significance threshold after Bonferroni correction at an $\alpha$ of 0.05 ($p <$ 1.11e-4 and $p <$ 6.2e-4, respectively; Table 4.2; Figure 4.2). HEY2, however, had 10 associated models, nine of which demonstrated a negative association with cardiovascular disease (CVD), eight with hypertension, and five with high blood pressure (Table 4.3; Figure 4.2). HEY2 expression in pre-frontal cortex brain tissue positively correlated with vascular/heart problems diagnosed by a doctor ($p = 2.50e-4$). All HEY2 relationships remained statistically significant after Bonferroni correction.

Through analyzing TWAS associations available through the PhenomeXcan platform (phenomexcan.org), we discovered 29 of the 427 significant phenotypes were significantly associated with tissue-specific expression of HEY1 were related to heart disease ($p < 0.01$; Table 4.2). Furthermore, the trend of association directionality continues as most cardiovascular-related conditions were negatively associated (Figure 4.2). Vascular/heart problems diagnosed by doctor with and without high blood pressure were associated with six regions of the basal ganglia, two with the pituitary, and two with the minor salivary gland. Among the most relevant associations was heart failure reported in four ways all with skeletal muscle expression of HEY1: heart failure ($p = 0.0012$), not strict heart failure ($p = 0.0012$), strict heart failure ($p = 0.0012$), and diagnostic code ICD10: I50 heart failure ($p = 0.0024$). Hypertension and ill-defined heart diseases were

significantly associated with HEY1 expression in five tissues (see Table 4.2). Furthermore, HEY1 expression in skeletal muscle was associated with endocarditis and acute and subacute endocarditis ($p = 0.00216$).

There were no heart-related disease associations for any tissues analyzed in the expression of HEY2 (Table 4.3). On the other hand, HEYL expression demonstrated relevant phenotypes in 21 tissues (Table 4.4). Vascular/heart problems diagnosed by a doctor: heart attack in the uterus, liver, prostate, left ventricle of the heart, vagina, adrenal gland, hippocampus, ovary, suprapubic skin not sun exposed, caudate basal ganglia, brain cortex, EBV-transformed lymphocyte cells ($p = 0.00042$ for each aforementioned), transverse colon ($p = 0.00042$), subcutaneous adipose tissue ($p = 0.00080$), gastroesophageal junction ($p = 0.0011$), stomach ($p = 0.0013$), coronary artery ($p = 0.0015$), amygdala ($p = 0.0017$), aorta ($p = 0.0018$), hypothalamus ($p = 0.0028$), and frontal cortex BA9 ($p = 0.0028$). Additionally, non-cancer illness code, self-reported: heart attack/myocardial infarction was significantly associated with HEYL expression in 19 tissues.

**Discussion**

Current confusion and controversy surround the role of GDF11 in many cardiovascular injuries and diseases and little is known regarding GDF11's genetic regulation. We utilized an unbiased phenome- and transcriptome-wide exploratory approach to analyze the controversy from a genetic basis while also identifying other contributors to the genetic regulation of complex heart conditions. Many interesting associations emerged

and were supported by a layered analysis between our genes of interest and cardiovascular-related conditions.

The PheWAS illuminated distinct heart conditions and hypertension, an important contributing factor to various cardiomyopathies [252]. Aortic valve disorder was the most strongly associated phenotype with the GDF11 gene locus, specifically at the rs568577713 variant, which had a positive effect size of 0.11 (Table 4.1; Figure 4.1). Interestingly, aortic valve disorder was also strongly associated with HEY1, HEY2, and HEYL variants, with HEYL reporting association with aortic valve stenosis, specifically. Aortic valve disorder is a condition that can be categorized as either regurgitations impairing backflow of the blood through the aortic valve, or aortic stenosis (AS) of the valve compromising anterograde flow [253]. Chronic causes of both aortic regurgitation (AR) and AS include infective endocarditis (IE), hypertension, calcification and fibrosis, and congenital bicuspid valve issues [253-255]. Aortic valve disorder is disproportionately more prevalent in the aged population and often results in left ventricular hypertrophy and heart failure [253, 256].

Endocarditis, a contributor to aortic valve disorder, was GDF11's second strongest associated trait across the phenome, at the SNP rs143006099. Endocarditis is the inflammation of the endocardium, or lining of the heart, chambers and valves. Its acute or subacute forms can be infective, from a bacterial origin, or non-infective, also known as sterile or aseptic [257]. Structural heart diseases can predispose to infective endocarditis, which is developed when the endocardium is damaged, and bacterial colonization follows

[257]. Non-infective endocarditis is commonly seen in advanced malignancy and is characterized by lesions of the heart valves, similar to those of infective endocarditis [258]. Without treatment, all forms of endocarditis can significantly impair valve function, increase the risk of a systemic embolism, contribute to heart failure, and, possibly, result in death [259].

In addition to phenome-wide association, endocarditis was positively associated with GDF11 expression in six different tissues (Table 4.1), supporting this gene-disease connection. Furthermore, the condition presents yet another potential pathway in which the HEY-GDF11 axis is involved. HEY1 variant rs186258783 was associated with the endocarditis phenotype, as was the gene's expression in five different tissues (Table 4.2). Likewise, variants of HEY2 and HEYL were both associated with the phenotypes acute and subacute infective endocarditis and endocarditis of an unspecified valve (Tables 4.3 and 4.4). Although HEY2 and HEYL tissue-specific expression did not display significant connection with endocarditis, the multi-layer evidence implicating GDF11 and the HEY genes in this disease pathway merit further investigation.

Hypertension, a leading cause of adverse cardiovascular outcomes [252, 260], also proved significant among GDF11, HEY1, and HEY2 as a phenotype and with tissue-specific gene expression (Tables 4.1-4.4). Chronic hypertension often manifests as left ventricular hypertrophy and can ultimately result in heart failure, myocardial infarction, stroke, and more [260, 261]. Due to its widespread prevalence and detrimental effects, identifying the genetic regulators of hypertension is a vital step in decreasing the

incidence of cardiovascular disease [260]. Specifically, we observed GDF11 showed significance in three different platforms, the first between SNP rs527651355 and the diagnostic code ICD10: I11.9: hypertensive heart disease without congestive heart failure. Then, GDF11's expression in the atrial appendage tissue and non-sun exposed suprapubic skin displayed positive associations with hypertensive heart and/or renal disease, hypertensive renal disease, and high blood pressure, and self-reported hypertension (Table 4.1). HEY1 and HEY2 demonstrated similar multi-platform associations with high significance (Tables 4.2 and 4.3). HEY2 in particular demonstrated tissue-specific significance with hypertension in nine models (Table 4.3). To corroborate these results, we observed a similar relationship with HEY2 and hypertension in GeneATLAS, a PheWAS database that aggregates trait-gene variant associations in 452,264 UK Biobank participants, totaling 778 traits (http://geneatlas.roslin.ed.ac.uk/region-phewas/) [262]. Within 1000 kb of the HEY2 chromosome region (GRCh37), hypertension was significantly associated ($p$ = 5.3e-15) at variant rs1343222.

While the bioinformatic investigation did not directly link GDF11 with the HEY genes, we observed overlap of many individual heart-related associations. For example, tissue-specific expression of GDF11 as observed through the TWAS Hub was positively associated with CVD, high blood pressure, and self-reported hypertension, and negatively associated with vascular/heart problems diagnosed by a doctor (Table 4.1). Meanwhile, HEY2 expression was also significantly associated with all four measures but with inverse relationships (Table 4.3; Figures 4.1 and 4.2). Again, GDF11's tissue-specific

expression association with endocarditis is positive, while HEY1's expression is negatively associated with disease in PhenomeXcan (Table 4.1 and 4.2). This mirroring effect suggests the regulation of GDF11 by HEY2 and potentially HEY1, known transcriptional repressors [199], in modulating heart health.

The regulation of GDF11 by members of the HEY family has yet to be explicitly investigated, however a study exploring the epigenomic and transcriptomic dynamics of heart organogenesis listed GDF11 as one of many genes with high connectivity, tissue-specific expression, and potential regulation by heart-specific enhancers such as HEY1, HEY2, and HEYL (Online Table X of [263]). Thus, combined with our findings, the HEY-GDF11 axis warrants mechanistic follow up, which is currently absent from the literature, to validate the HEY1/2/L binding sites upstream of GDF11 and determine their regulatory effects *in vitro* (see appendix).

PheWAS allow for novel gene-phenotype associations that are highly powered, and the identification of pleiotropic genetic variants, however, some limitations exist [221]. First, replication of PheWAS results may prove challenging if the SNP of interest is not the functional variant nor observed in multiple populations. Additionally, PheWAS and TWAS rely on ICD codes, which come from different healthcare professionals across many facilities, thus introducing variability in care and potential for human error. In order to address some of the variability innate in human coding, a patient must be coded two or more times for any ICD code to be considered a case [221, 264]. Additionally, the UK

Biobank participants are primarily Caucasian adults, thus genetic variability among races and ethnicities was not captured in our study [232].

Lastly, Bonferroni correction at an α of 0.05 was applied per model retrospectively to TWAS Hub results as a conservative effort to ensure significance, however this may not be an appropriate adjustment due to the lack of independence across the phenotypes examined [221]. Nevertheless, nearly associations remained significant after correction-besides heart disease as an illness of the father ($p = 0.0019$) and high blood pressure as an illness of the father ($p = 0.0042$) associations with HEY1 expression.

In addition to aortic valve disorder, endocarditis, and hypertension, several other important heart-related disease phenotypes showed significance with our genes of interest, though only on one level of analysis, such as myocardial infarction, CVD, and cardiomyopathy. Taken together, our results support the conclusion that GDF11 and the HEY genes play an important role in cardiovascular conditions, and that these roles seem to be opposite. GDF11 was largely positively associated with its related cardiovascular conditions, while the HEY genes (particularly HEY1 and HEY2) were positively associated. This relationship supports our previous findings that HEY1 may act as a transcriptional repressor of GDF11. In certain cardiovascular disease states, such as endocarditis, hypertension and heart failure, the repressive role of the HEY genes is inhibited, signaling an increase in GDF11 expression. Further investigation is needed to better understand the HEY-GDF11 axis in the pathological biology of cardiovascular conditions.

**Figures and Legends**

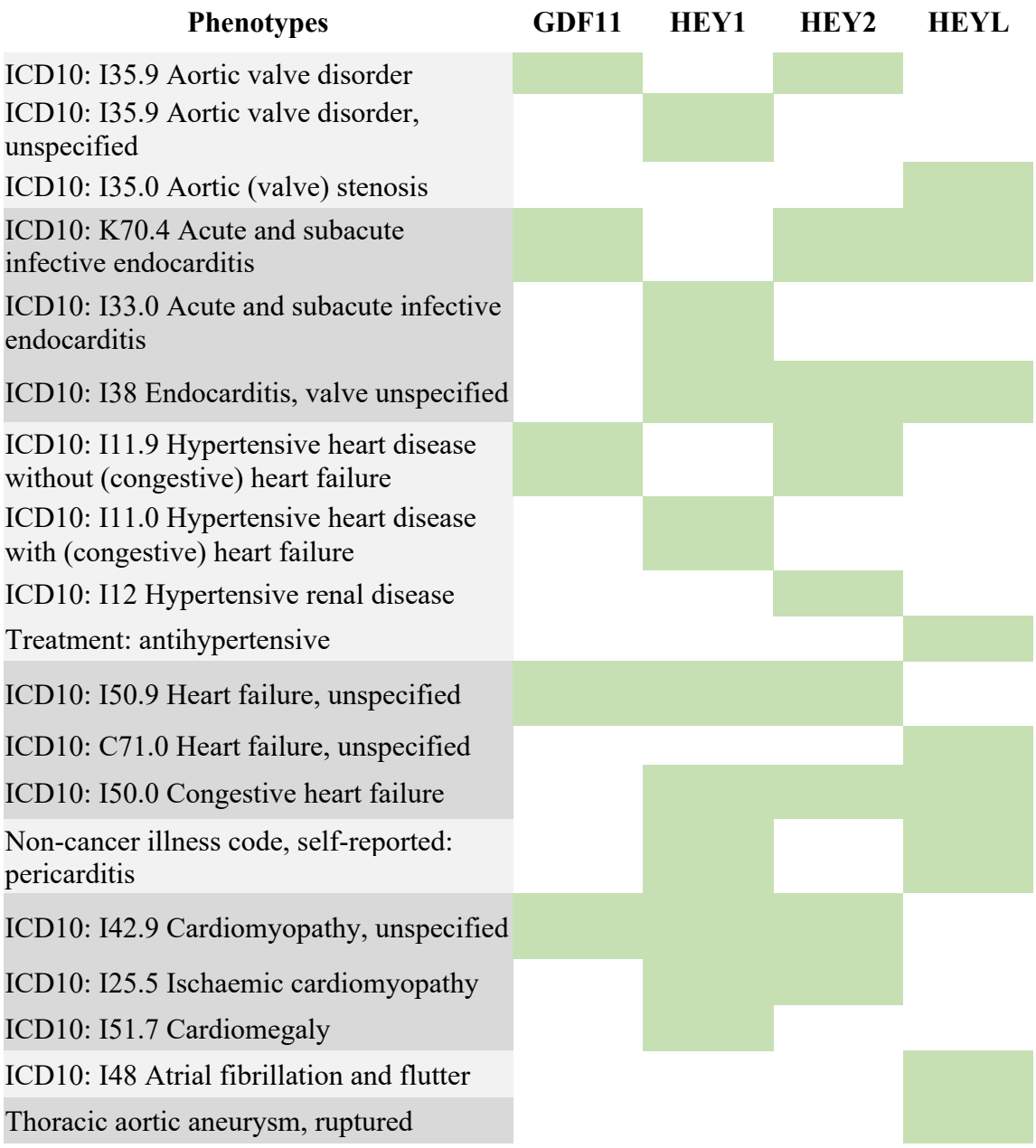


**FIGURE 4.1 - Heatmap of Significant Cardiovascular-Related Phenotypic Associations**. Phenotypes from Oxford BIG are grouped based on type of cardiovascular condition and listed on the left side. A significant association ($p < 5.0e-8$) between the gene and phenotype is indicated by green shading.

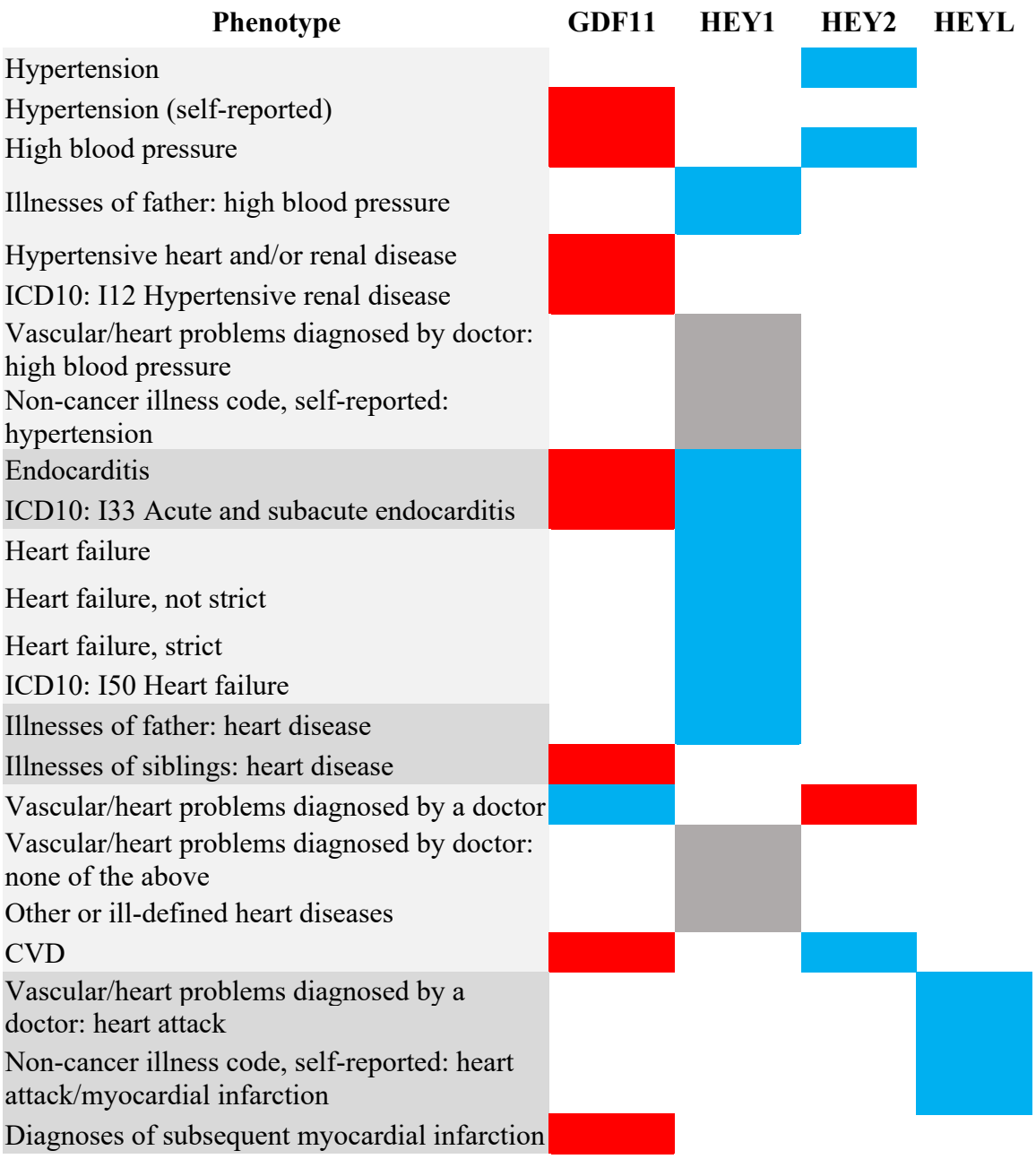


**FIGURE 4.2 - Heatmap of Transcriptome-Wide Associations.** Cardiovascular-related phenotypes from TWAS Hub and PhenomeXcan are grouped on the left according to condition. Red indicates a positive association, blue indicates negative, grey indicates an inconclusive direction, and white indicates no significant correlation. Significance was considered by database with PhenomeXcan results having a p-value of less than 0.01, and TWAS Hub associations having a p-value below the tissue-specific threshold determined by Bonferroni correction.

## Tables and Legends

**TABLE 4.1 - GDF11 Phenome-Wide and Transcriptome-Wide Heart-Related Associations.** All relevant phenotypic and trait associations listed for GDF11 are under their respective significance cut offs. For phenotypic associations extracted from Oxford BIG, significance is considered a $p < 5.0e-8$. Bonferroni correction was performed at an $\alpha = 0.05$ to determine the significance threshold for each tissue in the TWAS Hub. PhenomeXcan expression associations are considered significant at $p < 0.01$.

| **Phenome-Wide Associations** | | | | | |
|---|---|---|---|---|---|
| | **Heart-related Phenotype** | **P-value** | **SNP ID** | **Effect Allele** | **Effect Size** |
| **Oxford BIG** | ICD10: I35.9 Aortic valve disorder | 7.60E-18 | rs568577713 | A | 0.11 |
| | ICD10: K70.4 Acute and subacute infective endocarditis | 2.20E-14 | rs143006099 | C | 0.048 |
| | ICD10: I11.9 Hypertensive heart disease without (congestive) heart failure | 1.20E-13 | rs527651355 | A | 0.12 |
| | ICD10: I51.7 Cardiomegaly | 1.0e-9 | rs548170298 | C | 0.046 |
| | ICD10: I50.9 Heart failure, unspecified | 1.80E-09 | rs564889237 | T | 0.039 |
| | ICD10: I42.9 Cardiomyopathy, unspecified | 3.40E-09 | rs571113050 | A | 0.048 |
| **Transcriptome-Wide Associations** | | | | | |
| **TWAS Hub** | **Trait** | **Tissue** | | **P-value** | **Z-score** |
| | CVD | Skin not sun exposed suprapubic | | 3.80E-06 | 4.6 |
| | High blood pressure | | | 3.03E-05 | 4.1 |
| | Hypertension (self-reported) | | | 3.03E-05 | 4.1 |
| | Vascular/heart problems diagnosed by a doctor | | | 2.03E-05 | -4.2 |
| **PhenomeXcan** | **Trait** | **Tissue** | | **P-value** | **Z-score** |
| | Hypertensive heart and/or renal disease | Atrial appendage | | 0.00214 | 3.0558 |
| | ICD10: I12 Hypertensive renal disease | Atrial appendage | | 0.00596 | 2.7501 |
| | ICD10: I33 Acute and subacute endocarditis | Cell cultured fibroblasts | | 0.0038 | 2.8946 |
| | | Mammary breast tissue | | 0.00925 | 2.6026 |
| | | Brain/cervical spinal cord C-1 | | 0.00925 | 2.6026 |
| | | Tibial nerve | | 0.00925 | 2.6026 |
| | Endocarditis | Cell cultured fibroblasts | | 0.0068 | 2.7066 |
| | Diagnoses of subsequent myocardial infarction | Thyroid | | 0.00763 | 2.6681 |
| | | Brain/cervical spinal cord C-1 | | 0.0096 | 2.5898 |
| | | Tibial nerve | | 0.0096 | 2.5898 |
| | | Mammary breast tissue | | 0.0096 | 2.5898 |
| | | Cell cultured fibroblasts | | 0.0096 | 2.5897 |
| | Illnesses of siblings: heart disease | Thyroid | | 0.00331 | 2.937 |
| | | Mammary breast tissue | | 0.00889 | 2.6162 |
| | | Brain/cervical spinal cord C-1 | | 0.00889 | 2.6162 |
| | | Tibial nerve | | 0.00889 | 2.6162 |

**TABLE 4.2 - HEY1 Phenome-Wide and Transcriptome-Wide Heart-Related Associations.** All relevant phenotypic associations extracted from Oxford BIG for HEY1 listed reach significance at $p < 5.0e\text{-}8$. Bonferroni correction was performed at an experiment-wide α to determine the significance threshold for each tissue in the TWAS Hub, which was not reached by illnesses of father: heart disease ($p = 0.0019$), nor illnesses of father: high blood pressure ($p = 0.0042$), though their individual associations are below $p < 0.05$. PhenomeXcan expression associations are considered significant at $p < 0.01$.

| **Phenome-Wide Associations** | | | | | |
|---|---|---|---|---|---|
| | **Heart-related Phenotype** | **P-value** | **SNP ID** | **Effect Allele** | **Effect Size** |
| **Oxford BIG** | ICD10: I33.0 Acute and subacute infective endocarditis | 1.40E-19 | rs186258783 | A | 0.054 |
| | ICD10: I35.9 Aortic valve disorder, unspecified | 2.40E-19 | rs189726570 | A | 0.06 |
| | ICD10: I38 Endocarditis valve unspecified | 1.90E-16 | rs545253823 | G | 0.077 |
| | ICD10: I50.0 Congestive heart failure | 5.30E-16 | rs145405601 | A | 0.044 |
| | ICD10: I11.0 Hypertensive heart disease with (congestive) heart failure | 3.70E-15 | rs190327316 | A | 0.074 |
| | ICD10: I50.9 Heart failure, unspecified | 6.00E-15 | rs76299624 | G | 0.065 |
| | ICD10: I51.7 Cardiomegaly | 5.40E-13 | rs185362765 | G | 0.064 |
| | ICD10: I25.5 Ischaemic cardiomyopathy | 6.60E-11 | rs76818235 | A | 0.06 |
| | Non-cancer illness code, self-reported: pericarditis | 1.60E-08 | rs181849443 | T | 0.0021 |
| | ICD10: I42.9 Cardiomyopathy, unspecified | 2.20E-08 | rs76752315 | C | 0.027 |
| **Transcriptome-Wide Associations** | | | | | |
| | **Trait** | **Tissue** | | **P-value** | **Z-score** |
| **TWAS Hub** | Illnesses of father: heart disease* | Pre-frontal cortex | | 0.0019 | -2.1 |
| | Illnesses of father: high blood pressure* | Hypothalamus | | 0.0042 | -2.7 |
| | **Trait** | **Tissue** | | **P-value** | **Z-score** |
| **PhenomeXcan** | Vascular/heart problems diagnosed by doctor: high blood pressure | Nucleus accumbens basal ganglia | | 0.000168 | 3.763 |
| | | Caudate basal ganglia | | 0.000168 | 3.763 |
| | | Pituitary | | 0.000168 | 3.763 |
| | | Putamen basal ganglia | | 0.000168 | 3.763 |
| | | Minor salivary gland | | 0.00677 | -2.7082 |
| | Vascular/heart problems diagnosed by doctor: none of the above | Putamen basal ganglia | | 0.000151 | -3.7889 |
| | | Caudate basal ganglia | | 0.000151 | -3.7889 |
| | | Pituitary | | 0.000151 | -3.7889 |

| | | | | |
|---|---|---|---|---|
| | | Nucleus accumbens basal ganglia | 0.000151 | -3.7889 |
| | | Minor salivary gland | 0.00737 | 2.6796 |
| | Heart failure | Skeletal muscle | 0.00115 | -3.2513 |
| | Heart failure, not strict | Skeletal muscle | 0.00115 | -3.2513 |
| | Heart failure, strict | Skeletal muscle | 0.00115 | -3.2513 |
| | ICD10: I50 Heart Failure | Skeletal muscle | 0.00239 | -3.0366 |
| | Non-cancer illness code, self-reported: hypertension | Nucleus accumbens basal ganglia | 0.000104 | 3.8819 |
| | | Putamen basal ganglia | 0.000104 | 3.8819 |
| | | Pituitary | 0.000104 | 3.8819 |
| | | Caudate basal ganglia | 0.000104 | 3.8819 |
| | | Minor salivary gland | 0.00443 | -2.8458 |
| | Other or ill-defined heart diseases | Minor salivary gland | 0.00709 | 2.6925 |
| | | Caudate basal ganglia | 0.00914 | -2.6068 |
| | | Putamen basal ganglia | 0.00914 | -2.6068 |
| | | Nucleus accumbens basal ganglia | 0.00914 | -2.6068 |
| | | Pituitary | 0.00914 | -2.6068 |
| | Endocarditis | Putamen basal ganglia | 0.00203 | -3.0862 |
| | | Pituitary | 0.00203 | -3.0862 |
| | | Caudate basal ganglia | 0.00203 | -3.0862 |
| | | Nucleus accumbens basal ganglia | 0.00203 | -3.0862 |
| | ICD10: I33 Acute and subacute endocarditis | Skeletal muscle | 0.00216 | -3.0669 |

*Not statistically significant after Bonferroni correction at an experimental $\alpha = 0.05$

**TABLE 4.3 - HEY2 Phenome-Wide and Transcriptome-Wide Heart-Related Associations.** All relevant phenotypic and trait associations listed for HEY2 are under their respective significance cut offs. For phenotypic associations extracted from Oxford BIG, significance is considered a $p < 5.0e\text{-}8$. Bonferroni correction was performed at an experiment-wide $\alpha = 0.05$ to determine the significance threshold for each tissue in the TWAS Hub. There are no heart-related significant ($p < 0.01$) traits associated with HEY2 tissue-specific expression in PhenomeXcan. HTNS, hypertension.

| **Phenome-Wide Associations** | | | | | |
|---|---|---|---|---|---|
| | **Heart-Related Phenotype** | **P-value** | **SNP ID** | **Effect Allele** | **Effect Size** |
| **Oxford BIG** | ICD10: I35.9 Aortic valve disorder, unspecified | 6.50E-15 | rs759199133 | C | 0.089 |
| | ICD10: I38 Endocarditis valve unspecified | 2.30E-14 | rs147565513 | T | 0.064 |
| | ICD10: I50.9 Heart failure, unspecified | 5.80E-11 | rs192117947 | G | 0.047 |

| | | | | | |
|---|---|---|---|---|---|
| | ICD10: I25.5 Ischaemic cardiomyopathy | 2.40E-10 | rs527848217 | T | 0.054 |
| | ICD10: I42.9 Cardiomyopathy, unspecified | 4.50E-10 | rs751332699 | A | 0.094 |
| | ICD10: I50.0 Congestive heart failure | 1.60E-09 | rs182677449 | A | 0.049 |
| | ICD10: I33.0 Acute and subacute infective endocarditis | 4.80E-09 | rs565607641 | T | 0.023 |
| | ICD10: I12 Hypertensive renal disease | 1.00E-08 | rs191279762 | G | 0.0038 |
| | ICD10: I11.9 Hypertensive heart disease without (congestive) heart failure | 2.90E-08 | rs117891025 | G | 0.041 |

**Transcriptome-Wide Associations**

| | **Tissue** | **Panel** | **CVD** | | **Hypertension** | | **High blood pressure** | | **Vascular/heart problems diagnosed by doctor** | |
|---|---|---|---|---|---|---|---|---|---|---|
| | | | **P-value** | **Z-score** | **P-value** | **Z-score** | **P-value** | **Z-score** | **P-value** | **Z-score** |
| **TWAS Hub** | Model 1 - Pre-frontal Cortex | Common-Mind | 4.11E-07 | -5.0 | 4.33E-06 | -4.5 | 3.70E-05 | -4.0 | X | X |
| | Model 2 - Pancreas | GTEx | 8.00E-07 | -5.0 | 1.54E-05 | -4.3 | 1.05E-04 | -3.8 | X | X |
| | Model 3 - Testis | GTEx | 4.87E-07 | -5.1 | 2.84E-06 | -4.7 | 2.20E-05 | -4.2 | X | X |
| | Model 4 - Thyroid | GTEx | 4.32E-08 | -5.5 | 5.09E-07 | -5.0 | 5.01E-06 | -4.5 | X | X |
| | Model 5 - Adipose | METSIM | 1.02E-06 | -4.8 | 2.37E-05 | -4.1 | X | X | X | X |
| | Model 6 - Pre-frontal Cortex | ROS-MAP | 8.15E-08 | -5.3 | 1.00E-06 | -4.8 | 9.96E-06 | -4.3 | 2.49E-04 | 3.5 |
| | Model 8 - Kidney renal clear cell carcinoma | TCGA | 6.61E-06 | -4.4 | X | -3.4 | X | X | X | X |
| | Model 9 – Pheochromo-cytoma and paraganglioma | TCGA | 1.70E-06 | -4.8 | 9.99E-05 | -3.8 | X | X | X | X |
| | Model 10 - Thyroid carcinoma | TCGA | 1.70E-06 | -4.7 | 3.66E-05 | -4.0 | X | X | X | X |

**TABLE 4.4 - HEYL Phenome-Wide and Transcriptome-Wide Heart-Related Associations.** All relevant phenotypic and trait associations listed for HEYL are under their respective significance cut offs. PhenomeXcan expression associations are considered significant at $p < 0.01$. There are no significant associations between HEYL expression and heart-related traits in TWAS Hub.

| Phenome-Wide Associations | | | | | |
|---|---|---|---|---|---|
| | **Heart-related Phenotype** | **P-value** | **SNP ID** | **Effect Allele** | **Effect Size** |
| **Oxford BIG** | ICD10: C71.0 Heart failure, unspecified | 7.70E-13 | rs576022791 | T | 0.055 |
| | ICD10: I33.0 Acute and subacute infective endocarditis | 9.10E-13 | rs189205519 | T | 0.034 |
| | ICD10: I35.0 Aortic (valve) stenosis | 1.90E-11 | rs557823373 | T | 0.065 |
| | Thoracic aortic aneurysm, ruptured | 7.80E-11 | rs146137215 | T | 0.039 |
| | ICD10: I50.0 Congestive heart failure | 7.30E-10 | rs185811750 | A | 0.027 |
| | Non-cancer illness code, self reported: pericarditis | 6.90E-10 | rs577410243 | G | 0.0018 |
| | ICD10: I48 Atrial fibrillation and flutter | 5.40E-09 | rs576022791 | T | 0.055 |
| | Treatment: antihypertensive | 7.50E-09 | rs189967557 | C | 0.0017 |
| | ICD10: I38 Endocarditis, valve unspecified | 2.90E-08 | rs150729762 | C | 0.034 |

| Transcriptome-Wide Associations | | | | | |
|---|---|---|---|---|---|
| | **Tissue** | **Vascular/heart problems diagnosed by a doctor: heart attack** | | **Non-cancer illness code, self-reported: heart attack/myocardial infarction** | |
| | | **P-value** | **Z-score** | **P-value** | **Z-score** |
| **PhenomeXcan** | Uterus | 0.000416 | -3.5296 | 0.000522 | -3.4694 |
| | Liver | 0.000416 | -3.5296 | 0.000522 | -3.4694 |
| | Prostate | 0.000416 | -3.5296 | 0.000522 | -3.4694 |
| | Left ventricle of heart | 0.000416 | -3.5296 | 0.000522 | -3.4694 |
| | Vagina | 0.000416 | -3.5296 | 0.000522 | -3.4694 |
| | Adrenal gland | 0.000416 | -3.5296 | 0.000522 | -3.4694 |
| | Hippocampus | 0.000416 | -3.5296 | 0.000522 | -3.4694 |
| | Ovary | 0.000416 | -3.5296 | 0.000522 | -3.4694 |
| | Suprapubic skin not sun exposed | 0.000416 | -3.5296 | 0.000522 | -3.4694 |
| | Caudate basal ganglia | 0.000416 | -3.5296 | 0.000522 | -3.4694 |
| | Brain cortex | 0.000416 | -3.5296 | 0.000522 | -3.4694 |
| | EBV-transformed lymphocyte cells | 0.000416 | -3.5296 | 0.000522 | -3.4694 |
| | Transverse colon | 0.000417 | -3.5288 | 0.000504 | -3.4785 |
| | Subcutaneous adipose tissue | 0.000796 | -3.3542 | 0.000891 | -3.323 |
| | Gastroesophageal junction | 0.00111 | -3.2607 | 0.00146 | -3.182 |
| | Stomach | 0.00134 | -3.2078 | 0.00177 | -3.1256 |
| | Coronary artery | 0.00146 | -3.1824 | 0.00193 | -3.1016 |
| | Amygdala | 0.00168 | -3.1416 | 0.00224 | -3.0569 |
| | Aorta | 0.0018 | -3.122 | 0.00238 | -3.038 |

| | | | | | |
|---|---|---|---|---|---|
| | Hypothalamus | 0.00281 | -2.988 | X | X |
| | Frontal cortex BA9 | 0.00282 | -2.9869 | X | X |

# CHAPTER 5

# GDF11 AS A GENETIC INTERMEDIATE IN THE PATHOLOGICAL BIOLOGY OF HYPOTHYROIDISM AND ASTHMA[9]

[9] Starcher A, Ye K, Pazdro R. GDF11 as an intermediate genetic regulator of hypothyroidism and asthma. To be submitted to *Gene*.

**Abstract**

Growth Differentiation Factor 11 (GDF11) is a circulating blood-borne factor with defined roles in development, such as organogenesis and axial patterning, and some less determined roles in the adult mammal. It has been reported to have a regenerating effect in the heart, skeletal muscle, brain, and, more recently, lungs, however much controversy surrounds its true impact. Some of GDF11's rejuvenating property has been linked to its suppression of inflammation through activating TGF-β/Smad2/3 pathway, which could have major implications for chronic inflammatory diseases. Our study uses a layered bioinformatic approach to evaluate GDF11 as a genetic intermediate in the development of asthma and hypothyroidism and propose a regulatory pathway by which GDF11 is mediated in disease biology.

**Introduction**

Growth Differentiation Factor 11 (GDF11) is a widely expressed circulating protein that plays a key role in organogenesis and development in various species, including humans [86, 128, 265, 266]. In 2013, a parabiosis study reversed age-related cardiac hypertrophy in old mice, attributing the rejuvenating effect to GDF11, which they reported declined with age [41]. Furthermore, the research team demonstrated a similar impact from injection of recombinant GDF11 in aged mice [41]. Additional studies mirrored GDF11's rejuvenating effects in the heart [60], skeletal muscle [46], and brain [47]. However, subsequent studies reported conflicting results as to GDF11's true impact on various organs and tissues [50, 66] as well as its directionality in age [92].

Nevertheless, mounting evidence has demonstrated a significant relationship between GDF11 and inflammation, namely GDF11's attenuation of inflammatory factor expression by impeding nuclear factor kappa-light-chain-enhancer of activated B cells (NF-kB) and JNK signaling pathways through TGF-β/Smad2/3 activation [137-139, 267-269]. This antagonistic action proved beneficial in GDF11's protective effects against acute lung injury in C57BL/6 mice [137]. Furthermore, GDF11 expression and circulating plasma levels also declined chronic obstructive pulmonary disease (COPD) [269] and demonstrated a positive association with lung function in COPD individuals [270]. Additional therapeutic effects of GDF11's anti-inflammatory actions have been demonstrated in mice as a protection against inflammatory arthritis [139], endothelial injury and atherosclerotic lesion formation [138], and aging of the skin [267]. Lastly, GDF11 expression has been related to thyroid stimulating hormone (TSH) levels, and measures of metabolism, specifically of thyroid function, though with conflicting associations [56, 268].

In the present study, we take a layered bioinformatics approach to investigate GDF11 as a genetic intermediate in the pathogenesis of chronic inflammatory diseases, specifically asthma, and hypothyroidism [271-273]. Hypothyroidism is the pathological condition of deficient thyroid hormone status, and is characterized by high circulating levels of TSH [274]. In regions of Iodine sufficiency, the primary cause of hypothyroidism is Hashimoto's disease, a form of chronic autoimmune thyroiditis [275, 276]. Hypothyroidism diagnoses, seen in approximately 5% of the general population, are more common in individuals with autoimmune disorders such as Type 1 diabetes, celiac

disease, and autoimmone gastric atrophy [274, 275]. Asthma is likewise a very complex disease and involves an interplay among airflow obstruction, environmental triggers, bronchial hyper-responsiveness, and inflammation [271]. It is diagnosed in over 15 million Americans [277]. Clinical manifestations including coughing and wheezing are primarily the result of smooth muscle contraction and inflammation, which, when persistent, may lead to structural changes within the airway such as subepithelial fibrosis, mucus hypersecretion, blood vessel proliferation, and infiltration of inflammatory cells [271, 278, 279].

Sparse evidence has demonstrated associations between hypothyroidism and asthma, including an epidemiological study that used the Oxford Record Linkage Study dataset of statistical medical records [280]. The research team suggested a shared autoimmune-related etiology could be responsible for the disease connection. Alternatively, they proposed that thyroid hormones may enhance IgE production, directly influencing the inflammatory response involved in asthma [280-282]. Case studies reporting dramatically worsened asthma symptoms following the onset of thyrotoxicosis support this hypothesis [283, 284]. Other studies report conflicting, yet significant, relationships between measures of the two diseases, suggesting a complex interplay between asthma and thyroid hormones [285-287].

To begin our genetic investigation, we leveraged phenome-wide association studies (PheWAS) to extract valuable data from the thousands of associations between genetic variants and traits. PheWAS are unbiased, large-scale analyses often utilized in drug

development research due to their ability to identify pleiotropy (i.e. a single locus affecting multiple distinct phenotypes) [220, 224, 225]. For this reason and more, they are often used to compliment genome-wide association studies (GWAS) [221]. To define a phenome, PheWAS primarily relies on electronic medical records (EMR), which contain longitudinal health histories, family histories, procedure codes, and the International Classification of Disease (ICD) codes [221]. ICD codes allow for the standardization of disease status, and are internationally recognized. ICD-10-Clinical Modification (CM) is the current coding version used and contains approximated 68,000 medical codes [288].

An additional layer in our bioinformatics approach includes expression quantitative trait locus (eQTL) analysis. eQTLs contain variants in the DNA that affect the expression of a gene, as measured by either expression microarrays or RNA sequencing, and significantly contribute to phenotypic variation [289, 290]. *Cis*-eQTLs, also known as allele-specific expression (ASE) polymorphisms, are SNPs located in or near the promoter region of the gene of interest [291]. Generally, *cis*-eQTLs lie within 1 Mb of the transcription start site of the gene they modify [292]. By combining genetic information from genetically diverse individuals with expression data, *cis*-eQTLs help identify downstream expression effects of disease-associated risk factors [293].

Finally, we used integrative platforms housing transcriptome-wide association studies (TWAS) and functional genomics data to evaluate the connection between tissue-specific expression of a gene and human disease. TWAS are highly powered analyses that utilize

eQTLs in specific tissues pinpointed by GWAS to highlight functionally relevant loci in a disease or phenotype of interest [227-229]. They allow for identification of trait-associated SNPs by aggregating the effects of many different regulatory variants into a single testing unit, thus targeting causal mediators of a disease and providing valuable insight into the disease biology [230]. Through our stratified approach, we identified putative causal disease SNPs and provided evidence of GDF11 as a likely intermediate gene and potential therapeutic for asthma and hypothyroidism.

**Methods**[10]

Ethics Statement: UK Biobank is a globally accessible, large-scale biomedical database containing genetic and disease information from over 500,000 European individuals [232]. Participants ranged from 40 to 69 years of age between the years 2006 and 2010. The North West Multi-Centre Research Ethics Committee (11/NW/ 0382) approved the UK Biobank project. Informed consent was obtained from each participant prior to collection of biological and anthropometric measurements, lifestyle indicators, blood and urine biomarkers, and information from their medical records [232].

The Genotype-Tissue Expression (GTEx) project collected 15,201 RNA-sequencing samples from 49 tissues of 838 postmortem donors. The organ procurement organizations that collected the biospecimens, Biospecimen Source Sites (BSS) chose to submit a GTEx research protocol and undergo IRB review or, per the consultation of their Office of Research Subject Protection, forwent further review on account of deceased donors not

[10] Adapted from Starcher A, Pazdro R, Ye K. GDF11-HEY1/2/L axis as a genetic modulator of heart disease. Submitted to *G3*, June 7, 2021.

constituting as human subjects [233, 234]. However, due to the large amount of sequencing data that is made publicly available, GTEx required explicit next-of-kin or otherwise legally authorized representative authorization for study participation [233]. Specific training regulating how BSS obtained consent can be found at http://gtextraining.org/. Only de-identified data according to HIPPAA policy is distributed to GTEx project collaborators (http://www.hhs.gov/ocr/privacy/hipaa/administrative/privacyrule-/index.html).

Phenome-wide association study on GDF11 risk variants: To extract relevant thyroid- and respiratory-related phenome-wide associations, we utilized GeneATLAS and Oxford Brain Imaging Genetics (BIG) Server (version 2.0) (http://www.nealelab.is/uk-biobank/) [239, 262]. GeneATLAS utilizes the UK Biobank cohort (N = 452,264) of White British individuals to systematically catalogue associations between 778 traits and over 30 million variants [262]. The associations were computed by use of Mixed Linear Models in a large supercomputer using the DISSECT software. We utilized the GeneATLAS "search by region" function to extract PheWAS associations located +/- 1000 kb of our gene of interest and significance was determined at $p < 1.0e-8$. Oxford BIG is a similar integrative platform containing data from over 5,100 GWAS sourced from GWAS Brain Imaging Derived Phenotypes (n = 3,144 studies), [232, 235], amyotrophic lateral sclerosis GWAS [236], Alzheimer's disease GWAS [237], ADHD GWAS from the EAGLE consortium (https://tweelingenregister.vu.nl/eagle-gwa-meta-analyses-summary-results), Magnetic NMR GWAS [238], and BMI, waist circumference and waist/hip ratio from the GIANT consortium data files

(http://portals.broadinstitute.org/collaboration/giant/index.php/GIANT_-consortium_data_files). Association analysis was performed using BGENIE [239]. We used the significance threshold $p < 5.0e-8$, commonly used in GWAS [240], when analyzing associations among the relevant phenotypes and our genes interest.

Genetic variant regulators of GDF11 expression: eQTLGen Consortium pools results from testing the expression of 19,250 genes in the blood in 31,684 blood samples from 37 datasets including cohorts from GTEx and the Framingham Heart Study [294]. eQTLGen's *cis*-eQTL analysis included 11 million SNPs with a window size of 1 Mb and minor allele frequency (MAF) of less than or equal to 1%. To be included in the results, *cis*-eQTLs have to be within a distance of 1 Mb from the center of the gene and have been tested in at least two cohorts. We identified GDF11's most significant *cis*-eQTL (rs7302200; $p = 4.93e-15$) and conducted a PheWAS analysis via the PheWeb portal (version 1.3.9; http://pheweb.sph.umich.edu/-SAIGE-UKB/about) to identify phenotypic associations. PheWeb utilizes UK Biobank data to provide an analysis of over 1400 ICD-based traits, integrated through SAIGE, a generalized mixed model association test. All participating individuals were imputed using the Haplotype Reference Consortium panel which produced over 20 million genetic variants and all genomic positions are on GRCh37. Adjustments were made for genetic relatedness, birth year, and sex. Bonferroni correction was applied on the number of tested ICD main codes (N = 1,944 codes) for a corrected p-value threshold of 2.5e-5 [295].

Transcriptome-wide association study on GDF11: Transcriptome-wide analyses were performed through TWAS Hub [227]. GWAS and functional data for hundreds of traits and over 100,000 expression models were synthesized within the TWAS Hub [227]. Summary association statistics came from 30 large-scale (n = 20,000 subjects) GWAS studies, and SNPs with minor allele frequencies of less than 1% were removed [230]. RNA sequencing data originated from CommonMind Consortium (brain, n =613) [241], GTEx (41 tissues) [242], and the Metabolic Syndrome in Men study (adipose, N = 563) [243, 244], and expression microarray data from the Young Finns Study (blood, N = 1,264) [245, 246], and the Netherlands Twins Registry (N = 1,247) [230, 247]. Associations were considered significant if they reached the tissue-specific threshold determined by Bonferroni correction at an $\alpha$ of 0.05.

Integrative genomic associations: We extracted functional variant associations from Open Target Genetics (https://genetics.opentargets.org), which is an integrative platform that aggregates human GWAS and functional genomics data such as protein abundance, gene expression, QTL colocalization, gene expression, and more [296]. The data came from the UK Biobank and GWAS Catalog summary statistics repository and were included only at $p < 5.0e\text{-}8$ [296]. Primarily, GWAS within the database were retrieved from NHGRI-EBI GWAS Catalog summary statistics database (N = 300) [222]. The SAIGE study of 2139 binary case-control phenotypes and the Neale lab study of 1283 quantitative traits (http://www.nealelab.is/uk-biobank) were also integrated along with summary statistics [296, 297], and studies from the NHGRI-EBI GWAS Catalog without summary statistics were included (N = 14,013 studies). Functional genomics data housed

within the Open Targets Genomics platform are protein QTLs of 2,994 plasma proteins from European individuals (N = 3301) [298], and eQTLs from eQTL Catalogue, eQTLGen, and GTEx (https://www.gtexportal.org/home/) [294, 299]. Additional datasets provide evidence for variant to gene (V2G) associations, which are assigned based on a systematic categorization and scoring method [300-302]. All traits were mapped to the Experimental Factor Ontology (EFO) [303] prior to statistical analysis. Significance was considered $p < 5.0e-8$ for all studies [296].

Resources

Oxford Brain Imaging Genetics (BIG) Server (version 2.0): http://big.stats.ox.ac.uk/

eQTLGen: https://www.eqtlgen.org/

TWAS Hub: http://twas-hub.org/

GeneATLAS: http://geneatlas.roslin.ed.ac.uk/

PheWeb: http://pheweb.sph.umich.edu/SAIGE-UKB/about

Open Targets Genetics Portal: https://genetics.opentargets.org/

**Results**

Phenome-wide results demonstrate many associations between GDF11 and lung health

We began by examining gene-phenotype associations extracted from White European UK Biobank participants (N = 452,264) within GeneATLAS, which synthesizes trait-gene associations from 30 million variants determined by prior GWAS studies [262]. The GDF11 locus +/- 1000 kb returned 94 significant results ($p < 1.0e-8$), two of which were related to the respiratory system, and three related to thyroid dysfunction (Table 5.1).

Chronic lower respiratory diseases ($p$ = 3.30e-11), asthma ($p$ = 7.40e-23), hypothyroidism/myxoedema ($p$ = 9.41e-16), other hypothyroidism ($p$ = 1.57e-9), and a general thyroid problem diagnosis ($p$ = 5.97e-11) were associated with SNPs within GDF11's genomic region (Chr12:55136 kb – 57152 kb). Further investigation of each of the causal SNPs in PheWeb revealed all five variants were significantly positively associated ($p$ < 2.5e-5) with hypothyroidism not otherwise specified (NOS), hypothyroidism, asthma, and nasal polyps (Supplemental Figure 5.1).

We conducted a parallel PheWAS analysis on results extracted from over 5,100 GWAS using data from over 400,000 UK Biobank participants. Four of the 86 significant ($p$ < 5.0e-8) disease phenotypes associated with GDF11 gene variants were related to lung function, and no thyroid or metabolic phenotypes were observed (Table 5.1). Emphysema ($p$ = 1.40e-29), COPD with acute lower respiratory infection ($p$ = 1.30e-10), other specified respiratory disorders ($p$ = 1.10e-9), and pneumonia ($p$ = 1.50e-8) returned significant associations. COPD with acute lower respiratory infection associated with GDF11 variant rs568577713 had the strongest effect size (0.20) of the relevant phenotypes.

Tissue-specific expression of GDF11 is associated with asthma and hypothyroidism

Transcriptome-wide analyses were conducted to identify the associations between tissue-specific expression of GDF11 and human disease. The approach provides additional specificity beyond what single eQTL analyses and GWAS can by capturing the full *cis*-SNP signal [227]. GDF11 had one tissue model comprised of 196 GWAS results:

unexposed suprapubic skin (Table 5.1). Smoking status was the strongest associated phenotype ($p$ = 4.01e-7). Interestingly, this association was positive suggesting GDF11 expression may be upregulated by smoking. Conversely, other associated respiratory phenotypes such as asthma ($p$ = 9.67e-5), and self-reported asthma ($p$ = 4.49e-5) were negatively associated with expression of GDF11 in this tissue. Significant phenotypes related to thyroid function included hypothyroidism ($p$ = 1.35e-5), and hypothyroidism/myxoedema ($p$ = 3.03e-5). These also were negatively associated with GDF11 expression in unexposed suprapubic skin. All reported associations remained significant after Bonferroni correction at an α of 0.05 for the tissue model.

*Cis*-eQTL analysis revealed variant associated with hypothyroidism and asthma

eQTL analysis conducted in 31,684 blood samples revealed 89 *cis*-eQTLs associated with GDF11. The strongest association was with the SNP rs7302200 in position Chr12:56449435 ($p$ = 4.93e-15) and was negative (Table 5.1). Subsequent PheWAS analysis utilizing UK Biobank participants revealed that this SNP was associated with asthma ($p$ = 7.60e-10), nasal polyps ($p$ = 2.10e-8), hypothyroidism NOS ($p$ = 3.20e-6), and hypothyroidism ($p$ = 1.50e-5; Table 5.2). Interestingly, these associations between GDF11's *cis*-eQTL and the disease phenotypes were positive.

Integrative functional and genomics data analysis confirms *cis*-eQTL and its involvement in lung disease

We examined rs7302200 (G/A) through the Open Target Genetics portal, which allows for prioritization of candidate causal variants at disease-associated loci based on

heterogeneous sources of functional and biological data [304]. Rs7302200 is at a distance of 312,371 bp from its canonical transcription start site and is functionally implicated with GDF11 in the blood in an inverse relationship ($p$ = 4.9e-15). While this association in Open Target Genetics corroborates the eQTL relationship identified in eQTLGen, it is not entirely novel as it relies on eQTLGen data for the reported *cis*-eQTL association that was used in their V2G pipeline analysis. PheWAS in UK Biobank and the GWAS Catalog summary statistics repository reported significant associations between rs7302200 and our diseases of interest. Non-cancer illness code of asthma ($p$ = 4.4e-18), asthma with other respiratory complications ($p$ = 2.8e-17), asthma ($p$ = 7.6e-10), hypothyroidism/myxoedema ($p$ = 8.1e-11) and never smoking ($p$ = 6.4e-9) were significantly associated with rs7302200 (Table 5.2). The positive association with the respiratory conditions in contrast to GDF11 provides evidence for negative regulation of this *cis*-eQTL (Figure 5.1).

**Discussion**

Hypothyroidism and asthma are both complex, chronic conditions whose pathogeneses and progression are largely dictated by inflammation [271-273]. Both conditions are often diagnosed in individuals with autoimmune disorders, such as Type 1 diabetes [274, 305], and have recently been associated with each other [280-287]. One study identified a SNP in the thyroid hormone receptor gene that is associated with the bronchodilator response in individuals with asthma [306]. However, current understanding of the genetic architecture of these diseases is slim. There have been few GWAS conducted on hypothyroidism [307-309], and so far they have only been able to explain a small amount

of thyroid function variability [274, 310]. Likewise, GWAS of asthma have identified multiple risk alleles, yet only explain a small portion of the disease prevalence [311, 312], demonstrating the need for further investigation of these diseases. Because of GDF11's involvement in inflammation [137-139, 267-269] as well as its reputed regenerative role in the adult mammal [41, 46, 47, 60], it is an intriguing genetic intermediate of hypothyroidism and asthma development.

Our phenome-wide and transcriptome-wide results provide evidence to support GDF11's involvement in hypothyroidism as well as various forms of lung diseases and conditions, particularly asthma (Table 5.1). Each variant of GDF11 individually related to asthma, hypothyroidism and nasal polyps, when analyzed in a complimentary PheWAS portal, also demonstrated associations with all these phenotypes (Supplemental Figure 5.1). These findings support an interconnectedness in the genetic contribution to the pathological biology of these diseases.

Furthermore, the relationships of GDF11 variants and tissue-specific expression of GDF11 with these disease phenotypes are negative, suggesting a protective role of GDF11. Prior studies support a similar inverse relationship reporting lower circulating levels of GDF11 were associated with abnormal glycometabolism and an increase in metabolic syndrome morbidity [56], and reduced circulating and lung GDF11 in subjects with COPD [269]. The first study also reported an inverse relationship between TSH and GDF11 concentrations after correcting for age and sex, however the association was statistically insignificant [56].

eQTL analyses illuminated many *cis*-eQTLs associated with GDF11, the most strongly associated one at rs7302200. *Cis*-eQTLs are powerful tools not only in identifying disease-variants, but also in drug discovery [313, 314]. We identified phenotypes associated with the SNP that mirrored those associated with GDF11 in multiple platforms, suggesting GDF11 may be an intermediate trait in part negatively regulated by rs7302200 in the pathological biology of asthma and hypothyroidism (Figure 5.2). The associations between the predictive variant and lung- and thyroid-related phenotypes, were the opposite direction of those between GDF11 and the disease phenotypes (Table 5.2). These inverse associations suggest the variant may be disease-contributing and down-regulate GDF11 expression either in response to or in the development of the chronic conditions. Such findings support the need for further investigation into the eQTL-GDF11 pathway as a modulator of asthma and hypothyroidism.

One such inverse relationship we discovered was a strong positive association between smoking status and tissue-specific expression of GDF11 (Table 5.1), and a phenome-wide positive association between never smoking and the *cis*-eQTL variant (Table 5.2). It has been reported that treatment of GDF11 *in vitro* can inhibit cellular senescence induced by cigarette smoke extract in lung cells [269]. Interestingly, a population-based study reported a negative association between smoking tobacco and hypothyroidism, noting a lower prevalence of hypothyroidism among current smokers [315]. Considering these two studies in the context of our results, we posit the SNP rs7302200 is down-regulated and GDF11 subsequently upregulated in response to cigarette smoking as a

protective defense, and an inverse regulatory effect in the pathogenesis of hypothyroidism.

In our prior work, we provided evidence of members of the hairy and enhancer of split-related (HESR) family of basic helix-loop-helix (bHLH) transcriptional repressors [199] serving as genetic regulators of GDF11[11]. Presently, we noted significant phenotypic associations between the genes Hes Related Family BHLH Transcription Factor with YRPW Motif 1 (HEY 1), 2 (HEY2) and L (HEYL) and respiratory and thyroid conditions, as we did with GDF11 (Supplemental Table 5.1). These conditions included asthma, emphysema, unspecified respiratory disorders, bronchiectasis, COPD, lobar pneumonia, and acute upper respiratory infections. Furthermore, the tissue-specific expression of HEY1 was positively associated with hypothyroidism, while the same disease relationship with GDF11 expression was negative (Table 5.1).

While our results highlight a putative novel genetic pathway for the regulation of asthma and hypothyroidism, some limitations exist. ICD coding used in phenome-wide analyses allows for standardization and universal use of disease terminology, but is subject to sensitivity and specificity concerns, variability in practice across healthcare facilities, and human inputting error [316]. Additionally, since use of these platforms and bioinformatic methods is so recent, further evaluation is needed to validate the associations and define appropriate clinical significance thresholds [316]. We applied Bonferroni correction for many transcriptome-wide associations to establish a conservative significance threshold,

[11] Starcher A, Pazdro R, Ye K. HEY-GDF11 axis as a genetic modulator of heart disease. To be submitted to *Gene*.

but not all of our variables were truly independent [221]. Finally, our approach used multiple databases to enhance the quality of evidence supporting the associations, however it should be noted that these databases were not completely independent from one another. There was significant overlap between the data housed in each database, namely most phenome-wide associations were sourced from the UK Biobank participants.

In conclusion, our layered phenome- and transcriptome-wide results illuminated significant negative associations between GDF11 and asthma and hypothyroidism, implicating a potential therapeutic role of GDF11 in these diseases, possibly due to its anti-inflammatory function. Furthermore, powerful *cis*-eQTL analyses revealed significant associations with not only GDF11 (negative), but also with our disease phenotypes of interest (positive), suggesting rs7302200 may serve as a down-regulator of GDF11 expression in the development of these diseases. Additional scientific inquiry should be made to mechanistically validate the rs7302200-GDF11 axis, examine rs7302200 as a predictive disease variant, specifically in the development of asthma and hypothyroidism, and explore GDF11's role as a therapeutic in these diseases.

**Figures and Legends**

| Phenotype | Effect Size |
|---|---|
| Asthma \| non-cancer illness code, self-reported | 0.0672 |
| Asthma \| blood clot, dvt, bronchitis, emphysema, asthma, rhinitis, eczema, allergy diagnosed by doctor | 0.0657 |
| Asthma | 0.061 |
| Asthma* | 0.061 |
| Never \| smoking status | 0.148 |
| Nasal polyps | 0.0287 |
| Nasal polyps* | 0.15 |
| Hypothyroidism/myxodema \| non-cancer illness code, self-reported | 0.0741 |
| Hypothyroidism NOS* | 0.062 |
| Hypothyroidism* | 0.056 |

**Key:** 0.0-0.03 | 0.031-0.06 | 0.061-0.09 | 0.091-.12

**FIGURE 5.1 - Heatmap of Phenome-Wide Effect Sizes for Hypothyroid- and Respiratory-Related Conditions Associated with Variant rs7302200.** Phenotypes with * indicate the association was from PheWeb, while all other phenotype associations were from the Open Target Genetics portal. Phenotypes were grouped according to disease/condition.

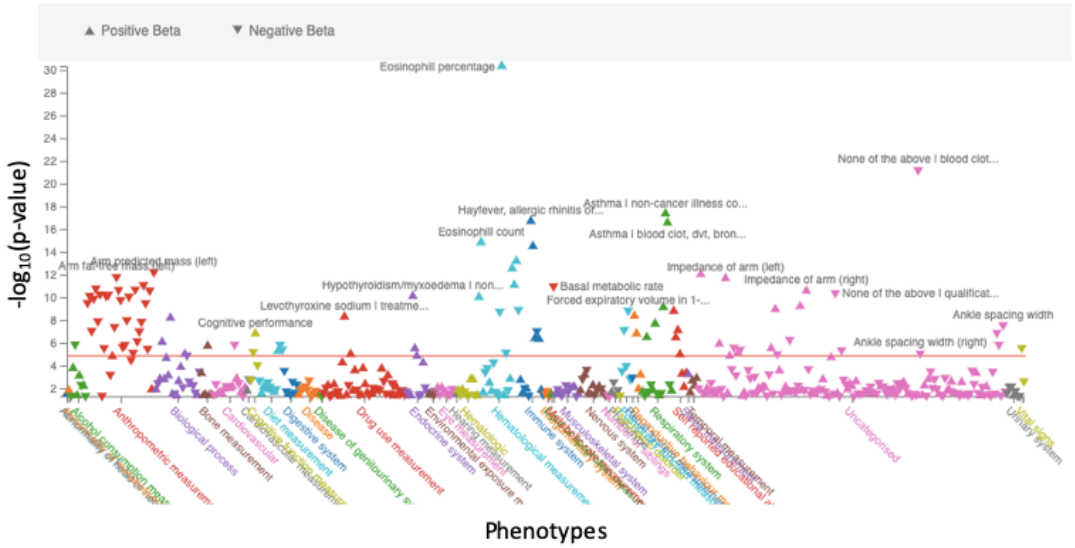


**FIGURE 5.2 - Phenotypic Associations with rs7302200**. Many phenotypic associations with the SNP rs7302200 reached significance ($p < 2.5e\text{-}5$) within the PheWeb portal. The strongest association was with eosinophil percentage ($p = 4.5e\text{-}31$). Our phenotypes of interest are the two asthma traits ($p = 4.40e\text{-}18$ and $p = 2.8e\text{-}17$), hypothyroidism/myxoedema ($p = 8.10e\text{-}11$), smoking status never ($p = 6.40e\text{-}9$), and nasal polyps ($p = 2.10e\text{-}8$).

**Tables and Legends**

**TABLE 5.1 - Significant Associations of Lung and Thyroid Phenotypes and *cis*-eQTLs with GDF11.** Phenome-wide analysis revealed associations between variants near and within the GDF11 locus and disease traits. The significance threshold for GeneATLAS was $p < 1.0e-8$, and $p < 5.0e-8$ for Oxford BIG. TWAS analyses through the TWAS Hub identified significant associations between lung and thyroid phenotypes and tissue-specific GDF11 expression associations. The significance threshold for TWAS Hub results was determined to be $p < 2.55e-4$ after Bonferroni correction at α of 0.05. eQTLGen data revealed the most significant *cis*-eQTL for GDF11: rs7302200 at position Chr12: 56449435.

| **PheWAS** | | | | | |
|---|---|---|---|---|---|
| **GeneATLAS** | **Trait** | **P-value** | **Position** | | **SNP ID** |
| | ICD10: J40-J47 Chronic lower respiratory diseases | 3.30E-11 | Chr12:56427808 | | rs1702877 |
| | Asthma | 7.40E-23 | Chr12:56396768 | | rs1689510 |
| | Hypothyroidism/myxoedema | 9.41E-16 | Chr12:56390636 | | rs1689510 |
| | ICD10: E03 Other Hypothyroidism | 1.57E-09 | Chr12:56384804 | | rs705699 |
| | Thyroid problem (not cancer) | 5.97E-11 | Chr12:56390636 | | rs705702 |
| **Oxford BIG** | **Trait** | **P-value** | **SNP ID** | **Effect Allele** | **Effect Size** |
| | ICD10: J43.9 Emphysema, unspecified | 1.40E-29 | rs141445925 | A | 0.076 |
| | ICD10: J44.0 Chronic obstructive pulmonary disease with acute lower respiratory infection | 1.30E-10 | rs568577713 | A | 0.20 |
| | ICD10: J98.8 Other specified respiratory disorders | 1.10E-09 | rs185488818 | A | 0.02 |
| | ICD10: J18.9 Pneumonia, unspecified | 1.50E-08 | rs185654642 | A | 0.048 |
| **TWAS Analysis** | | | | | |
| **TWAS Hub** | **Trait** | **Tissue** | | **P-value** | **Z-score** |
| | Smoking status | Skin not sun exposed suprapubic | | 4.01E-07 | 5.1 |
| | Hypothyroidism | | | 1.35E-05 | -4.3 |
| | Hypothyroidism/myxoedema | | | 3.03E-05 | -4.1 |
| | Asthma | | | 9.67E-05 | -3.8 |

| | | | | |
|---|---|---|---|---|
| | Asthma (self-reported) | | 4.49E-05 | -4 |
| **Most Significant *cis*-eQTL** | | | | |
| **eQTLGen** | **SNP** | **Position (hg19)** | **P-value for GDF11** | **Z-score** |
| | rs7302200 | 56449435 | 4.93E-15 | -7.83 |

**TABLE 5.2 - PheWAS Analysis of the Variant rs7302200 Responsible for the Significant *cis*-eQTL for GDF11.** PheWeb associations were considered significant at $p < 2.5e-5$. Phenome-wide associations from Open Target Genetics were considered significant at a p-value of less than 5.0e-8. Hypothyroidism NOS, hypothyroidism not otherwise specified; dvt, deep vein thrombosis.

| **PheWAS** | | | |
|---|---|---|---|
| **PheWeb** | **Associated Traits** | **P-value** | **Effect Size** |
| | Asthma | 7.60E-10 | 0.061 |
| | Nasal polyps | 2.10E-08 | 0.15 |
| | Hypothyroidism NOS | 3.20E-06 | 0.062 |
| | Hypothyroidism | 1.50E-05 | 0.056 |

| **Functional Genomics Analysis** | | | | |
|---|---|---|---|---|
| **Open Targets Genetics** | **eQTL Gene Association** | **Tissue** | **P-value** | **Effect Size** |
| | GDF11 | Blood | 4.9e-15 | -0.0669 |
| | **Trait** | | **P-value** | **Effect Size** |
| | Asthma \| non-cancer illness code, self-reported | | 4.40E-18 | 0.0672 |
| | Asthma \| blood clot, dvt, bronchitis, emphysema, asthma, rhinitis, eczema, allergy diagnosed by doctor | | 2.80E-17 | 0.0657 |

| | | | |
|---|---|---|---|
| | Hypothyroidism/myxoedema \| non-cancer illness code, self-reported | 8.10E-11 | 0.0741 |
| | Asthma | 7.6E-10 | 0.0610 |
| | Never \| smoking status | 6.40E-09 | 0.148 |
| | Nasal polyps | 2.10E-08 | 0.0287 |

**Supplemental Information**

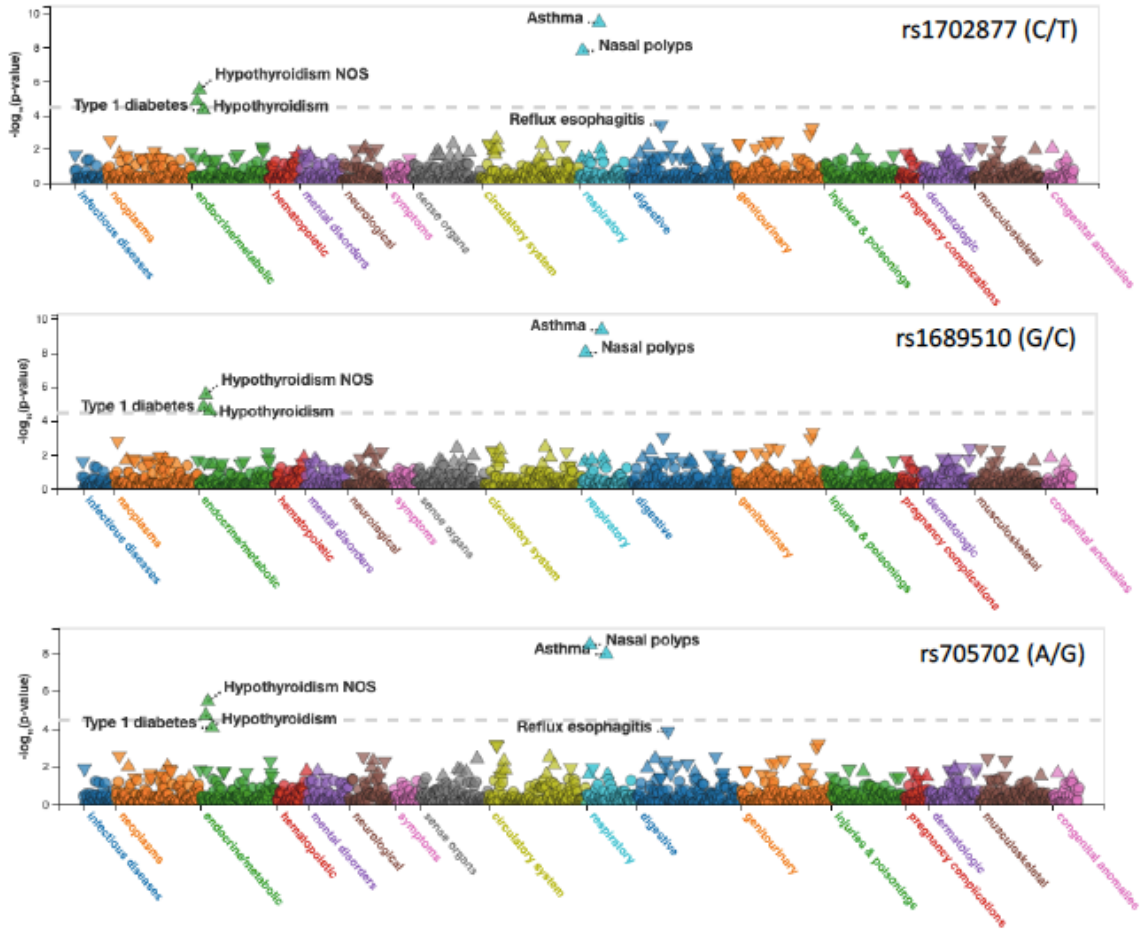

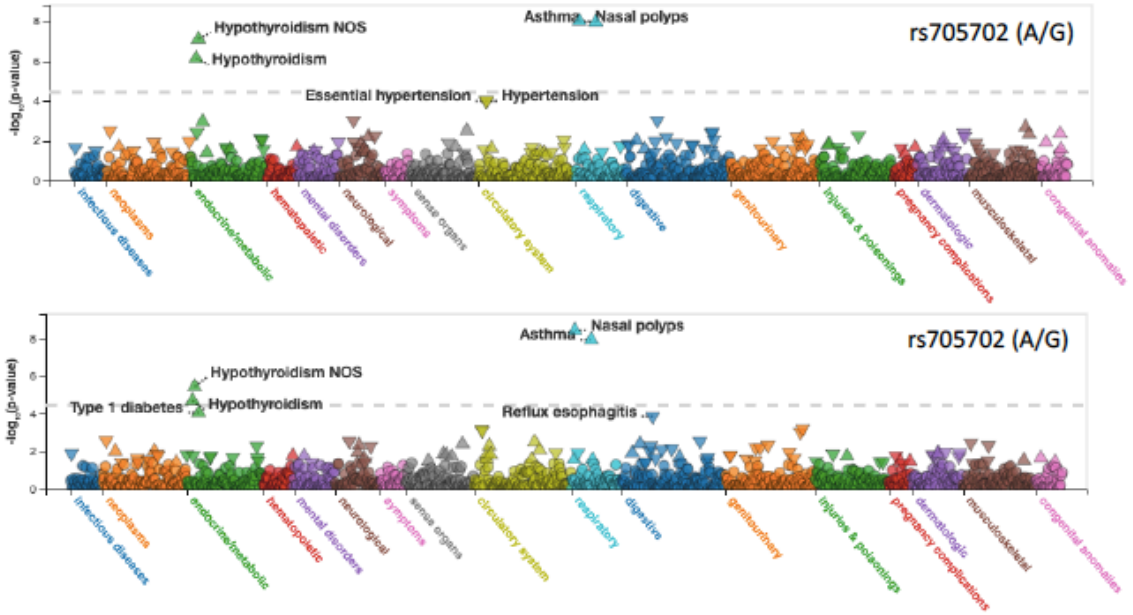


**SUPPLEMENTAL FIGURE 5.1 - GDF11 Variants Associated with Nasal Polyps, Asthma, Hypothyroidism NOS, and Hypothyroidism.** GeneATLAS revealed hypothyroid- and respiratory-related variants associated with GDF11. In PheWeb, each of these five variants were associated with the four listed phenotypes.

**SUPPLEMENTAL TABLE 5.1 - HEY1, HEY2, and HEYL Displayed Phenotypic and Transcriptomic Significance with Respiratory- and Thyroid-Related Conditions.** The phenome-wide analysis conducted in Oxford BIG resulted in many significant ($p < 5.0e-8$) associations with lung- and thyroid-related phenotypes. Transcriptome-wide analysis yielded significant ($p < 0.05$) relationships between the phenotypes of interest and tissue-specific HEY1 expression, alone.

| **HEY1** | | | | | |
|---|---|---|---|---|---|
| **PheWAS** | | | | | |
| **Oxford BIG** | **Respiratory-Related Phenotype** | **P-value** | **SNP ID** | **Effect Allele** | **Effect Size** |
| | ICD10: J98.8 Other specified respiratory disorders | 9.90E-17 | rs34087850 | C | 0.026 |
| | ICD10: J45.9 Asthma, unspecified | 8.40E-15 | rs182759854 | A | 0.036 |

| | | | | | |
|---|---|---|---|---|---|
| | ICD10: J43.9 Emphysema, unspecified | 4.50E-12 | rs144719766 | C | 0.058 |
| | ICD10: J47 Bronchiectasis | 5.00E-12 | rs190569778 | A | 0.077 |
| **TWAS** | | | | | |
| **PhenomeXcan** | **Thyroid-related Phenotype** | **Tissue** | **P-value** | **Z-score** | |
| | Non-cancer illness code, self-reported: thyroid problem (not cancer) | Minor salivary gland | 0.00906 | -2.6099 | |
| | | Hypothalamus | 0.0153 | -2.4248 | |
| | Hypothyroidism (congenital or acquired) | Testis | 0.00989 | 2.5798 | |
| **HEY2** | | | | | |
| **PheWAS** | | | | | |
| **Oxford BIG** | **Respiratory-related Phenotype** | **P-value** | **SNP ID** | **Effect Allele** | **Effect Size** |
| | ICD10: J44.1 Chronic obstructive pulmonary disease with acute exacerbation, unspecified | 9.60E-16 | rs570840849 | T | 0.13 |
| | ICD10: J18.1 Lobar pneumonia, unspecified | 4.10E-13 | rs117797136 | C | 0.037 |
| | ICD10: J18.0 Bronchopneumonia, unspecified | 5.80E-10 | rs192093804 | C | 0.043 |
| | ICD10: J47 Bronchiectasis | 7.40E-10 | rs574118179 | C | 0.064 |
| | ICD10: J45.9 Asthma, unspecified | 7.50E-10 | rs149354201 | A | 0.024 |
| | **Thyroid-related Phenotype** | **P-value** | **SNP ID** | **Effect Allele** | **Effect Size** |
| | ICD10: E05 Thyrotoxicosis [hyperthyroidism] | 5.60E-09 | rs570840849 | T | 0.0068 |
| **HEYL** | | | | | |
| **PheWAS** | | | | | |
| **Oxford BIG** | **Respiratory-related Phenotype** | **P-value** | **SNP ID** | **Effect Allele** | **Effect Size** |

| | | | | | |
|---|---|---|---|---|---|
| | ICD10: J98.8 Other specified respiratory disorders | 3.10E-44 | rs55113969 | A | 0.1 |
| | ICD10: J43.9 Emphysema, unspecified | 6.40E-27 | rs564586303 | T | 0.069 |
| | ICD10: J18.1 Lobar pneumonia, unspecified | 2.90E-24 | rs879876972 | G | 0.078 |
| | ICD10: J44.1 Chronic obstructive pulmonary disease with acute exacerbation, unspecified | 6.20E-10 | rs183808824 | A | 0.054 |
| | ICD10: J06 Acute upper respiratory infections of multiple and unspecified sites | 2.00E-08 | rs555799546 | A | 0.0059 |

***Supplemental file information***:

PhenomeXcan: http://apps.hakyimlab.org/phenomexcan/

PhenomeXcan includes transcriptome-wide gene expression results from 49 tissues using the latest GTEx (v8) data [248] that were then refined by a locus regional colocalization probability (locus RCP) [226]. Locus RCP was used to define putative causal gene contributors (locus RCP > 0.1). In our analyses, we considered p-values of < 0.01 to be significant at a threshold of 650 results to encompass all significant associations.

# CHAPTER 6

# CONCLUSION

In summary, the findings presented in this thesis provide evidence for the regulation of GDF11 by HEY genes, primarily HEY1 and HEY2, and for GDF11 as an intermediate trait in the pathological biology of asthma and hypothyroidism. As for the contentiously debated age-reversing effects of GDF11 in the heart, we were unable to strongly affirm or negate the relationship. However, we did find evidence of tissue-specific expression and variants of GDF11 positively associated with several cardiovascular disease conditions (Chapter four). Furthermore, findings in Chapter three underscore a relatively weak, inconsistent relationship between total serum GDF11 levels and cardiac hypertrophy in a genetically-diverse population of adult mice and support a stronger, consistent anti-hypertrophic role for its homolog, myostatin.

Genetic mapping of serum GDF11 illuminated a QTL near HEY1, a transcriptional repressor with putative binding sites located in close proximity to the GDF11 gene in the mouse and human genomes (Chapter three). The Hey1 protein shares this binding motif with its relatives Hey2 and HeyL, which are all part of the Notch pathway, a signaling cascade that mediates the proliferation and differentiation of cardiomyocytes as well as remodeling the developed heart under stress. These results form the necessary foundation for future studies, which will further interrogate the Hey proteins as regulators of GDF11 and cardiovascular disease, and lead to a better understanding of the cardiovascular impact of GDF11 in older adults.

We provided further evidence for the HEY-GDF11 axis by noting common, yet opposite associations between GDF11 with cardiovascular conditions and HEY1/2/L with cardiovascular conditions in human genetics portals (Chapter four). We leveraged UK Biobank data as well as other GWAS results, GTEx expression information, and more to identify human disease associations with tissue-specific expression and variants of our genes of interest. GDF11 demonstrated mostly positive phenome-wide and transcriptome-wide associations with heart impairments including aortic valve disorder, endocarditis, hypertension, heart failure, and cardiomyopathy. HEY1 and HEY2 in particular were largely negatively associated with heart conditions such as hypertension, endocarditis, and cardiovascular disease. The overlapping and inverse relationships add evidence of the negative regulation of GDF11 by HEY genes.

Furthermore, the inverse relationships with disease states between GDF11 and HEY members continued in our exploration of thyroid and respiratory conditions (Chapter 5). When examining transcriptome-wide associations, we found GDF11 was negatively associated with asthma and hypothyroidism and positively associated with smoking status, whereas HEY1 was negatively associated with hypothyroidism and HEY2 positively associated with hyperthyroidism. GDF11 also shared several common phenome-wide respiratory disease associations with HEY1, HEY2, and HEYL such as asthma, chronic obstructive pulmonary disease, and emphysema.

Additionally, powerful *cis*-eQTL analyses revealed significant associations with not only GDF11 (negative), but also with our disease phenotypes of interest (positive), suggesting rs7302200 may serve as a down-regulator of GDF11 expression in the pathological biology of asthma and hypothyroidism (Chapter 5). GDF11's negative

associations with these diseases makes it an intriguing potential therapeutic, especially due to its documented anti-inflammatory effects through the inhibition of the nuclear factor kappa-light-chain-enhancer of activated B cells (NF-kB) and JNK signaling pathways by TGF-β/Smad2/3 activation. Additional mechanistic studies are needed to validate rs7302200-GDF11 regulation, examine rs7302200 as a predictive disease variant in the development of asthma and hypothyroidism, and explore GDF11's role as a therapeutic in these diseases.

**References:**


1. *WHO reveals leading causes of death and disability worldwide: 2000-2019*. 2020: WHO.

2. Virani Salim, S., et al., *Heart Disease and Stroke Statistics—2020 Update: A Report From the American Heart Association.* Circulation, 2020. **141**(9): p. e139-e596.

3. Benjamin, E.J., et al., *Heart Disease and Stroke Statistics-2019 Update: A Report From the American Heart Association.* Circulation, 2019. **139**(10): p. e56-e528.

4. Heidenreich, P.A., et al., *Forecasting the impact of heart failure in the United States: a policy statement from the American Heart Association.* Circulation. Heart failure, 2013. **6**(3): p. 606-619.

5. Díez-Villanueva, P. and F. Alfonso, *Heart failure in the elderly.* Journal of geriatric cardiology : JGC, 2016. **13**(2): p. 115-117.

6. Ziaeian, B. and G.C. Fonarow, *Epidemiology and aetiology of heart failure.* Nature reviews. Cardiology, 2016. **13**(6): p. 368-378.

7. Inamdar, A.A. and A.C. Inamdar, *Heart Failure: Diagnosis, Management and Utilization.* Journal of clinical medicine, 2016. **5**(7): p. 62.

8. Tham, Y.K., et al., *Pathophysiology of cardiac hypertrophy and heart failure: signaling pathways and novel therapeutic targets.* Arch Toxicol, 2015. **89**(9): p. 1401-38.

9. Ramaraj, R., *Hypertrophic Cardiomyopathy: Etiology, Diagnosis, and Treatment.* Cardiology in Review, 2008. **16**(4).

10. Dai, D.-F., et al., *Cardiac aging: from molecular mechanisms to significance in human health and disease.* Antioxidants & redox signaling, 2012. **16**(12): p. 1492-1526.

11. Tardiff, J.C., *Cardiac hypertrophy: stressing out the heart.* The Journal of clinical investigation, 2006. **116**(6): p. 1467-1470.

12. Mihl, C., W.R.M. Dassen, and H. Kuipers, *Cardiac remodelling: concentric versus eccentric hypertrophy in strength and endurance athletes.* Netherlands heart journal : monthly journal of the Netherlands Society of Cardiology and the Netherlands Heart Foundation, 2008. **16**(4): p. 129-133.

13. Bujak, M., et al., *Aging-related defects are associated with adverse cardiac remodeling in a mouse model of reperfused myocardial infarction.* J Am Coll Cardiol, 2008. **51**(14): p. 1384-92.

14. Olivetti, G., et al., *Cardiomyopathy of the aging human heart. Myocyte loss and reactive cellular hypertrophy.* Circ Res, 1991. **68**(6): p. 1560-8.

15. Lorell, B.H., et al., *Diastolic function in left ventricular hypertrophy: clinical and experimental relationships.* Eur Heart J, 1990. **11 Suppl G**: p. 54-64.

16. Chiao, Y.A. and P.S. Rabinovitch, *The Aging Heart.* Cold Spring Harbor perspectives in medicine, 2015. **5**(9): p. a025148-a025148.

17. Lakatta, E.G. and D. Levy, *Arterial and cardiac aging: major shareholders in cardiovascular disease enterprises: Part II: the aging heart in health: links to heart disease.* Circulation, 2003. **107**(2): p. 346-54.

18. Foo, R.S., K. Mani, and R.N. Kitsis, *Death begets failure in the heart.* J Clin Invest, 2005. **115**(3): p. 565-71.

19. Berk, B.C., K. Fujiwara, and S. Lehoux, *ECM remodeling in hypertensive heart disease.* J Clin Invest, 2007. **117**(3): p. 568-75.

20. Spinale, F.G., *Myocardial matrix remodeling and the matrix metalloproteinases: influence on cardiac form and function.* Physiol Rev, 2007. **87**(4): p. 1285-342.

21. Lee, R.T., *Matrix metalloproteinase inhibition and the prevention of heart failure.* Trends Cardiovasc Med, 2001. **11**(5): p. 202-5.

22. Volders, P.G., et al., *Interstitial collagen is increased in the non-infarcted human myocardium after myocardial infarction.* J Mol Cell Cardiol, 1993. **25**(11): p. 1317-23.

23. Dai, D.F., et al., *Overexpression of catalase targeted to mitochondria attenuates murine cardiac aging.* Circulation, 2009. **119**(21): p. 2789-97.

24. Hobai, I.A. and B. O'Rourke, *Decreased sarcoplasmic reticulum calcium content is responsible for defective excitation-contraction coupling in canine heart failure.* Circulation, 2001. **103**(11): p. 1577-84.

25. O'Rourke, B., et al., *Mechanisms of altered excitation-contraction coupling in canine tachycardia-induced heart failure, I: experimental studies.* Circ Res, 1999. **84**(5): p. 562-70.

26. Cruickshank, J.M., *The role of coronary perfusion pressure.* Eur Heart J, 1992. **13 Suppl D**: p. 39-43.

27. Dai, D.F., et al., *Mitochondrial oxidative stress mediates angiotensin II-induced cardiac hypertrophy and Galphaq overexpression-induced heart failure.* Circ Res, 2011. **108**(7): p. 837-46.

28. Rabinowitz, M. and R. Zak, *Mitochondria and cardiac hypertrophy.* Circ Res, 1975. **36**(3): p. 367-76.

29. Raskoff, W.J., S. Goldman, and K. Cohn, *The "athletic heart". Prevalence and physiological significance of left ventricular enlargement in distance runners.* Jama, 1976. **236**(2): p. 158-62.

30. Hart, G., *Exercise-induced cardiac hypertrophy: a substrate for sudden death in athletes?* Exp Physiol, 2003. **88**(5): p. 639-44.

31. Bevegård, B.S. and J.T. Shepherd, *Regulation of the circulation during exercise in man.* Physiol Rev, 1967. **47**(2): p. 178-213.

32. Wakatsuki, T., J. Schlessinger, and E.L. Elson, *The biochemical response of the heart to hypertension and exercise.* Trends Biochem Sci, 2004. **29**(11): p. 609-17.

33. Selvetella, G., et al., *Adaptive and maladaptive hypertrophic pathways: points of convergence and divergence.* Cardiovascular Research, 2004. **63**(3): p. 373-380.

34. Nauta, J.F., et al., *Concentric vs. eccentric remodelling in heart failure with reduced ejection fraction: clinical characteristics, pathophysiology and response to treatment.* European Journal of Heart Failure, 2020. **22**(7): p. 1147-1155.

35. Nakamura, M. and J. Sadoshima, *Mechanisms of physiological and pathological cardiac hypertrophy.* Nat Rev Cardiol, 2018. **15**(7): p. 387-407.

36. de Simone, G., *Concentric or Eccentric Hypertrophy: How Clinically Relevant Is the Difference?* Hypertension, 2004. **43**(4): p. 714-715.

37. Gaasch, W.H. and M.R. Zile, *Left ventricular structural remodeling in health and disease: with special emphasis on volume, mass, and geometry.* J Am Coll Cardiol, 2011. **58**(17): p. 1733-40.

38. Metra, M., et al., *Acute heart failure in elderly patients: worse outcomes and differential utility of standard prognostic variables. Insights from the PROTECT trial.* Eur J Heart Fail, 2015. **17**(1): p. 109-18.

39. Metra, M., et al., *Acute heart failure in the elderly: differences in clinical characteristics, outcomes, and prognostic factors in the VERITAS Study.* J Card Fail, 2015. **21**(3): p. 179-88.

40. Simoni-Nieves, A., et al., *GDF11 Implications in Cancer Biology and Metabolism. Facts and Controversies.* Frontiers in Oncology, 2019. **9**(1039).

41. Loffredo, F.S., et al., *Growth differentiation factor 11 is a circulating factor that reverses age-related cardiac hypertrophy.* Cell, 2013. **153**(4): p. 828-39.

42. Yoshioka, J., et al., *Targeted deletion of thioredoxin-interacting protein regulates cardiac dysfunction in response to pressure overload.* Circ Res, 2007. **101**(12): p. 1328-38.

43. Yin, F.C., et al., *Use of tibial length to quantify cardiac hypertrophy: application in the aging rat.* Am J Physiol, 1982. **243**(6): p. H941-7.

44. Jackson, M.F., et al., *The aging myostatin null phenotype: reduced adiposity, cardiac hypertrophy, enhanced cardiac stress response, and sexual dimorphism.* J Endocrinol, 2012. **213**(3): p. 263-75.

45. McPherron, A.C., *METABOLIC FUNCTIONS OF MYOSTATIN AND GDF11.* Immunol Endocr Metab Agents Med Chem, 2010. **10**(4): p. 217-231.

46. Sinha, M., et al., *Restoring systemic GDF11 levels reverses age-related dysfunction in mouse skeletal muscle.* Science, 2014. **344**(6184): p. 649-52.

47. Katsimpardi, L., et al., *Vascular and neurogenic rejuvenation of the aging mouse brain by young systemic factors.* Science, 2014. **344**(6184): p. 630-4.

48. Takei, Y., *Age-dependent decline in neurogenesis of the hippocampus and extracellular nucleotides.* Hum Cell, 2019. **32**(2): p. 88-94.

49. Egerman, M.A., et al., *GDF11 Increases with Age and Inhibits Skeletal Muscle Regeneration.* Cell Metab, 2015. **22**(1): p. 164-74.

50. Smith, S.C., et al., *GDF11 does not rescue aging-related pathological hypertrophy.* Circ Res, 2015. **117**(11): p. 926-32.

51. Chen, Y., et al., *Relationship of serum GDF11 levels with bone mineral density and bone turnover markers in postmenopausal Chinese women.* Bone Res, 2016. **4**: p. 16012.

52. Zhang, Y., et al., *Growth differentiation factor 11 is a protective factor for osteoblastogenesis by targeting PPARgamma.* Gene, 2015. **557**(2): p. 209-14.

53. Liu, A., et al., *Growth differentiation factor 11 worsens hepatocellular injury and liver regeneration after liver ischemia reperfusion injury.* Faseb j, 2018. **32**(9): p. 5186-5198.

54. Ahn, S.-T., et al., *Evaluation of growth differentiation factor 11 (GDF11) levels in dogs with chronic mitral valve insufficiency.* Canadian journal of veterinary research = Revue canadienne de recherche veterinaire, 2016. **80**(1): p. 90-92.

55. Yang, R., et al., *Quantitation of circulating GDF-11 and β2-MG in aged patients with age-related impairment in cognitive function.* Clin Sci (Lond), 2017. **131**(15): p. 1895-1904.

56. Xu, B., et al., *Serum growth differentiation factor 11 is closely related to metabolic syndrome in a Chinese cohort.* Journal of Diabetes Investigation, 2021. **12**(2): p. 234-243.

57. Kalampouka, I., A. van Bekhoven, and B.T. Elliott, *Differing Effects of Younger and Older Human Plasma on C2C12 Myocytes in Vitro.* Front Physiol, 2018. **9**: p. 152.

58. Tian, J., et al., *The effects of aging, diabetes mellitus, and antiplatelet drugs on growth factors and anti-aging proteins in platelet-rich plasma.* Platelets, 2019. **30**(6): p. 773-792.

59. Añón-Hidalgo, J., et al., *Circulating GDF11 levels are decreased with age but are unchanged with obesity and type 2 diabetes.* Aging (Albany NY), 2019. **11**(6): p. 1733-1744.

60. Poggioli, T., et al., *Circulating Growth Differentiation Factor 11/8 Levels Decline With Age.* Circ Res, 2016. **118**(1): p. 29-37.

61. Natsuume-Sakai, S., K. Motonishi, and S. Migita, *Quantitative estimations of five classes of immunoglobulin in inbred mouse strains.* Immunology, 1977. **32**(6): p. 861-6.

62. Walker, R.G., et al., *Biochemistry and Biology of GDF11 and Myostatin: Similarities, Differences, and Questions for Future Investigation.* Circulation research, 2016. **118**(7): p. 1125-1142.

63. Olson, K.A., et al., *Association of growth differentiation factor 11/8, putative anti-ageing factor, with cardiovascular outcomes and overall mortality in humans: analysis of the Heart and Soul and HUNT3 cohorts.* Eur Heart J, 2015. **36**(48): p. 3426-34.

64. Rodgers, B.D. and J.A. Eldridge, *Reduced Circulating GDF11 Is Unlikely Responsible for Age-Dependent Changes in Mouse Heart, Muscle, and Brain.* Endocrinology, 2015. **156**(11): p. 3885-8.

65. Bergen, H.R., 3rd, et al., *Myostatin as a mediator of sarcopenia versus homeostatic regulator of muscle mass: insights using a new mass spectrometry-based assay.* Skelet Muscle, 2015. **5**: p. 21.

66. Schafer, M.J., et al., *Quantification of GDF11 and Myostatin in Human Aging and Cardiovascular Disease.* Cell Metab, 2016. **23**(6): p. 1207-1215.

67. Semba, R.D., et al., *Relationship of Circulating Growth and Differentiation Factors 8 and 11 and Their Antagonists as Measured Using Liquid Chromatography-Tandem Mass Spectrometry With Age and Skeletal Muscle Strength in Healthy Adults.* J Gerontol A Biol Sci Med Sci, 2019. **74**(1): p. 129-136.

68. Camparini, L., et al., *Targeted Approach to Distinguish and Determine Absolute Levels of GDF8 and GDF11 in Mouse Serum.* PROTEOMICS, 2020. **n/a**(n/a): p. 1900104.

69. Du, G.Q., et al., *Targeted myocardial delivery of GDF11 gene rejuvenates the aged mouse heart and enhances myocardial regeneration after ischemia-reperfusion injury.* Basic Res Cardiol, 2017. **112**(1): p. 7.

70. Fife, E., et al., *Relationship of muscle function to circulating myostatin, follistatin and GDF11 in older women and men.* BMC geriatrics, 2018. **18**(1): p. 200-200.

71. Padyana, A.K., et al., *Crystal structure of human GDF11.* Acta Crystallogr F Struct Biol Commun, 2016. **72**(Pt 3): p. 160-4.

72. Walker, R.G., et al., *Structural basis for potency differences between GDF8 and GDF11.* BMC Biol, 2017. **15**(1): p. 19.

73. Ge, G., et al., *GDF11 forms a bone morphogenetic protein 1-activated latent complex that can modulate nerve growth factor-induced differentiation of PC12 cells.* Molecular and cellular biology, 2005. **25**(14): p. 5846-5858.

74. Kim, J., et al., *GDF11 controls the timing of progenitor cell competence in developing retina.* Science, 2005. **308**(5730): p. 1927-30.

75. Souza, T.A., et al., *Proteomic identification and functional validation of activins and bone morphogenetic protein 11 as candidate novel muscle mass regulators.* Mol Endocrinol, 2008. **22**(12): p. 2689-702.

76. McPherron, A.C., T.V. Huynh, and S.J. Lee, *Redundancy of myostatin and growth/differentiation factor 11 function.* BMC Dev Biol, 2009. **9**: p. 24.

77. Lee, S.J. and A.C. McPherron, *Regulation of myostatin activity and muscle growth.* Proc Natl Acad Sci U S A, 2001. **98**(16): p. 9306-11.

78. Langley, B., et al., *Myostatin inhibits myoblast differentiation by down-regulating MyoD expression.* J Biol Chem, 2002. **277**(51): p. 49831-40.

79. Oh, S.P., et al., *Activin type IIA and IIB receptors mediate Gdf11 signaling in axial vertebral patterning.* Genes Dev, 2002. **16**(21): p. 2749-54.

80. Philip, B., Z. Lu, and Y. Gao, *Regulation of GDF-8 signaling by the p38 MAPK.* Cell Signal, 2005. **17**(3): p. 365-75.

81. Rebbapragada, A., et al., *Myostatin signals through a transforming growth factor beta-like signaling pathway to block adipogenesis.* Mol Cell Biol, 2003. **23**(20): p. 7230-42.

82. Sidis, Y., et al., *Biological activity of follistatin isoforms and follistatin-like-3 is dependent on differential cell surface binding and specificity for activin, myostatin, and bone morphogenetic proteins.* Endocrinology, 2006. **147**(7): p. 3586-97.

83. Kondás, K., et al., *Both WFIKKN1 and WFIKKN2 have high affinity for growth and differentiation factors 8 and 11.* J Biol Chem, 2008. **283**(35): p. 23677-84.

84. Suh, J. and Y.-S. Lee, *Similar sequences but dissimilar biological functions of GDF11 and myostatin.* Experimental & Molecular Medicine, 2020. **52**(10): p. 1673-1693.

85. Chang, K.T., et al., *Aminode: Identification of Evolutionary Constraints in the Human Proteome.* Sci Rep, 2018. **8**(1): p. 1357.

86. Zhang, Y., et al., *Role of growth differentiation factor 11 in development, physiology and disease.* Oncotarget, 2017. **8**(46): p. 81604-81616.

87. Lee, Y.S. and S.J. Lee, *Regulation of GDF-11 and myostatin activity by GASP-1 and GASP-2.* Proc Natl Acad Sci U S A, 2013. **110**(39): p. E3713-22.

88. Mosher, D.S., et al., *A mutation in the myostatin gene increases muscle mass and enhances racing performance in heterozygote dogs.* PLoS Genet, 2007. **3**(5): p. e79.

89. Clop, A., et al., *A mutation creating a potential illegitimate microRNA target site in the myostatin gene affects muscularity in sheep.* Nat Genet, 2006. **38**(7): p. 813-8.

90. Schuelke, M., et al., *Myostatin mutation associated with gross muscle hypertrophy in a child.* N Engl J Med, 2004. **350**(26): p. 2682-8.

91. McPherron, A.C., A.M. Lawler, and S.J. Lee, *Regulation of anterior/posterior patterning of the axial skeleton by growth/differentiation factor 11.* Nat Genet, 1999. **22**(3): p. 260-4.

92. Egerman, M.A. and D.J. Glass, *The role of GDF11 in aging and skeletal muscle, cardiac and bone homeostasis.* Crit Rev Biochem Mol Biol, 2019. **54**(2): p. 174-183.

93. Zhou, Y., et al., *Circulating Concentrations of Growth Differentiation Factor 11 Are Heritable and Correlate With Life Span.* The Journals of Gerontology: Series A, 2016. **71**(12): p. 1560-1563.

94. Bueno, J.L., et al., *Growth differentiation factor 11 (GDF11) - a promising anti-ageing factor - is highly concentrated in platelets.* Vox Sang, 2016. **111**(4): p. 434-436.

95. Ahamed, J., et al., *In vitro and in vivo evidence for shear-induced activation of latent transforming growth factor-beta1.* Blood, 2008. **112**(9): p. 3650-60.

96. Duran, J., et al., *GDF11 Modulates Ca(2+)-Dependent Smad2/3 Signaling to Prevent Cardiomyocyte Hypertrophy.* Int J Mol Sci, 2018. **19**(5).

97. Zhang, C., et al., *GDF11 Attenuated ANG II-Induced Hypertrophic Cardiomyopathy and Expression of ANP, BNP and Beta-MHC Through Down-Regulating CCL11 in Mice.* Curr Mol Med, 2018. **18**(10): p. 661-671.

98. (US), I.o.M., *Cardiovascular Disability: Updating the Social Security Listings*, in *Ischemic Heart Disease*, C.o.S.S.C.D. Criteria, Editor. 2010, National Academies Press (US): Washington (DC). p. 7.

99. Kalogeris, T., et al., *Cell biology of ischemia/reperfusion injury.* International review of cell and molecular biology, 2012. **298**: p. 229-317.

100. Kalogeris, T., et al., *Ischemia/Reperfusion.* Comprehensive Physiology, 2016. **7**(1): p. 113-170.

101. Hudobenko, J., et al., *Growth differentiation factor-11 supplementation improves survival and promotes recovery after ischemic stroke in aged mice.* Aging, 2020. **12**(9): p. 8049-8066.

102. Su, H.H., et al., *Exogenous GDF11 attenuates non-canonical TGF-β signaling to protect the heart from acute myocardial ischemia-reperfusion injury.* Basic Res Cardiol, 2019. **114**(3): p. 20.

103. McNally, E.M., *Questions and Answers About Myostatin, GDF11, and the Aging Heart.* Circulation research, 2016. **118**(1): p. 6-8.

104. Harper, S.C., et al., *Is Growth Differentiation Factor 11 a Realistic Therapeutic for Aging-Dependent Muscle Defects?* Circ Res, 2016. **118**(7): p. 1143-50; discussion 1150.

105. Jin, Q., et al., *Neonatal Systemic AAV-Mediated Gene Delivery of GDF11 Inhibits Skeletal Muscle Growth.* Molecular therapy : the journal of the American Society of Gene Therapy, 2018. **26**(4): p. 1109-1117.

106. Bernardo, B.C., et al., *Molecular distinction between physiological and pathological cardiac hypertrophy: experimental findings and therapeutic strategies.* Pharmacol Ther, 2010. **128**(1): p. 191-227.

107. McMullen, J.R. and G.L. Jennings, *Differences between pathological and physiological cardiac hypertrophy: novel therapeutic strategies to treat heart failure.* Clin Exp Pharmacol Physiol, 2007. **34**(4): p. 255-62.

108. Zhang, X.-J., et al., *Growth differentiation factor 11 is involved in isoproterenol-induced heart failure.* Molecular medicine reports, 2019. **19**(5): p. 4109-4118.

109. Yu, X., et al., *Growth Differentiation Factor 11 Promotes Abnormal Proliferation and Angiogenesis of Pulmonary Artery Endothelial Cells.* Hypertension, 2018. **71**(4): p. 729-741.

110. Akhmedov, A., et al., *P290GDF11 promotes increased sensitivity of the murine heart to ischemic injury.* Cardiovascular Research, 2018. **114**(suppl_1): p. S74-S74.

111. Fried, L.P., et al., *Frailty in older adults: evidence for a phenotype.* J Gerontol A Biol Sci Med Sci, 2001. **56**(3): p. M146-56.

112. Harper, S.C., et al., *GDF11 Decreases Pressure Overload-Induced Hypertrophy, but Can Cause Severe Cachexia and Premature Death.* Circulation research, 2018. **123**(11): p. 1220-1231.

113. Zimmers, T.A., et al., *Exogenous GDF11 induces cardiac and skeletal muscle dysfunction and wasting.* Basic Res Cardiol, 2017. **112**(4): p. 48.

114. Hammers, D.W., et al., *Supraphysiological levels of GDF11 induce striated muscle atrophy.* EMBO Mol Med, 2017. **9**(4): p. 531-544.

115. Fan, X., et al., *The Growth Differentiation Factor 11 (GDF11) and Myostatin (MSTN) in tissue specific aging.* Mech Ageing Dev, 2017. **164**: p. 108-112.

116. Roh, J.D., et al., *Activin type II receptor signaling in cardiac aging and heart failure.* Sci Transl Med, 2019. **11**(482).

117. Jin, Q., et al., *Neonatal Systemic AAV-Mediated Gene Delivery of GDF11 Inhibits Skeletal Muscle Growth.* Mol Ther, 2018. **26**(4): p. 1109-1117.

118. Leibowitz, D., *Left Ventricular Hypertrophy and Chronic Renal Insufficiency in the Elderly.* Cardiorenal Medicine, 2014. **4**(3-4): p. 168-175.

119. Almodovar, A.J., et al., *Genomic structure and genetic drift in C57BL/6 congenic metabolic mutant mice.* Mol Genet Metab, 2013. **110**(3): p. 396-400.

120. Zimmers, T.A., et al., *Induction of cachexia in mice by systemically administered myostatin.* Science, 2002. **296**(5572): p. 1486-8.

121. McPherron, A.C., A.M. Lawler, and S.J. Lee, *Regulation of skeletal muscle mass in mice by a new TGF-beta superfamily member.* Nature, 1997. **387**(6628): p. 83-90.

122. Nakashima, M., et al., *Expression of growth/differentiation factor 11, a new member of the BMP/TGFbeta superfamily during mouse embryogenesis.* Mech Dev, 1999. **80**(2): p. 185-9.

123. Gamer, L.W., et al., *A novel BMP expressed in developing mouse limb, spinal cord, and tail bud is a potent mesoderm inducer in Xenopus embryos.* Dev Biol, 1999. **208**(1): p. 222-32.

124. Gokoffski, K.K., et al., *Activin and GDF11 collaborate in feedback control of neuroepithelial stem cell proliferation and fate.* Development (Cambridge, England), 2011. **138**(19): p. 4131-4142.

125. Wu, H.H., et al., *Autoregulation of neurogenesis by GDF11.* Neuron, 2003. **37**(2): p. 197-207.

126. Harmon, E.B., et al., *GDF11 modulates NGN3+ islet progenitor cell number and promotes beta-cell differentiation in pancreas development.* Development, 2004. **131**(24): p. 6163-74.

127. Jamaiyar, A., et al., *The versatility and paradox of GDF 11.* Pharmacol Ther, 2017. **175**: p. 28-34.

128. Farooq, M., et al., *Histone deacetylase 3 (hdac3) is specifically required for liver development in zebrafish.* Dev Biol, 2008. **317**(1): p. 336-53.

129. Gamer, L.W., et al., *Gdf11 is a negative regulator of chondrogenesis and myogenesis in the developing chick limb.* Dev Biol, 2001. **229**(2): p. 407-20.

130. Zhang, X., et al., *Activation of the growth-differentiation factor 11 gene by the histone deacetylase (HDAC) inhibitor trichostatin A and repression by HDAC3.* Mol Cell Biol, 2004. **24**(12): p. 5106-18.

131. Gerardo-Ramírez, M., et al., *GDF11 exhibits tumor suppressive properties in hepatocellular carcinoma cells by restricting clonal expansion and invasion.* Biochim Biophys Acta Mol Basis Dis, 2019. **1865**(6): p. 1540-1554.

132. Bajikar, S.S., et al., *Tumor-Suppressor Inactivation of GDF11 Occurs by Precursor Sequestration in Triple-Negative Breast Cancer.* Dev Cell, 2017. **43**(4): p. 418-435.e13.

133. Yokoe, T., et al., *Clinical significance of growth differentiation factor 11 in colorectal cancer.* Int J Oncol, 2007. **31**(5): p. 1097-101.

134. Qin, X., et al., *Coexpression of growth differentiation factor 11 and reactive oxygen species in metastatic oral cancer and its role in inducing the epithelial to mesenchymal transition.* Oral Surg Oral Med Oral Pathol Oral Radiol, 2017. **123**(6): p. 697-706.

135. Horner, A., et al., *Expression and distribution of transforming growth factor-beta isoforms and their signaling receptors in growing human bone.* Bone, 1998. **23**(2): p. 95-102.

136. Weiss, A. and L. Attisano, *The TGFbeta superfamily signaling pathway.* Wiley Interdiscip Rev Dev Biol, 2013. **2**(1): p. 47-63.

137. Xu, H.B., et al., *Growth differentiation factor 11 relieves acute lung injury in mice by inhibiting inflammation and apoptosis.* Eur Rev Med Pharmacol Sci, 2020. **24**(12): p. 6908-6918.

138. Mei, W., et al., *GDF11 Protects against Endothelial Injury and Reduces Atherosclerotic Lesion Formation in Apolipoprotein E-Null Mice.* Molecular therapy : the journal of the American Society of Gene Therapy, 2016. **24**(11): p. 1926-1938.

139. Li, W., et al., *GDF11 antagonizes TNF-α-induced inflammation and protects against the development of inflammatory arthritis in mice.* Faseb j, 2019. **33**(3): p. 3317-3329.

140. Funkenstein, B. and E. Olekh, *Growth/differentiation factor-11: an evolutionary conserved growth factor in vertebrates.* Dev Genes Evol, 2010. **220**(5-6): p. 129-37.

141. Brown, G.R., et al., *Gene: a gene-centered information resource at NCBI.* Nucleic Acids Res, 2015. **43**(Database issue): p. D36-42.

142. Yates, A.D., et al., *Ensembl 2020.* Nucleic Acids Res, 2020. **48**(D1): p. D682-d688.

143. Fagerberg, L., et al., *Analysis of the human tissue-specific expression by genome-wide integration of transcriptomics and antibody-based proteomics.* Mol Cell Proteomics, 2014. **13**(2): p. 397-406.

144. Uhlén, M., et al., *Proteomics. Tissue-based map of the human proteome.* Science, 2015. **347**(6220): p. 1260419.

145. Esquela, A.F. and S.J. Lee, *Regulation of metanephric kidney development by growth/differentiation factor 11.* Dev Biol, 2003. **257**(2): p. 356-70.

146. Essalmani, R., et al., *In vivo functions of the proprotein convertase PC5/6 during mouse development: Gdf11 is a likely substrate.* Proc Natl Acad Sci U S A, 2008. **105**(15): p. 5750-5.

147. Tsuda, T., et al., *PCSK5 and GDF11 expression in the hindgut region of mouse embryos with anorectal malformations.* Eur J Pediatr Surg, 2011. **21**(4): p. 238-41.

148. Hardy, C.L., J.M. Rolland, and R.E. O'Hehir, *The immunoregulatory and fibrotic roles of activin A in allergic asthma.* Clinical and experimental allergy : journal of the British Society for Allergy and Clinical Immunology, 2015. **45**(10): p. 1510-1522.

149. Harrison, C.A., S.L. Al-Musawi, and K.L. Walton, *Prodomains regulate the synthesis, extracellular localisation and activity of TGF-β superfamily ligands.* Growth Factors, 2011. **29**(5): p. 174-86.

150. Schneyer, A.L., et al., *Differential antagonism of activin, myostatin and growth and differentiation factor 11 by wild-type and mutant follistatin.* Endocrinology, 2008. **149**(9): p. 4589-95.

151. Hill, J.J., et al., *The myostatin propeptide and the follistatin-related gene are inhibitory binding proteins of myostatin in normal serum.* J Biol Chem, 2002. **277**(43): p. 40735-41.

152. Hill, J.J., et al., *Regulation of myostatin in vivo by growth and differentiation factor-associated serum protein-1: a novel protein with protease inhibitor and follistatin domains.* Mol Endocrinol, 2003. **17**(6): p. 1144-54.

153. Robertson, R.D. and A. Mukherjee, *Synexpression group analyses identify new functions of FSTL3, a TGFβ ligand inhibitor.* Biochem Biophys Res Commun, 2012. **427**(3): p. 568-73.

154. Gilson, H., et al., *Follistatin induces muscle hypertrophy through satellite cell proliferation and inhibition of both myostatin and activin.* Am J Physiol Endocrinol Metab, 2009. **297**(1): p. E157-64.

155. Thies, R.S., et al., *GDF-8 propeptide binds to GDF-8 and antagonizes biological activity by inhibiting GDF-8 receptor binding.* Growth Factors, 2001. **18**(4): p. 251-9.

156. Wolfman, N.M., et al., *Activation of latent myostatin by the BMP-1/tolloid family of metalloproteinases.* Proc Natl Acad Sci U S A, 2003. **100**(26): p. 15842-6.

157. Li, Z., et al., *Transgenic overexpression of bone morphogenetic protein 11 propeptide in skeleton enhances bone formation.* Biochem Biophys Res Commun, 2011. **416**(3-4): p. 289-92.

158. Wang, Z., et al., *GDF11 induces differentiation and apoptosis and inhibits migration of C17.2 neural stem cells via modulating MAPK signaling pathway.* PeerJ, 2018. **6**: p. e5524.

159. Demontis, F., et al., *Intertissue control of the nucleolus via a myokine-dependent longevity pathway.* Cell Rep, 2014. **7**(5): p. 1481-1494.

160. Poniatowski, Ł.A., et al., *Transforming growth factor Beta family: insight into the role of growth factors in regulation of fracture healing biology and potential clinical applications.* Mediators of inflammation, 2015. **2015**: p. 137823-137823.

161. Inman, G.J., *Linking Smads and transcriptional activation.* Biochem J, 2005. **386**(Pt 1): p. e1-e3.

162. Liu, J.P., *The function of growth/differentiation factor 11 (Gdf11) in rostrocaudal patterning of the developing spinal cord.* Development, 2006. **133**(15): p. 2865-74.

163. Zhang, Y.H., et al., *GDF11/BMP11 activates both smad1/5/8 and smad2/3 signals but shows no significant effect on proliferation and migration of human umbilical vein endothelial cells.* Oncotarget, 2016. **7**(11): p. 12063-74.

164. Moustakas, A. and C.H. Heldin, *Non-Smad TGF-beta signals.* J Cell Sci, 2005. **118**(Pt 16): p. 3573-84.

165. Horbelt, D., A. Denkis, and P. Knaus, *A portrait of Transforming Growth Factor β superfamily signalling: Background matters.* Int J Biochem Cell Biol, 2012. **44**(3): p. 469-74.

166. Zhang, Y.E., *Non-Smad pathways in TGF-beta signaling.* Cell Res, 2009. **19**(1): p. 128-39.

167. Bryant, C.D., *The blessings and curses of C57BL/6 substrains in mouse genetic studies.* Annals of the New York Academy of Sciences, 2011. **1245**: p. 31-33.

168. Yang, H., et al., *On the subspecific origin of the laboratory mouse.* Nat Genet, 2007. **39**(9): p. 1100-7.

169. Churchill, G.A., et al., *The Diversity Outbred mouse population.* Mamm Genome, 2012. **23**(9-10): p. 713-8.

170. *The genome architecture of the Collaborative Cross mouse genetic reference population.* Genetics, 2012. **190**(2): p. 389-401.

171. Axton, E., *JAX Diversity Outbred mice: a genetically diverse mouse for a diverse human population*. 2020: The Jackson Laboratory.

172. Schmidt, C.W., *Diversity outbred: a new generation of mouse model.* Environmental health perspectives, 2015. **123**(3): p. A64-A67.

173. Lambert, R. *J:DO mice: novel tools for high-resolution genetic mapping*. 2012 [cited 2021; Available from: https://pharmaphorum.com/views-and-analysis/jdo_mice_novel_tools_for_high-resolution_genetic_mapping_/.

174. Müller, A.L. and N.S. Dhalla, *Differences in Concentric Cardiac Hypertrophy and Eccentric Hypertrophy*, in *Cardiac Adaptations: Molecular Mechanisms*, B. Ostadal and N.S. Dhalla, Editors. 2013, Springer New York: New York, NY. p. 147-166.

175. Chen-Scarabelli, C., et al., *Dilemmas in end-stage heart failure.* Journal of geriatric cardiology : JGC, 2015. **12**(1): p. 57-65.

176. Azad, N. and G. Lemay, *Management of chronic heart failure in the older population.* Journal of geriatric cardiology : JGC, 2014. **11**(4): p. 329-337.

177. Rodgers, B.D., *The Immateriality of Circulating GDF11.* Circulation Research, 2016. **118**(10): p. 1472-1474.

178. Morissette, M.R., et al., *Myostatin inhibits IGF-I-induced myotube hypertrophy through Akt.* Am J Physiol Cell Physiol, 2009. **297**(5): p. C1124-32.

179. Carnac, G., B. Vernus, and A. Bonnieu, *Myostatin in the pathophysiology of skeletal muscle.* Current genomics, 2007. **8**(7): p. 415-422.

180. Tobin, J.F. and A.J. Celeste, *Myostatin, a negative regulator of muscle mass: implications for muscle degenerative diseases.* Curr Opin Pharmacol, 2005. **5**(3): p. 328-32.

181. Rodriguez, J., et al., *Myostatin and the skeletal muscle atrophy and hypertrophy signaling pathways.* Cell Mol Life Sci, 2014. **71**(22): p. 4361-71.

182. Morissette, M.R., et al., *Myostatin regulates cardiomyocyte growth through modulation of Akt signaling.* Circ Res, 2006. **99**(1): p. 15-24.

183. Lee, S.J. and A.C. McPherron, *Myostatin and the control of skeletal muscle mass.* Curr Opin Genet Dev, 1999. **9**(5): p. 604-7.

184. McKoy, G., et al., *Developmental expression of myostatin in cardiomyocytes and its effect on foetal and neonatal rat cardiomyocyte proliferation.* Cardiovasc Res, 2007. **74**(2): p. 304-12.

185. Biesemann, N., et al., *Myostatin regulates energy homeostasis in the heart and prevents heart failure.* Circ Res, 2014. **115**(2): p. 296-310.

186. Morgan, A.P., et al., *The Mouse Universal Genotyping Array: From Substrains to Subspecies.* G3 (Bethesda), 2015. **6**(2): p. 263-79.

187. Broman, K.W., et al., *R/qtl2: software for mapping quantitative trait loci with high-dimensional data and multi-parent populations.* Genetics, 2018. **211**(211): p. 495-502.

188. Broman, K.W. and Ś. Sen, *A Guide to QTL Mapping with R/qtl*. 2009, Springer: New York.

189. Yang, J., et al., *Advantages and pitfalls in the application of mixed-model association methods.* Nature genetics, 2014. **46**(2): p. 100-106.

190. Churchill, G.A. and R.W. Doerge, *Empirical threshold values for quantitative trait mapping.* Genetics, 1994. **138**(3): p. 963-71.

191. Thorvaldsdóttir, H., J.T. Robinson, and J.P. Mesirov, *Integrative Genomics Viewer (IGV): high-performance genomics data visualization and exploration.* Briefings in bioinformatics, 2013. **14**(2): p. 178-192.

192. Howe, K.L., et al., *Ensembl Genomes 2020—enabling non-vertebrate genomic research.* Nucleic Acids Research, 2019. **48**(D1): p. D689-D695.

193. Johnson, W.E., C. Li, and A. Rabinovic, *Adjusting batch effects in microarray expression data using empirical Bayes methods.* Biostatistics, 2007. **8**(1): p. 118-27.

194. Lee, S.J., *Extracellular Regulation of Myostatin: A Molecular Rheostat for Muscle Mass.* Immunol Endocr Metab Agents Med Chem, 2010. **10**: p. 183-194.

195. Joulia-Ekaza, D. and G. Cabello, *Myostatin regulation of muscle development: molecular basis, natural mutations, physiopathological aspects.* Exp Cell Res, 2006. **312**(13): p. 2401-14.

196. Mendias, C.L., et al., *Haploinsufficiency of myostatin protects against aging-related declines in muscle function and enhances the longevity of mice.* Aging Cell, 2015. **14**(4): p. 704-6.

197. Rodgers, B.D., et al., *Myostatin represses physiological hypertrophy of the heart and excitation-contraction coupling.* The Journal of physiology, 2009. **587**(Pt 20): p. 4873-4886.

198. Cohn, R.D., et al., *Myostatin does not regulate cardiac hypertrophy or fibrosis.* Neuromuscular disorders : NMD, 2007. **17**(4): p. 290-296.

199. Weber, D., et al., *Mechanisms of epigenetic and cell-type specific regulation of Hey target genes in ES cells and cardiomyocytes.* J Mol Cell Cardiol, 2015. **79**: p. 79-88.

200. Fischer, A. and M. Gessler, *Delta-Notch--and then? Protein interactions and proposed modes of repression by Hes and Hey bHLH factors.* Nucleic Acids Res, 2007. **35**(14): p. 4583-96.

201. Rutenberg, J.B., et al., *Developmental patterning of the cardiac atrioventricular canal by Notch and Hairy-related transcription factors.* Development (Cambridge, England), 2006. **133**(21): p. 4381-4390.

202. Fischer, A., et al., *Hey bHLH factors in cardiovascular development.* Cold Spring Harb Symp Quant Biol, 2002. **67**: p. 63-70.

203. Fischer, A., et al., *Combined Loss of Hey1 and HeyL Causes Congenital Heart Defects Because of Impaired Epithelial to Mesenchymal Transition.* Circulation Research, 2007. **100**(6): p. 856-863.

204. Xiang, F., et al., *Transcription factor CHF1/Hey2 suppresses cardiac hypertrophy through an inhibitory interaction with GATA4.* American journal of physiology. Heart and circulatory physiology, 2006. **290**(5): p. H1997-H2006.

205. Nakagawa, O., et al., *Members of the HRT family of basic helix-loop-helix proteins act as transcriptional repressors downstream of Notch signaling.* Proc Natl Acad Sci U S A, 2000. **97**(25): p. 13655-60.

206. Sun, J., et al., *Regulation of myogenic terminal differentiation by the hairy-related transcription factor CHF2.* J Biol Chem, 2001. **276**(21): p. 18591-6.

207. Kent, W.J., et al., *The human genome browser at UCSC.* Genome Res, 2002. **12**(6): p. 996-1006.

208. Soutoglou, E., N. Katrakili, and I. Talianidis, *Acetylation regulates transcription factor activity at multiple levels.* Mol Cell, 2000. **5**(4): p. 745-51.

209. Ronnebaum, S.M. and C. Patterson, *The FoxO family in cardiac function and dysfunction.* Annual review of physiology, 2010. **72**: p. 81-94.

210. Hosaka, T., et al., *Disruption of forkhead transcription factor (FOXO) family members in mice reveals their functional diversification.* Proc Natl Acad Sci U S A, 2004. **101**(9): p. 2975-80.

211. Ni, Y.G., et al., *FoxO transcription factors activate Akt and attenuate insulin signaling in heart by inhibiting protein phosphatases.* Proceedings of the National Academy of Sciences of the United States of America, 2007. **104**(51): p. 20517-20522.

212. Xu, M., et al., *FoxO1: a novel insight into its molecular mechanisms in the regulation of skeletal muscle differentiation and fiber type specification.* Oncotarget, 2017. **8**(6): p. 10662-10674.

213. Beharry, A.W., et al., *HDAC1 activates FoxO and is both sufficient and required for skeletal muscle atrophy.* J Cell Sci, 2014. **127**(Pt 7): p. 1441-53.

214. Allen, D.L. and T.G. Unterman, *Regulation of myostatin expression and myoblast differentiation by FoxO and SMAD transcription factors.* Am J Physiol Cell Physiol, 2007. **292**(1): p. C188-99.

215. Seiliez, I., N. Sabin, and J.C. Gabillard, *FoxO1 is not a key transcription factor in the regulation of myostatin (mstn-1a and mstn-1b) gene expression in trout myotubes.* Am J Physiol Regul Integr Comp Physiol, 2011. **301**(1): p. R97-104.

216. Auguste, G., et al., *Suppression of Activated FOXO Transcription Factors in the Heart Prolongs Survival in a Mouse Model of Laminopathies.* Circ Res, 2018. **122**(5): p. 678-692.

217. Niessen, K. and A. Karsan, *Notch signaling in cardiac development.* Circ Res, 2008. **102**(10): p. 1169-81.

218. MacGrogan, D., J. Münch, and J.L. de la Pompa, *Notch and interacting signalling pathways in cardiac development, disease, and regeneration.* Nature Reviews Cardiology, 2018. **15**(11): p. 685-704.

219. Heisig, J., et al., *Target gene analysis by microarrays and chromatin immunoprecipitation identifies HEY proteins as highly redundant bHLH repressors.* PLoS genetics, 2012. **8**(5): p. e1002728-e1002728.

220. Robinson, J.R., et al., *Genome-wide and Phenome-wide Approaches to Understand Variable Drug Actions in Electronic Health Records.* Clinical and translational science, 2018. **11**(2): p. 112-122.

221. Hebbring, S.J., *The challenges, advantages and future of phenome-wide association studies.* Immunology, 2014. **141**(2): p. 157-65.

222. Buniello, A., et al., *The NHGRI-EBI GWAS Catalog of published genome-wide association studies, targeted arrays and summary statistics 2019.* Nucleic Acids Res, 2019. **47**(D1): p. D1005-d1012.

223. McCarthy, M.I., et al., *Genome-wide association studies for complex traits: consensus, uncertainty and challenges.* Nat Rev Genet, 2008. **9**(5): p. 356-69.

224. Stearns, F.W., *One hundred years of pleiotropy: a retrospective.* Genetics, 2010. **186**(3): p. 767-773.

225. Diogo, D., et al., *Phenome-wide association studies across large population cohorts support drug target validation.* Nature Communications, 2018. **9**(1): p. 4285.

226. Pividori, M., et al., *PhenomeXcan: Mapping the genome to the phenome through the transcriptome.* Sci Adv, 2020. **6**(37).

227. Gusev, A., et al., *Integrative approaches for large-scale transcriptome-wide association studies.* Nat Genet, 2016. **48**(3): p. 245-52.

228. Bhattacharya, A., et al., *A framework for transcriptome-wide association studies in breast cancer in diverse study populations.* Genome Biology, 2020. **21**(1): p. 42.

229. Gamazon, E.R., et al., *A gene-based association method for mapping traits using reference transcriptome data.* Nat Genet, 2015. **47**(9): p. 1091-8.

230. Mancuso, N., et al., *Integrating Gene Expression with Summary Association Statistics to Identify Genes Associated with 30 Complex Traits.* Am J Hum Genet, 2017. **100**(3): p. 473-487.

231. Barbeira, A.N., et al., *Widespread dose-dependent effects of RNA expression and splicing on complex diseases and traits.* bioRxiv, 2019: p. 814350.

232. Bycroft, C., et al., *The UK Biobank resource with deep phenotyping and genomic data.* Nature, 2018. **562**(7726): p. 203-209.

233. Carithers, L.J., et al., *A Novel Approach to High-Quality Postmortem Tissue Procurement: The GTEx Project.* Biopreservation and biobanking, 2015. **13**(5): p. 311-319.

234. Siminoff, L.A., et al., *Consent to a Postmortem Tissue Procurement Study: Distinguishing Family Decision Makers' Knowledge of the Genotype-Tissue Expression Project.* Biopreserv Biobank, 2018. **16**(3): p. 200-206.

235. Miller, K.L., et al., *Multimodal population brain imaging in the UK Biobank prospective epidemiological study.* Nature Neuroscience, 2016. **19**(11): p. 1523-1536.

236. van Rheenen, W., et al., *Genome-wide association analyses identify new risk variants and the genetic architecture of amyotrophic lateral sclerosis.* Nat Genet, 2016. **48**(9): p. 1043-8.

237. Lambert, J.C., et al., *Meta-analysis of 74,046 individuals identifies 11 new susceptibility loci for Alzheimer's disease.* Nat Genet, 2013. **45**(12): p. 1452-8.

238. Kettunen, J., et al., *Genome-wide study for circulating metabolites identifies 62 loci and reveals novel systemic effects of LPA.* Nat Commun, 2016. **7**: p. 11122.

239. Elliott, L.T., et al., *Genome-wide association studies of brain imaging phenotypes in UK Biobank.* Nature, 2018. **562**(7726): p. 210-216.

240. Kanai, M., T. Tanaka, and Y. Okada, *Empirical estimation of genome-wide significance thresholds based on the 1000 Genomes Project data set.* Journal of Human Genetics, 2016. **61**(10): p. 861-866.

241. Fromer, M., et al., *Gene expression elucidates functional impact of polygenic risk for schizophrenia.* Nat Neurosci, 2016. **19**(11): p. 1442-1453.

242. Consortium, G.T., *The Genotype-Tissue Expression (GTEx) project.* Nature genetics, 2013. **45**(6): p. 580-585.

243. Stancáková, A., et al., *Hyperglycemia and a common variant of GCKR are associated with the levels of eight amino acids in 9,369 Finnish men.* Diabetes, 2012. **61**(7): p. 1895-902.

244. Stancáková, A., et al., *Changes in insulin sensitivity and insulin release in relation to glycemia and glucose tolerance in 6,414 Finnish men.* Diabetes, 2009. **58**(5): p. 1212-21.

245. Raitakari, O.T., et al., *Cohort profile: the cardiovascular risk in Young Finns Study.* Int J Epidemiol, 2008. **37**(6): p. 1220-6.

246. Nuotio, J., et al., *Cardiovascular risk factors in 2011 and secular trends since 2007: the Cardiovascular Risk in Young Finns Study.* Scand J Public Health, 2014. **42**(7): p. 563-71.

247. Wright, F.A., et al., *Heritability and genomics of gene expression in peripheral blood.* Nat Genet, 2014. **46**(5): p. 430-7.

248. *The GTEx Consortium atlas of genetic regulatory effects across human tissues.* Science, 2020. **369**(6509): p. 1318-1330.

249. Fischer, A. and M. Gessler, *Hey Genes in Cardiovascular Development.* Trends in Cardiovascular Medicine, 2003. **13**(6): p. 221-226.

250. Fischer, A., et al., *The Notch target genes Hey1 and Hey2 are required for embryonic vascular development.* Genes & development, 2004. **18**(8): p. 901-911.

251. Tateya, T., et al., *Cooperative functions of Hes/Hey genes in auditory hair cell and supporting cell development.* Dev Biol, 2011. **352**(2): p. 329-40.

252. Subramaniam, V. and G.Y. Lip, *Hypertension to heart failure: a pathophysiological spectrum relating blood pressure, drug treatments and stroke.* Expert Rev Cardiovasc Ther, 2009. **7**(6): p. 703-13.

253. Wenn P, Z.R., *Aortic Valve Disease*, I. StatPearls, Editor. [Updated 2021 Jan 21], StatPearls Publishing: Treasure Island (FL).

254. Roberts, W.C., et al., *Causes of pure aortic regurgitation in patients having isolated aortic valve replacement at a single US tertiary hospital (1993 to 2005).* Circulation, 2006. **114**(5): p. 422-9.

255. Bekeredjian, R. and P.A. Grayburn, *Valvular heart disease: aortic regurgitation.* Circulation, 2005. **112**(1): p. 125-34.

256. Czarny, M.J. and J.R. Resar, *Diagnosis and management of valvular aortic stenosis.* Clinical Medicine Insights. Cardiology, 2014. **8**(Suppl 1): p. 15-24.

257. Holland, T.L., et al., *Infective endocarditis.* Nature reviews. Disease primers, 2016. **2**: p. 16059-16059.

258. Le Bot, A., et al., *[Non-infective endocarditis].* Rev Med Interne, 2018. **39**(10): p. 782-791.

259. Hurrell, H., R. Roberts-Thomson, and B.D. Prendergast, *Non-infective endocarditis.* Heart, 2020. **106**(13): p. 1023.

260. Fuchs, F.D. and P.K. Whelton, *High Blood Pressure and Cardiovascular Disease.* Hypertension, 2020. **75**(2): p. 285-292.

261. Kjeldsen, S.E., *Hypertension and cardiovascular risk: General aspects.* Pharmacol Res, 2018. **129**: p. 95-99.

262. Canela-Xandri, O., K. Rawlik, and A. Tenesa, *An atlas of genetic associations in UK Biobank.* Nat Genet, 2018. **50**(11): p. 1593-1599.

263. VanOudenhove, J., et al., *Epigenomic and Transcriptomic Dynamics During Human Heart Organogenesis.* Circ Res, 2020. **127**(9): p. e184-e209.

264. McCarty, C.A., et al., *Healthy People 2010 disease prevalence in the Marshfield Clinic Personalized Medicine Research Project cohort: opportunities for public health genomic research.* Per Med, 2007. **4**(2): p. 183-190.

265. Dichmann, D.S., H. Yassin, and P. Serup, *Analysis of pancreatic endocrine development in GDF11-deficient mice.* Dev Dyn, 2006. **235**(11): p. 3016-25.

266. Rochette, L., et al., *Growth and differentiation factor 11 (GDF11): Functions in the regulation of erythropoiesis and cardiac regeneration.* Pharmacol Ther, 2015. **156**: p. 26-33.

267. Rochette, L., et al., *Anti-Aging Effects of GDF11 on Skin.* International journal of molecular sciences, 2020. **21**(7): p. 2598.

268. Añón-Hidalgo, J., et al., *Circulating Concentrations of GDF11 are Positively Associated with TSH Levels in Humans.* Journal of clinical medicine, 2019. **8**(6): p. 878.

269. Onodera, K., et al., *Decrease in an anti-ageing factor, growth differentiation factor 11, in chronic obstructive pulmonary disease.* Thorax, 2017. **72**(10): p. 893-904.

270. Tanaka, R., et al., *Physical inactivity is associated with decreased growth differentiation factor 11 in chronic obstructive pulmonary disease.* Int J Chron Obstruct Pulmon Dis, 2018. **13**: p. 1333-1342.

271. Ishmael, F.T., *The inflammatory response in the pathogenesis of asthma.* J Am Osteopath Assoc, 2011. **111**(11 Suppl 7): p. S11-7.

272. Murdoch, J.R. and C.M. Lloyd, *Chronic inflammation and asthma.* Mutation research, 2010. **690**(1-2): p. 24-39.

273. Mancini, A., et al., *Thyroid Hormones, Oxidative Stress, and Inflammation.* Mediators of inflammation, 2016. **2016**: p. 6757154-6757154.

274. Chaker, L., et al., *Hypothyroidism.* Lancet (London, England), 2017. **390**(10101): p. 1550-1562.

275. Chiovato, L., F. Magri, and A. Carlé, *Hypothyroidism in Context: Where We've Been and Where We're Going.* Advances in therapy, 2019. **36**(Suppl 2): p. 47-58.

276. Mincer, D.L. and I. Jialal, *Hashimoto Thyroiditis*, in *StatPearls*. 2021, StatPearls Publishing
Copyright © 2021, StatPearls Publishing LLC.: Treasure Island (FL).

277. Redd, S.C., *Asthma in the United States: burden and current theories.* Environ Health Perspect, 2002. **110 Suppl 4**(Suppl 4): p. 557-60.

278. Barnes, P.J., *Immunology of asthma and chronic obstructive pulmonary disease.* Nat Rev Immunol, 2008. **8**(3): p. 183-92.

279. Holgate, S.T., *Pathogenesis of asthma.* Clin Exp Allergy, 2008. **38**(6): p. 872-97.

280. Goldacre, M., et al., *Use of large medical databases to study associations between diseases.* Qjm, 2000. **93**(10): p. 669-75.

281. Manzolli, S., et al., *Allergic airway inflammation in hypothyroid rats.* J Allergy Clin Immunol, 1999. **104**(3 Pt 1): p. 595-600.

282. Sato, A., et al., *A possible role of immunoglobulin E in patients with hyperthyroid Graves' disease.* J Clin Endocrinol Metab, 1999. **84**(10): p. 3602-5.

283. Hoffman, D.A. and W.M. McConahey, *Thyrotoxicosis and asthma.* Lancet, 1982. **1**(8275): p. 808.

284. Ursu, H.I., et al., *Graves'-Basedow's disease--asthma association. Presentation of five cases.* Rom J Endocrinol, 1993. **31**(1-2): p. 89-94.

285. Bingyan, Z. and W. Dong, *Impact of thyroid hormones on asthma in older adults.* The Journal of international medical research, 2019. **47**(9): p. 4114-4125.

286. Qashqary, M., et al., *Prevalence of Suspected Cases of Hyperthyroidism in Jeddah by Using Wayne's Scoring Index.* Cureus, 2020. **12**(11): p. e11538-e11538.

287. Oppedal, R.J., D.A. Khan, and E.S. Brown, *Hypothyroidism in patients with asthma and major depressive disorder.* Primary care companion to the Journal of clinical psychiatry, 2007. **9**(6): p. 467-468.

288. Cartwright, D.J., *ICD-9-CM to ICD-10-CM Codes: What? Why? How?* Advances in wound care, 2013. **2**(10): p. 588-592.

289. Albert, F.W. and L. Kruglyak, *The role of regulatory variation in complex traits and disease.* Nature Reviews Genetics, 2015. **16**(4): p. 197-212.

290. Skelly, D.A., J. Ronald, and J.M. Akey, *Inherited variation in gene expression.* Annu Rev Genomics Hum Genet, 2009. **10**: p. 313-32.

291. Qu, W., et al., *Identification of Splicing Quantitative Trait Loci (sQTL) in Drosophila melanogaster with Developmental Lead (Pb(2+)) Exposure.* Frontiers in genetics, 2017. **8**: p. 145-145.

292. Yao, C., et al., *Dynamic Role of trans Regulation of Gene Expression in Relation to Complex Traits.* The American Journal of Human Genetics, 2017. **100**(4): p. 571-580.

293. van der Wijst, M., et al., *The single-cell eQTLGen consortium.* eLife, 2020. **9**: p. e52155.

294. Võsa, U., et al., *Unraveling the polygenic architecture of complex traits using blood eQTL metaanalysis.* bioRxiv, 2018: p. 447367.

295. Laisk, T., M. Lepamets, and R. Mägi, *Genome-wide association study identifies five risk loci for pernicious anemia and implicates the role of HLA-DR15 haplotype*. 2020, medRxiv.

296. Ghoussaini, M., et al., *Open Targets Genetics: systematic identification of trait-associated genes using large-scale genetics and functional genomics.* Nucleic Acids Research, 2021. **49**(D1): p. D1311-D1320.

297. Zhou, W., et al., *Efficiently controlling for case-control imbalance and sample relatedness in large-scale genetic association studies.* Nat Genet, 2018. **50**(9): p. 1335-1341.

298. Sun, B.B., et al., *Genomic atlas of the human plasma proteome.* Nature, 2018. **558**(7708): p. 73-79.

299. Kerimov, N., et al., *eQTL Catalogue: a compendium of uniformly processed human gene expression and splicing QTLs*. 2020, bioRxiv.

300. Jung, I., et al., *A compendium of promoter-centered long-range chromatin interactions in the human genome.* Nat Genet, 2019. **51**(10): p. 1442-1449.

301. Andersson, R., et al., *An atlas of active enhancers across human cell types and tissues.* Nature, 2014. **507**(7493): p. 455-461.

302. Thurman, R.E., et al., *The accessible chromatin landscape of the human genome.* Nature, 2012. **489**(7414): p. 75-82.

303. Malone, J., et al., *Modeling sample variables with an Experimental Factor Ontology.* Bioinformatics, 2010. **26**(8): p. 1112-8.

304. Carvalho-Silva, D., et al., *Open Targets Platform: new developments and updates two years on.* Nucleic Acids Research, 2019. **47**(D1): p. D1056-D1065.

305. Tedeschi, A. and R. Asero, *Asthma and autoimmunity: a complex but intriguing relation.* Expert Rev Clin Immunol, 2008. **4**(6): p. 767-76.

306. Duan, Q.L., et al., *A polymorphism in the thyroid hormone receptor gene is associated with bronchodilator response in asthmatics.* The pharmacogenomics journal, 2013. **13**(2): p. 130-136.

307. Eriksson, N., et al., *Novel associations for hypothyroidism include known autoimmune risk loci.* PLoS One, 2012. **7**(4): p. e34442.

308. Denny, J.C., et al., *Variants near FOXE1 are associated with hypothyroidism and other thyroid conditions: using electronic medical records for genome- and phenome-wide studies.* Am J Hum Genet, 2011. **89**(4): p. 529-42.

309. Pickrell, J.K., et al., *Detection and interpretation of shared genetic influences on 42 human traits.* Nat Genet, 2016. **48**(7): p. 709-17.

310. Porcu, E., et al., *A meta-analysis of thyroid-related traits reveals novel loci and gender-specific differences in the regulation of thyroid function.* PLoS Genet, 2013. **9**(2): p. e1003266.

311. Kim, K.W. and C. Ober, *Lessons Learned From GWAS of Asthma.* Allergy Asthma Immunol Res, 2019. **11**(2): p. 170-187.

312. Han, Y., et al., *Genome-wide analysis highlights contribution of immune system pathways to the genetic architecture of asthma.* Nature Communications, 2020. **11**(1): p. 1776.

313. Vitali, F., et al., *Precision drug repurposing via convergent eQTL-based molecules and pathway targeting independent disease-associated polymorphisms.* Pacific Symposium on Biocomputing. Pacific Symposium on Biocomputing, 2019. **24**: p. 308-319.

314. Westra, H.-J. and L. Franke, *From genome to function by studying eQTLs.* Biochimica et Biophysica Acta (BBA) - Molecular Basis of Disease, 2014. **1842**(10): p. 1896-1902.

315. Asvold, B.O., et al., *Tobacco smoking and thyroid function: a population-based study.* Arch Intern Med, 2007. **167**(13): p. 1428-32.

316. Denny, J.C., et al., *PheWAS: demonstrating the feasibility of a phenome-wide scan to discover gene-disease associations.* Bioinformatics, 2010. **26**(9): p. 1205-10.

317. Iso, T., L. Kedes, and Y. Hamamori, *HES and HERP families: multiple effectors of the Notch signaling pathway.* J Cell Physiol, 2003. **194**(3): p. 237-55.

318. Salie, R., et al., *Ubiquitous overexpression of Hey1 transcription factor leads to osteopenia and chondrocyte hypertrophy in bone.* Bone, 2010. **46**(3): p. 680-94.

319. Sakamoto, M., et al., *The basic helix-loop-helix genes Hesr1/Hey1 and Hesr2/Hey2 regulate maintenance of neural precursor cells in the brain.* J Biol Chem, 2003. **278**(45): p. 44808-15.

320. Itoh, F., et al., *Synergy and antagonism between Notch and BMP receptor signaling pathways in endothelial cells.* Embo j, 2004. **23**(3): p. 541-51.

321. Buas, M.F., S. Kabak, and T. Kadesch, *The Notch effector Hey1 associates with myogenic target genes to repress myogenesis.* J Biol Chem, 2010. **285**(2): p. 1249-58.

322. Kokubo, H., et al., *Hesr1 and Hesr2 regulate atrioventricular boundary formation in the developing heart through the repression of Tbx2.* Development, 2007. **134**(4): p. 747-55.

323. Yin, X., et al., *Hey1 functions as a positive regulator of odontogenic differentiation in odontoblast-lineage cells.* International journal of molecular medicine, 2018. **41**(1): p. 331-339.

324. Zavadil, J., et al., *Integration of TGF-beta/Smad and Jagged1/Notch signalling in epithelial-to-mesenchymal transition.* Embo j, 2004. **23**(5): p. 1155-65.

325. Wöltje, K., M. Jabs, and A. Fischer, *Serum induces transcription of Hey1 and Hey2 genes by Alk1 but not Notch signaling in endothelial cells.* PLoS One, 2015. **10**(3): p. e0120547.

326. Gade, P. and D.V. Kalvakolanu, *Chromatin immunoprecipitation assay as a tool for analyzing transcription factor activity.* Methods in molecular biology (Clifton, N.J.), 2012. **809**: p. 85-104.

327. Jennings, B.H., D.M. Tyler, and S.J. Bray, *Target specificities of Drosophila enhancer of split basic helix-loop-helix proteins.* Molecular and cellular biology, 1999. **19**(7): p. 4600-4610.

328. Davis, R.L. and D.L. Turner, *Vertebrate hairy and Enhancer of split related proteins: transcriptional repressors regulating cellular differentiation and embryonic patterning.* Oncogene, 2001. **20**(58): p. 8342-57.

329. Leal, M.C., et al., *Notch signaling proteins HES-1 and Hey-1 bind to insulin degrading enzyme (IDE) proximal promoter and repress its transcription and activity: implications for cellular Aβ metabolism.* Biochimica et biophysica acta, 2012. **1823**(2): p. 227-235.

330. Perna, D., et al., *Genome-wide mapping of Myc binding and gene regulation in serum-stimulated fibroblasts.* Oncogene, 2012. **31**(13): p. 1695-709.

331. Takata, T. and F. Ishikawa, *Human Sir2-related protein SIRT1 associates with the bHLH repressors HES1 and HEY2 and is involved in HES1- and HEY2-mediated transcriptional repression.* Biochem Biophys Res Commun, 2003. **301**(1): p. 250-7.

332. Gordon, H. and H.H. Sweets, *A Simple Method for the Silver Impregnation of Reticulum.* The American journal of pathology, 1936. **12**(4): p. 545-552.1.

333. Maier, M.M. and M. Gessler, *Comparative analysis of the human and mouse Hey1 promoter: Hey genes are new Notch target genes.* Biochem Biophys Res Commun, 2000. **275**(2): p. 652-60.

334. Steidl, C., et al., *Characterization of the human and mouse HEY1, HEY2, and HEYL genes: cloning, mapping, and mutation screening of a new bHLH gene family.* Genomics, 2000. **66**(2): p. 195-203.

335. Gessler, M., et al., *Mouse gridlock: no aortic coarctation or deficiency, but fatal cardiac defects in Hey2 -/- mice.* Curr Biol, 2002. **12**(18): p. 1601-4.

336. Donovan, J., et al., *Tetralogy of fallot and other congenital heart defects in Hey2 mutant mice.* Curr Biol, 2002. **12**(18): p. 1605-10.

337. Luxán, G., et al., *Endocardial Notch Signaling in Cardiac Development and Disease.* Circ Res, 2016. **118**(1): p. e1-e18.

338. Fischer, A., et al., *Hey basic helix-loop-helix transcription factors are repressors of GATA4 and GATA6 and restrict expression of the GATA target gene ANF in fetal hearts.* Molecular and cellular biology, 2005. **25**(20): p. 8960-8970.

# APPENDIX

## STRATEGIC AIMS TO MECHANISTICALLY TEST THE HEY-GDF11 AXIS

### A.1. Background and Preliminary Data

In our prior work, association mapping of the GDF11 serum level phenotype produced a suggestive QTL peak ($p < 0.1$) on chromosome 3 within the Bayesian credible interval of [3.039589 – 9.983782] Mbp. Further analysis indicated the candidate gene was hairy/enhancer-of-split related with YRPW motif 1 (Hey 1), a member of the basic helix-loop-helix family and a downstream effector of canonical Notch signaling [317]. Hey1 is critical for the embryonic development of many tissues including bone, muscle, nerve, and the heart [318-323]. Interestingly, *Hey1* expression can be induced independent of Notch by TGF-β/BMP signaling [324, 325], which is the signaling pathway initiated by GDF11 and its related proteins [86]. As of yet, no studies to our knowledge have established a relationship between Hey1 and GDF11 specifically.

Our third aim explores Hey1 as a potential transcriptional regulator of heart function in the adult mammal by delineating the relationship between GDF11 expression and Hey1 by *in vitro* and *in vivo* methods. It will also distinguish the role of Hey1 from its closely related proteins, Hey2 and HeyL.

## A.2. Study Design

The foremost aim will be to validate Hey1's binding site *in vitro* in relation to the human *GDF11* and murine *Gdf11* genes via Chromatin Immunoprecipitation coupled with quantitative PCR (ChIP-qPCR). Once the exact binding sites have been located, we will determine Hey1's effect on *GDF11/Gdf11* expression through plasmid transfection on both human and mouse cell lines. Subsequently, we will observe the effects of Hey1 *in vivo* through a floxed constituent knockout mouse model. By selectively eliminating *Hey1* in the adult mouse, we can examine the gene's effects on heart health as well as serum GDF11 concentration. Finally, the *in vitro* experimentation (ChIP-qPCR and transfection) will be repeated with Hey2 and HeyL, respectively, to further explore the differences and overlapping roles between the related transcription factors.

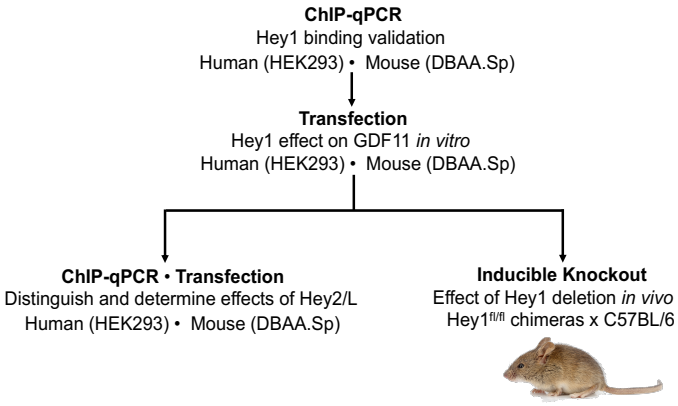


**Figure A.1:** Study Design

### A.2.1. Determine precise binding site of Hey1 and its effect on GDF11 *in vitro*

Using online data bases and bioinformatic techniques, we identified the most likely binding sites for Hey1 in relation to *GDF11/Gdf11* based on genomic location and acetylation activity. This aim will use reliable mechanistic techniques to determine the precise binding sites of Hey1 in relation to our gene of interest.

### A.2.1.1. Validate Binding Site of Hey1 by Performing ChIP-qPCR

Chromatin immunoprecipitation with quantitative PCR (ChIP-qPCR) provides protein-DNA association information that allows for transcription factor binding sites to be located in a specific area of the genome [326]. Several studies have shown that Hey1, and its related proteins, bind to the highly conserved canonical E-box sequence 5'-CACGTG-3' across mammalian species [202, 327], however some findings suggest additional or alternative binding motifs [219, 328]. In order to confirm our proposed binding site in relation to the *Gdf11/GDF11* gene (Figure A.2), we will perform ChIP-qPCR on human

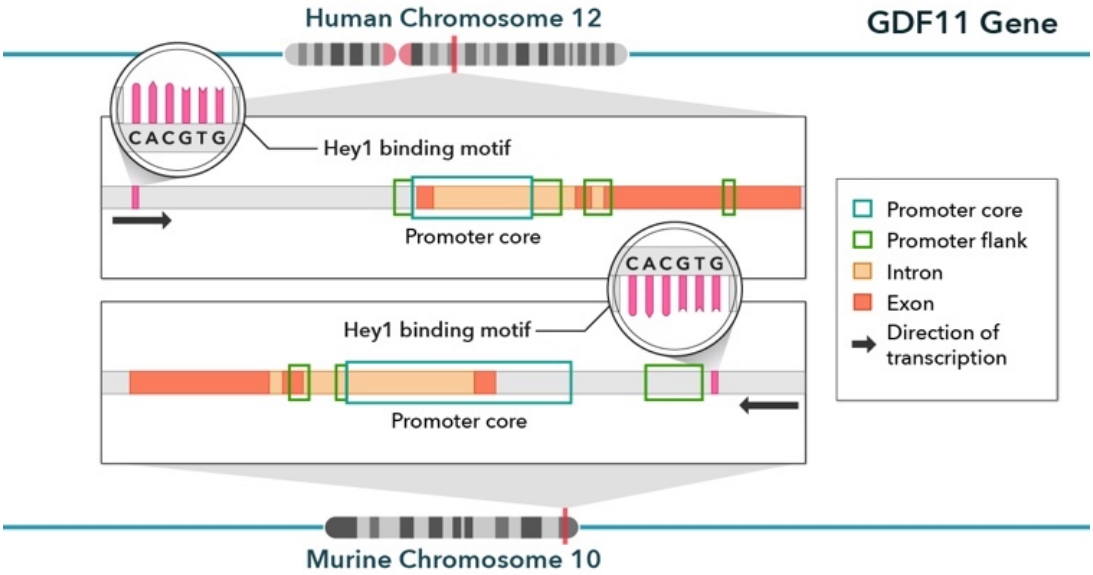


**Figure A.2**: Putative Binding Site Predicted by Prior Bioinformatic Analysis.

embryonic kidney (HEK293 from ATCC) and adult mouse spleen (DBA A.Sp from ATCC) cells in parallel (Figure A.3).

Cell Culture Conditions: HEK293 cells as well as the DBA A.Sp cells will be maintained in Dulbecco's modified Eagle's medium containing 10% fetal bovine serum and 1% penicillin. Incubator will be kept at 37°C with 5% CO2.

ChIP Procedure: Each cell line will be induced with 50 ng/ml doxycycline for 48 h for low level overexpression of Hey1 proteins. For fixation, 1% formaldehyde will be added to four dishes - two of which containing $3x10^7$ mouse cells and two containing $3x10^7$ HEK293 cells - for 10 minutes at room temperature. Then 0.2 M of glycine will be added to halt annealing and cells will be rinsed three times with 10 mL of cold PBS. After centrifugation, the samples will be lysed in a cell lyses buffer containing 1% SDS and incubated for 10 minutes. The chromatin will be sheared by sonification (FisherBrand Model 50 Sonic Dismembrator) to produce segments approximately 500 bp each. Centrifugation will pellet the cell debris for immunoprecipitation, and DNA will be purified and the concentration quantified. A portion of the pelleted cell debris will also be held as a control sample prior to the addition of the antibody. A Hey1 antibody purchased from Proteintech will be used to capture the Hey1-GDF11 fragments in the input samples, along with a species-matched IgG as a control. The samples will then be incubated with Protein A/G Plus–Agarose beads (Santa Cruz Biotechnology). Following a series of salt washes, we will elute the DNA in an elution buffer and centrifuge again. The supernatant containing the protein/DNA complex will undergo reverse cross-linking by protein kinase K and phenol:chloroform DNA extraction.

qPCR Analysis:

Next, oligonucleotide primers will be used to amplify immunoprecipitated DNA fragments at specific loci by qPCR. We will custom design the primers by utilizing Ensembl exon boundary information and the primerQuest tool on the Integrated DNA Technologies website for both humans and mice. The genomic fragments for both cell lines will be amplified by PCR using the same primers and the genomic regions of the

binding sites will be determined.

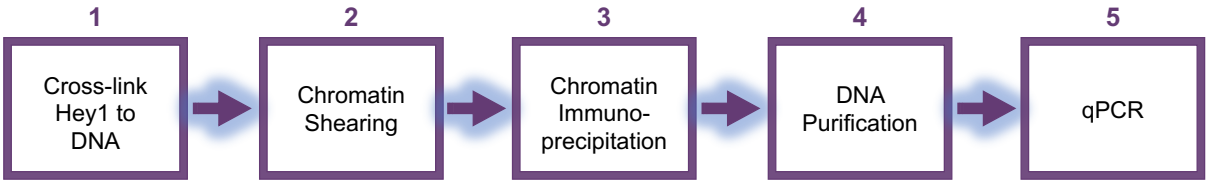


**Figure A.3:** ChIP-qPCR

Potential Complications and Solutions: As noted above, there is uncertainty in the current literature as to what consensus sequence Hey1 functionally binds *in vivo* and whether or not that is consistent for all of the genes it regulates along the genome [219]. Though the core motif 5'-CACGTG-3' has proven necessary for some genes *in vivo* [329], it does not always have to be present for Hey1 to regulate its target gene [219], implicating a relaxed criteria for DNA binding, additional binding motifs, and/or, as Perna et al. suggested, Hey1 may bind sequentially in such a way that does not require sequence specificity initially [330]. After validating the binding site, and if *in vivo* experimentation outlined in A.2.2. shows a significant role of Hey1 in GDF11 serum concentration, then follow up studies should be conducted to determine the functional binding site in a living mouse model.

Expected Outcomes: We expect Hey1 to bind upstream of human GDF11 at approximately Chr12:55,729,183-55,729,189 and upstream of the mouse GDF11 gene at Chr10:128,898,596-128,898,601 according to our prior bioinformatics investigation (Figure A.2).

### A.2.1.2. Determining the effect of Hey1 on GDF11 expression *in vitro* via Hey1 transfections

Cell Culture Conditions: Both human and murine cell lines will be maintained as described above.

Hey1 Transfection: A standard transient transfection will be performed on the human and mouse cell lines noted above. The Hey1 expression plasmids will be transfected by the addition of the Lipofectamine® LTX Reagent (ThermoFisher) into HEK293 cells, which will have been plated into 60mm culture dishes at a concentration of $5.5x10^5$ with growth medium. Approximately 24 hours later, the cells will be harvested for quantification of GDF11 expression. The procedure will be repeated using DBA A.Sp cells and a mouse Hey1 plasmid. For the control, HEK293 and DBA A.Sp cells will be cultured in parallel under the same conditions without injection of the plasmids.

Test Genetic Expression: Both the control cell lines and the plasmid-transfected cell lines will undergo genetic testing to determine baseline and experimental expression levels of Hey1 and GDF11. Cells will be pelleted, harvested and undergo total RNA extraction (Qiagen: RNeasy Mini Kit). DNase will be used to digest DNA in the sample, ensuring purity of RNA product. Then we will use the NanoDrop Spectrophotometer (NDS) to assess for contaminants and total RNA concentrations will be quantified. Total RNA will undergo reverse transcription (Applied Biosystems: High Capacity cDNA Reverse Transcription Kit) to obtain stable cDNA. Finally, primers and housekeeping genes will be optimized and used for qRT-PCR (GGBC: LightCycler 480 System) for quantification of Hey1 and GDF11 expression.

Expected Results: Members of the basic helix-loop-helix family of transcription factors, including the hairy/Enhancer of split-related subfamily, act as transcriptional repressors of their target genes through various pathways [202, 328, 331]. We expect that the overexpression of Hey1 will cause a sharp reduction, of GDF11 transcription when compared to the non-transfected control cell lines.

**A.2.2.1. Examine impact of Hey1 deletion in an adult mouse by inducible knockout**

An inducible Hey1 knockout mouse model allows for comparison of a gene's effect within the same test subject. Hey1 has been implicated in cardiac development [202, 250, 322], so by maintaining this gene until the adult stage will eliminate potential embryonic malformations to examine Hey1's effect in adulthood specifically.

Inducible knockout methodology: Floxed Hey1 mice crossed with a recombinase-expressing line will be designed by the ingenious targeting laboratory (Ronkonkoma, NY) to allow for heart-specific Hey1 deletion via Cre-recombinase treatment once the mice are four months old. Half of the mice (N = 10) will not undergo genetic deletion and will serve as our control group.

Genetic validation: Effectiveness of the Hey1 knockout will be determined via genotyping. Prior to sacrifice, tail tips from the intervention group will be collected and sent to NEOGEN Genomics (Lincoln, NE) for DNA isolation and genotyping via the Giga Mouse Universal Genotyping Array (GigaMuga) [186].

Assess impact of Hey1 deletion: A blood draw from the submandibular vein will be performed on all mice 1) at four months of age immediately prior to the induced Hey1 deletion in the experimental group, and 2) one to two months later before sacrifice in order to quantify expressed circulating GDF11. Serum will be sent to the Brigham

Research Assay Core at Brigham and Women's Hospital (Boston, MA) for GDF11 quantification via liquid chromatography-mass spectrometry (LC-MS/MS). LC-MS/MS specifically and reliably measures GDF11, while distinguishing it from its homolog myostatin [103]. One month after the gene silencing of the experimental group, all mice will be euthanized and the hearts isolated and prepared for histological analysis. Tissue will be sectioned and the hematoxylin and eosin stain will be applied as standard histopathologic analysis protocol, then the Gordon and Sweet's reticulin stain for determination of cardiomyocyte cross sectional area [332], and finally Masson's trichome stain for visualization of percent fibrosis, as done before. The FIJI software (ImageJ) will be used to measure left ventricular wall thickness, cardiomyocyte cross sectional area, and percent fibrosis.

Potential complications: Due to the pioneering nature of our study, the ideal amount of time between deletion of Hey1 in mice and euthanasia has not been determined. Therefore, half of the mice in the intervention group (N = 5) will be sacrificed one month after selective gene deletion and the other half (N = 5) will be sacrificed two months after. Phenotypic data from the two cohorts will be collected and compared.

Expected results: Our prior study revealed a positive correlation between serum GDF11 levels and cardiomyocyte cross sectional area ($r = 0.136$, $p < 0.046$) in a genetically diverse adult population, suggesting a mild pro-hypertrophic effect of GDF11. We hypothesize that Hey1 will serve as a transcriptional repressor of GDF11, and that the deletion of Hey1 will result in increased cardiomyocyte cross sectional area.

### A.2.3. Determine behavior of Hey2 and HeyL *in vitro*

All three *Hey* genes are present in both the human and mouse genomes [333] and share similar genomic structure [334]. *Hey1* and *Hey2* exhibit partially overlapping expression patterns in many mouse tissues during embryonic development [333]. Specifically, *Hey1* is highly expressed in the atria and *Hey2* is expressed in the ventricular cardiomyocytes of developing mouse heart [250]. Although the *Hey* genes share many similarities, *Hey2* knockout mice die prematurely due to severe vascular effects [250, 335, 336], while *Hey1* or *HeyL* single knockout mice have shown minimal [322] to no apparent phenotypic changes [250] in development (Table A.1). Combination deletion of *Hey1* and *HeyL* in mice present with defects in the right outflow tract of the developing heart [203, 337] and *Hey1-Hey2* knockout mice are nonviable [338]. This information suggests a synergistic effect of the Hey proteins in their roles as transcription factors [203]. Thus, in this aim we will further differentiate the roles of each Hey family member as it relates to human and murine GDF11 regulation *in vitro*.

| Mouse Model | Phenotype |
|---|---|
| **Hey2$^{-/-}$** | Ventricular septal defect, atrial septum defect, pulmonary artery stenosis, tetralogy of Fallot, tricuspid valve atresia, atrioventricular valve dysfunction; embryonic lethal |
| **Hey1$^{-/-}$;Hey2$^{-/-}$** | Defective cardiac looping, hypoplastic endocardial cushion and impaired trabeculation; peri/postnatal lethality |
| **Hey1$^{-/-}$;HeyL$^{-/-}$** | Ventricular septal defect, atrioventricular valve defects; perinatal lethality |

**Table A.1:** Hey Knockouts. Adapted from "Endocardial Notch Signaling in Cardiac Development and Disease" Luxan, et al.

#### A.2.3.1. Validate binding site of Hey2 and HeyL

Cell Culture Conditions: Both human and murine cell lines will be maintained as described above.

ChIP-qPCR Analysis: The ChIP-qPCR protocol will be replicated as described above for Hey2 and HeyL respectively.

Expected Results: Current literature suggest that all members of the Hey family of bHLH transcription factors share the same binding site [202, 327]. Thus, we hypothesize that Hey2 and HeyL will result in the same binding locations as each other and as Hey1.

**A.2.3.2. Determine distinct roles of Hey2 and HeyL on GDF11**

Employ transfection: Transfections will be conducted as described above in A.2.1.2. using first a Hey2 plasmid on both human and mouse cell lines, then also transfecting with HeyL for both species.

Genetic testing: Expression quantification of GDF11 as well as Hey2 and Hey3 will be performed as outlined in A.2.1.2.

Expected Results: The Notch target genes Hey1 and Hey2 show overlapping roles in the developing heart [250]. We expect transfections of Hey2 and HeyL to result in a decrease of GDF11 to the same extent as Hey1 will alone in A.2.1.2.